4-26-2019

Uncovering the Mechanisms of Staphylococcus aureus Enterotoxin A-induced Systemic and Pulmonary Inflammation

Julia Ryan
University of Connecticut - Storrs, julryan@uchc.edu

Doctor of Philosophy Dissertation

Uncovering the Mechanisms of *Staphylococcus aureus* Enterotoxin A-induced Systemic and Pulmonary Inflammation

By Julia Svedova, PhD

University of Connecticut, 2019

Abstract

Staphylococcus aureus is a component of normal flora colonizing skin and nares, but it is also one of the most common causes of serious infections, especially sepsis. The dysfunctional immune response during sepsis often leads to tissue damage and organ failure, including acute lung injury. Among the virulence factors that likely drive the high morbidity and mortality associated with *S. aureus* sepsis and tissue injury are enterotoxins, including *S. aureus* enterotoxin A (SEA). SEA directly crosslinks MHC II molecules and specific Vβ chains of T cell receptors resulting in oligoclonal activation of T cells and massive immune response. Previous studies showed that SEA inhalation in mice caused a rapid activation of SEA-specific T cells and cytokine release into circulation. This systemic inflammatory response was followed by SEA-specific T cell expansion in lymphoid tissues and lung, which was accompanied by development of pulmonary pathology and increased vascular permeability. The aims of this study were to (1) define the crosstalk between adaptive immunity and innate immune cells during the systemic inflammatory response, (2) further characterize SEA-induced pulmonary inflammation and understand the mechanism leading to increased permeability in lung, and (3) determine the role of alveolar macrophages in the systemic inflammatory response due to SEA inhalation. The results demonstrated that after inhalation, SEA disseminated systemically via blood and triggered rapid transcriptional changes in T cells followed by a systemic recruitment of neutrophils and monocytes into circulation and lymphoid tissues. TNF and CD28 signaling

played unique but also overlapping roles in the migration of innate immune cells. Furthermore, this study shows that the injury to the pulmonary endothelial cells was dependent both on early immune responses due to T cell activation as well as on later inflammatory processes through CD54 engagement. Finally, alveolar macrophages were shown to play a critical role in binding SEA within the lung mucosa and their ablation was associated with increased T cell activation and cytokine release. Altogether, these findings demonstrated the elaborate pathways involved in SEA-evoked inflammation. Understanding the mechanisms of *S. aureus* enterotoxin-induced systemic and pulmonary response may unravel novel therapeutic options for *S. aureus* infections.

Uncovering the Mechanisms of *Staphylococcus aureus* Enterotoxin A-Induced Systemic and Pulmonary Inflammation

By Julia Svedova

B.S., Trinity College (Hartford, CT), 2011

A Dissertation

Submitted in Partial Fulfillment of the

Requirements for the Degree of

Doctor of Philosophy

At the

University of Connecticut

2019

APPROVAL PAGE

Doctor of Philosophy Dissertation

Uncovering the Mechanisms of *Staphylococcus aureus* Enterotoxin A-induced Systemic and Pulmonary Inflammation

Presented by

Julia Svedova, B.S.

Major Advisor _____
Anthony T. Vella

Associate Advisor_____
Hector L. Aguila

Associate Advisor_____
Linda S. Cauley

Associate Advisor_____
Kamal M. Khanna

University of Connecticut
2019

Acknowledgments

I would like to thank my mentor, Dr. Anthony Vella, for teaching me how to think like a scientist. When I entered graduate school, my main goal was to learn how to independently design a hypothesis, how to test it, and how to interpret the results. I believe I learned all of that and much more. Thank you for being a supporting and patient mentor who didn't give up on me even when I was stubborn and emotional.

I would also like to thank my thesis committee and all of the past and current members of Dr. Vella's lab for their immense support, advice on experimental design and analysis, and assistance during data collection.

I would like to thank my family and friends who stood by me through all of the ups and downs of graduate school and always believed in me. Thank you for making time for me to talk and for listening to my complaints and frustrations.

Finally, I would thank my husband Joe Ryan, because his constant encouragement, help, and support were what kept me going each day through to the end. Thank you for making me laugh even when I was stressed and exhausted and for always making me see the light at the end of the tunnel while also stopping along the way to enjoy the view.

Table of Contents

List of Figures and Tables

Chapter 1: Introduction

General comments

Acute inflammation is a rapid and vital reaction to injury, trauma or infection. The goal of acute inflammatory response is to activate local cells (e.g. tissue macrophages or endothelium), recruit leukocytes and induce a milieu of pro- and anti-inflammatory mediators, which eventually leads to resolution of inflammation, healing and tissue regeneration. In certain instances, however, it may also result in further propagation of the inflammatory response and organ dysfunction (1). Typical examples of excessive inflammatory response causing tissue damage include systemic inflammatory response syndrome (SIRS) and the related sepsis as well as acute lung injury (ALI)/acute respiratory distress syndrome (ARDS). Understanding how acute inflammation is contained, how it subsides and how it becomes uncontrolled and exaggerated is crucial for the development of better therapeutic strategies.

A key cellular component of acute inflammatory response is the innate immune system, particularly, neutrophils, monocytes, and macrophages. These cells can be quickly activated and recruited to the site of injury. Furthermore, they can mount relatively nonspecific defense mechanisms against various inflammatory, nocuous, or alarm signals. These mechanisms include phagocytosis and release of reactive oxygen species, cytokines, chemokines, lytic enzymes and other mediators (2-4). Because of their ability to elicit a rapid and robust nonspecific immune response, innate immune cells are thought to be the mediators of tissue damage in cases of overly activated immune response, i.e. in SIRS/sepsis or ALI/ARDS. Thus, innate immune responses and particularly neutrophils have been targeted in many studies in order to develop novel treatments for these life-threatening conditions (5, 6). Unfortunately, there is currently no approved pharmacotherapy for the treatment of SIRS/sepsis and ALI/ARDS (7, 8). A part of the issue is undoubtedly the fact that these conditions have an overly complex etiology and pathophysiology, and they involve a plethora of villainous mediators. Thus,

targeting a single agent may not be sufficient to achieve therapeutic success in all patients. However, it is also likely that an important part of the immune response has been neglected over the years in the study of injurious, excessive inflammation: the adaptive immunity and particularly T cells.

Adaptive immune response is usually considered delayed compared to the innate immunity. Nevertheless, it can also induce a rapid and over-exuberant inflammation when stimulated with specific agents. This is particularly relevant in the case of superantigens. Superantigens, such as *S. aureus* enterotoxins, are known for their ability to trigger oligoclonal activation of T cells and a cytokine storm. This rapid T-cell mediated inflammatory response can cause serious organ injury and even death (9, 10). This work explores the mechanisms of *S. aureus* enterotoxin-induced inflammation and uncovers potential therapeutic targets. The first chapter introduces the topics of *S. aureus* enterotoxins, SIRS and ALI. The second chapter contains materials and methods used in the experimental studies. Chapter 3 investigates systemic inflammatory response in the context of *S. aureus* enterotoxin. Chapter 4 focuses on the mechanisms of pulmonary inflammation due to S. aureus enterotoxin. Chapter 5 explores the role of alveolar macrophages in *S. aureus* enterotoxin-induced inflammation. Finally, chapter 6 offers concluding remarks and future directions.

Staphylococcus aureus **and superantigens**

Staphylococcus aureus is a Gram-positive, facultative aerobe that colonizes anterior nares, pharynx, or skin in asymptomatic individuals. In fact, 20% (range 12-30%) of the general population has a persistent nasal carriage of *S. aureus* and 30% (range 16-70%) are intermittent carriers (11). However, in addition to being a commensal organism, *S. aureus* is also recognized as one of most significant causes of life-threatening infectious diseases in the United States (9, 12). In particular, the methicillin-resistant form of *S. aureus* (MRSA) poses a major threat in hospital settings (12, 13) and although the incidence of MRSA in the United

States has been declining likely due to better prevention strategies, it is currently estimated to cause over 80,000 cases of invasive infections annually (14). Because of its versatile virulence factors, *S. aureus* can evade the immune defenses of the host and cause a variety of infections: including benign soft tissue abscesses as well as life-threatening infections such as bacteremia and sepsis, pneumonia, endocarditis or osteomyelitis (12, 15). Among the wide array of secreted or surface-bound virulence factors is a group of toxins known as superantigens.

Superantigens, such as *S. aureus* enterotoxins, are nonglycosylated low-molecular-weight exotoxins (9). There are about 40 different bacterial superantigens that are typically produced by *S. aureus* or *Streptococci* species (10). Staphylococcal superatigens are usually encoded by accessory genetic elements, such as prophages, plasmids, transposons, or pathogenicity islands and thus, they are not uniformly present in all clinical isolates (10). Nevertheless, it has been reported that the majority of strains carry at least one superantigen gene (9, 16-18). The regulation of superantigen synthesis by the bacteria is currently not well understood but at least in the case of *S. aureus* enterotoxins it appears to be induced during or at the end of the exponential growth phase (19, 20).

Superantigens have a unique ability to bypass antigen processing and directly bind to the major histocompatibility complex class II (MHC II) of antigen presenting cells (APCs). In fact, even metabolically inactivated APCs are still capable of presenting a superantigen (21, 22). The binding of superantigens to MHC II is extremely stable and can generally occur through the α chain and in some cases also the β chain of MHC II (10). After directly binding to MHC II, superantigens can then crosslink it with specific Vβ chains of T cell receptors (TCRs). The engagement of Vβ chains is determined by the shallow cavity at the top of the protein (10, 23). Superantigens are also much more promiscuous compared to other antigens. Each superantigen can bind to several different Vβ regions; for example, in mice, *S. aureus* enterotoxin A (SEA) can bind to Vβ1, 3, 10, 11 and 17. Furthermore, whereas conventional antigens are restricted by MHC I and MHC II binding, superantigens can activate both $CD4^+$ and

$CD8^+$ T cells with a specific TCR Vβ chain (23). Thus, compared to conventional antigens which usually activate $1/10^4$-10^6 T cells, superantigens can stimulate up to 1/4 T cells (22). This rapid activation of a large number of T cells causes a cytokine storm and the elevated levels of IL-2, TNF and IFNγ in the bloodstream are generally believed to be the main cause of toxicity (10).

Furthermore, as the term "enterotoxin" indicates, some *S. aureus* enterotoxins possess a strong emetic activity and in fact, ingestion of superantigens is a major cause of food poisoning (24). The mechanism of emesis induction is not completely understood. However, the presence of a cystine loop seems be required for emetic activity while it appears to be independent of MHC II and TCR binding (9, 24), In addition to their ability to induce systemic or enteric toxicity, most superantigens are remarkably stable: they are resistant to heat, boiling, acids, proteolysis and dessication. Thus, their biological toxicity and environmental stability makes them extremely dangerous agents and some are currently categorized as potential weapons of bioterrorism (9).

Although all superantigens share their ability to stimulate a large number of T cells, they exhibit different binding properties to MHC II as well as different emetic activity depending on the presence of the cystine loop. These structural features can be used to separate superantigens into 5 groups. Table 1.1 represents categorization of staphylococcal superantigens (adapted from Spaulding et al. (9)). The ability to engage not only the α chain but also the β chain of MHC II appears to play a critical role in the overall potency. In particular, the second binding site to the β chain of MHC II also known as Zn^{2+}-dependent MHC II binding site increases the persistence of a superantigen on cell surface and may allow for crosslinking of adjacent APCs (25, 26). Thus, superantigens that bind both the α and the β chains of MHC II have about 10- to 100-fold greater toxicity compared to superantigens binding only to the α chain (9). Finally, recent studies identified two other important engagement sites for superantigens, the costimulatory receptor CD28 on T cells and its ligand CD86 on APCs (27, 28). Direct binding of a superantigen to these sites enhances the CD28/CD86 costimulation

axis and it appears to play a crucial role in the extent of T cell activation, cytokine storm and overall lethality due to a superantigen exposure (27-29).

Immune response to superantigens

The ability of superantigens like *S. aureus* enterotoxins to directly bind to MHC II molecules and bridge them with specific Vβ chains of TCRs triggers a potent immune response. First, the high affinity of superantigens for MHC II induces a rapid activation of T cells. In fact, as early as 1 h after SEA inhalation, the early T cell activation antigen CD69 was upregulated on about 80% of SEA-specific T cells in mediastinal lymph nodes (LNs) and by 5 h, about 80% of SEA-specific T cells were positive for both CD69 and IL-2 receptor, CD25 (30). Upon activation, T cells and APCs respond by releasing a number of different cytokines and chemokines. In particular, the production of IL-2, TNF, and IFNγ by T cells is a pronounced feature of a superantigen exposure (31-33). Together with other cytokines and chemokines, such as IL-6, IL-12, or CCL2 (34, 35), this so-called cytokine storm is thought to mediate the serious symptoms of toxic shock (10, 36).

Superantigens and particularly *S. aureus* enterotoxins were initially described as potent T cell mitogens (37, 38). Following activation, superantigen-specific T cell populations undergo 5-6 rounds of division, resulting in a significant accumulation of T cells (23, 34, 39, 40). For instance, in a model of SEA inhalation in mice, $V\beta3^+$ SEA-specific T cells underwent a massive expansion in all lymphoid tissues as well as the lung by 2 days after exposure. Apart from the actual numbers, the percentage of $V\beta3^+$ T cells in the spleen increased from about 3% to 30% of the total T cell population (39). In addition, superantigen-stimulated T cells exhibit effector and cytotoxic phenotype. In particular, 2 or 3 days following *S. aureus* enterotoxin exposure, $CD8^+$ T cells were shown to express high levels of IFNγ, granzyme B, and perforin (30, 39, 41) and their accumulation in lung was associated with increased cell number and protein concentration in the bronchoalveolar lavage (BAL) fluid, indicating tissue injury (39).

Following expansion, superantigen-specific T cells undergo clonal deletion or programmed death (42-45). The activation-induced cell death (AICD) due to *S. aureus* enterotoxin was found to only occur in proliferating T cells and the apoptotic cells upregulated CD95 (Fas) as well as CD178 (FasL) (46, 47). Interestingly, AICD could be prevented when mice were simultaneously exposed to bacterial lipopolysaccharide (LPS). The survival of T cells was dependent on TNF and to a lesser extent IFNγ and the rescued T cells were unresponsive to Fas engagement (48).

Not all specific T cells become deleted and these cells display an anergic phenotype (49-51), defined as inability to proliferate or produce cytokines upon restimulation (52). There are two proposed mechanisms of superantigen-induced T cell anergy: intrinsic and extrinsic. An intrinsic deficit is characterized as inert change in cell signaling or transcriptional activity. Several studies reported molecular changes in TCR signaling of anergic cells, particularly defective protein phosphorylation and altered function of transcriptional factor AP-1 (53, 54). The presence of an intrinsic anergic state was also shown using *in vivo* transfer experiments where anergic T cells transferred to a naïve recipient failed to proliferate upon *S. aureus* enterotoxin restimulation while naïve T cells transferred into an anergic recipient proliferated (55). In contrast, an extrinsic deficit would be attributed to an outside suppressor, such as cytokine or cell-to-cell contact. In particular, mechanistically, it was shown that anergy of $CD4^+$ T cells was dependent on the presence of myeloid cells, NO synthase activity, reactive oxygen species, and IFNγ (52, 56). An important source of IFNγ are $CD8^+$ T cells (39); indeed, $CD4^+$ T cell anergy was enforced by $CD8^+$ T cells (57). Furthermore, the unresponsiveness of superantigens could be attributed to immunosuppression due to augmentation of Treg population (58-60). Recently, it was also proposed that superantigen interaction with APCs not only induces pro-inflammatory responses but also plays a role in inducing unresponsiveness through increased expression of IL-10, programmed death ligand-1 (PD-L1), also immunosuppressive molecule indoleamine 2,3-dioxygenase - IDO (61).

Finally, it is important to note that there are some differences between human and mouse responses to superantigens. Human T cells are exquisitely sensitive to superantigens. In some cases, human T cells cultured *in vitro* can respond to 1 fg/mL of superantigen (10). Furthermore, it has been estimated that an amount of 0.0013 μg/kg of body weight could be life threatening to a human. In contrast, mice are quite resistant to superantigens and unless they are genetically modified or pre-treated with sensitizing agents, such as D-galactosamine, they do not generally develop symptoms of toxic shock or succumb to superantigens (62). Nevertheless, similarly to humans, murine immune system responds to superantigens by oligoclonal activation and expansion of T cells, cytokine release, as well as the subsequent T cell anergy (31-33, 40, 44, 63, 64). Thus, studying these responses can lead to a better understanding of the pathology and eventually to a development of novel treatments.

Role of superantigens in systemic and pulmonary diseases

Superantigens were initially associated with a condition known as toxic shock syndrome during its outbreak in children in the late 1970s (65). Since then, the involvement of superantigens in the pathology of various human diseases has been a focus of many studies. Some of the recognized illnesses linked to superantigens include food poisoning, atopic dermatitis, and allergic rhinitis (10). Recent evidence has also demonstrated a causal relationship between staphylococcal superantigens and *S. aureus* pneumonia and sepsis (9). These conditions are discussed below in greater detail.

Toxic shock syndrome

Toxic shock syndrome is a systemic response to superantigen exposure, particularly toxic shock syndrome toxin-1 (TSST-1) and *S. aureus* enterotoxins. By 1980, several studies reported development of toxic shock in young menstruating women, which was related to the use of high absorbency tampons and the presence of TSST-1 (9, 66-68). In contrast, non-

menstrual toxic shock syndrome may result from any primary *S. aureus* infection and can be caused by TSST-1 as well as *S. aureus* enterotoxin A, B, or C (36, 69). In addition, while there was no mortality in menstrual toxic shock syndrome, non-menstrual toxic shock syndrome cases had a mortality of 22% (70). The classical symptoms of toxic shock syndrome resemble influenza-like illness and include high fever, vomiting, diarrhea, headache, sore throat, myalgia, and erythematous, desquamating rash (10, 36). Following the outbreak of menstrual toxic shock syndrome in the 1980s, the incidence of the disease has been considered relatively low; however, it is likely that a lack of a diagnostic test and the stringent definition of characteristic symptoms lead to an underestimation of the actual rates (69).

Systemic inflammatory response syndrome and sepsis

SIRS and the related sepsis are devastating medical conditions with increasing incidence worldwide and no available pharmacotherapy (7). SIRS is a broad term used to define a group of systemic symptoms that occur as a physiologic response to a variety of acute insults, such as infection, trauma, hemorrhage or immune-mediated organ injury (71) . A recent study estimated that SIRS occurs in over 16 million adult patients in the emergency department within the United States annually (71). The symptoms of SIRS include tachycardia (heart rate >90 beats/min), tachypnea (respiratory rate >20 breaths/min or partial pressure of carbon dioxide $PaCO_2$ <32 mmHg), fever or hypothermia (temperature >38.5°C or <35°C) and changes in white blood cell count (WBC); either increase in WBC of more than 12,000 cells/mm^3 or decrease in WBC of less than 4000 cells/mm^3 (7, 72). Sepsis is often defined as SIRS in the presence of a known or suspected infection and is thought to affect more than 1,000,000 people in the United States every year (7, 73). Although recent advances in critical care reduced the overall rate of in-hospital deaths, the mortality due to sepsis remains unacceptably high with estimates between 20-30%. Furthermore, the surviving patients remain at increased risk for death even after recovery and may suffer from impaired physical and neurocognitive functioning (72).

The general mechanism of SIRS/sepsis pathophysiology is shown in Fig. 1.1. Following an inflammatory trigger, such as pneumonia, trauma or surgery, the immune system and specifically innate cells - neutrophils, monocytes and macrophages - become activated (e.g. through pattern recognition receptors) and trigger a robust inflammatory response, involving cytokines, chemokines, the complement system as well as platelets. Similarly, the adaptive immunity and particularly T cells can get stimulated upon interaction with APCs. Both pro- and anti-inflammatory factors can be released simultaneously; therefore, patients may present with either hyperinflammatory state (SIRS) or immunosuppressive state (compensatory anti-inflammatory response syndrome or CARS). These changes may be accompanied by coagulation abnormalities, which can manifest as disseminated intravascular coagulation (DIC) as well as impaired neuroendocrine regulation that normally controls aspects of immunosuppressive mechanisms. Together, these systemic responses can lead to increased oxidative stress, tissue hypoperfusion, and loss of barrier function (72, 74, 75). Tissue injury may lead to organ dysfunction and if several organs are involved (e.g. lung or kidney), it is known as multiple organ dysfunction syndrome (7). Finally, if patients suffer from hypotension refractory to fluid resuscitation, they are in septic shock, a serious condition with a high mortality rate (72).

While initially the predominant causative organisms were Gram-negative bacteria, more recent data demonstrated an increasing incidence of Gram-positive bacteria and fungi. In particular, Gram-positive bacteria were found in 37.6% of cases (76). Even more recently, a large epidemiologic study of serious infections in intensive care units found Gram-positive bacteria in 47% of patients with *S. aureus* present in 20% (77). In Gram-negative bacteria, LPS plays a dominant role in initiating the inflammatory cascade in sepsis. However, Gram-positive bacteria do not have LPS and possess other virulence factors, such as superantigens (78). In fact, superantigen-expressing *S. aureus* strains or superantigen proteins were found in septic patients, and the prevalence of SEA correlated with the severity of the disease (79-81). SEA

was also found in 25% of burn injury patients (population susceptible to serious infections and sepsis) and its presence increased the likelihood of mortality by 11% (82). Furthermore, a recent study demonstrated that neutralization of superantigen *S. aureus* enterotoxin K present in the common MRSA strain USA300 increased survival in an intravenous challenge model in mice (83). Similarly, neutralization of *S. aureus* enterotoxin B in a mouse model of MRSA infection prevented lethal sepsis and reduced skin tissue invasion and abscess formation (84). Finally, the presence of superantigen *S. aureus* enterotoxin C was critical in inducing tissue injury and driving lethality in a rabbit model of *S. aureus* sepsis (85).

Pneumonia, acute lung injury and acute respiratory distress syndrome

ALI/ARDS affects 200,000 adults in the United States annually and has a mortality of about 40% (86). Furthermore, a recent multinational epidemiologic study identified that over 10% of intensive care unit patients develop this devastating condition, suggesting that ALI/ARDS is largely underdiagnosed (87). ALI is characterized by bilateral pulmonary infiltrates with arterial hypoxemia due to accumulation of edema fluid and impaired gas exchange (the concentration of arterial oxygen divided by the inspired fraction of oxygen PaO_2/FiO_2 <300). If PaO_2/FiO_2 <200, the patient is diagnosed with ARDS (88). ALI/ARDS can be caused by direct (pulmonary) and indirect (extrapulmonary) causes. Direct causes include pneumonia, aspiration, pulmonary contusion, or toxic inhalation, whereas indirect causes include sepsis, extrathoracic trauma, burn injury, drug overdose, or pancreatitis (89). However, pneumonia and sepsis represent the most common triggers. The hallmark of ALI/ARDS pathology is increased vascular permeability due to endothelial injury. This is accompanied by injury to the lung epithelial cells, pulmonary edema, accumulation of red blood cells and immune cells in the lung tissue, particularly neutrophils, macrophages, and monocytes (88). The mechanism of ALI/ARDS is not fully understood; however, because of the significant neutrophil infiltration, neutrophils are often considered to be a critical part of the pathogenesis (88).

Despite a number of clinical trials, there is currently no pharmacotherapy for the treatment of ALI/ARDS. These included clinical trials testing treatments focused on inhibition of neutrophil and macrophage function, such as neutrophil elastase inhibitor or antioxidant N-acetylcysteine, and they showed no change in mortality (8). Thus, it is likely that other mechanisms are in place that may drive the pathology in ALI/ARDS. In particular, the role of T cells in the pathogenesis of ARDS is only now beginning to emerge (90). Previous studies demonstrated that there were elevated numbers of lymphocytes in the blood and BAL fluid of ALI/ARDS patients (91, 92). Furthermore, ALI/ARDS patients also showed an increase in a T cell specific cytokine IL-2 in the BAL fluid and its levels were correlated with increased mortality (93, 94). One potential explanation for the presence of T cells in ALI/ARDS is superantigens. In fact, the involvement of superantigens in a number of airway diseases, such as allergic rhinitis, nasal polyposis and asthma has been a focus of many studies (95). Moreover, recent reports demonstrated that preimmunization against superantigens prevented fatal necrotizing pneumonia in rabbits infected with a common USA200 MRSA strain (96, 97). Finally, aerosolized *S. aureus* enterotoxin caused serious pulmonary inflammation and death in 3 out of 6 rhesus monkeys (98). Unfortunately, there is currently a lack of human studies that would link superantigens to sepsis- or pneumonia-induced ALI/ARDS. Such studies will be necessary to confirm the role of superantigens in ALI/ARDS.

The model of *S. aureus* enterotoxin inhalation in mice

S. aureus enterotoxins and other superantigens are known to induce robust systemic responses, but how they spread systemically is not clear. One possibility is that they are directly produced in blood during *S. aureus* bacteremia. However, several studies demonstrated that hemoglobin peptides inhibit superantigen production by *S. aureus* (99, 100) and therefore, they likely disseminate systemically from focal sites of infection rather than being synthesized in the bloodstream by the bacteria (9). The anterior nares are known to be the most common

colonization site of *S. aureus,* which can be attributed to the route of transmission: *S. aureus* is commonly transferred from various surfaces by hands to the nasal niche via “nose picking” (11). Nasal carriage of *S. aureus* and particularly MRSA was shown to increase the risk of acquiring an infection with this pathogen 4-fold (101-103). Thus, inhalation of *S. aureus* enterotoxin may closely resemble the route of dissemination in humans. In fact, several reports of accidental exposure to aerosolized *S. aureus* enterotoxin in humans showed systemic symptoms of chills, headache, fever, myalgia, cough, dyspnea, vomiting and diarrhea (104).

In mice, *S. aureus* enterotoxin inhalation initiates an inflammatory cascade through systemic activation of specific T cells, accompanied by a robust cytokine release into circulation, including, IL-6, TNF or IFNγ. In addition to the systemic changes, *S. aureus* enterotoxin-specific αβ T cells in the lung induce IL-17 release by γδ T cells, which aids recruitment of neutrophils into the airways. This early systemic inflammatory response occurs within several hours after inhalation. By 48 h, *S. aureus* enterotoxin-specific T cells expand in all lymphoid tissues as well as the lung. The increased protein concentration and cell number in the BAL fluid (particularly, innate cells, NK cells and T cells) are indicative of pulmonary injury. Histologically, the lung tissue showed perivascular and peribronchial inflammation, disruption of terminal vessels, and accumulation of red blood cells, leukocytes and proteins (30, 34, 39, 105, 106). Although these studies highlighted key features of *S. aureus* enterotoxin-induced inflammation, there are many remaining questions. In particular, it is not known how *S. aureus* enterotoxin spreads systemically following inhalation, what is the crosstalk between the adaptive immune system and innate cells and how *S. aureus* enterotoxin drives lung injury and increased vascular permeability. The following studies investigate the mechanisms of systemic and pulmonary immune responses after SEA inhalation.

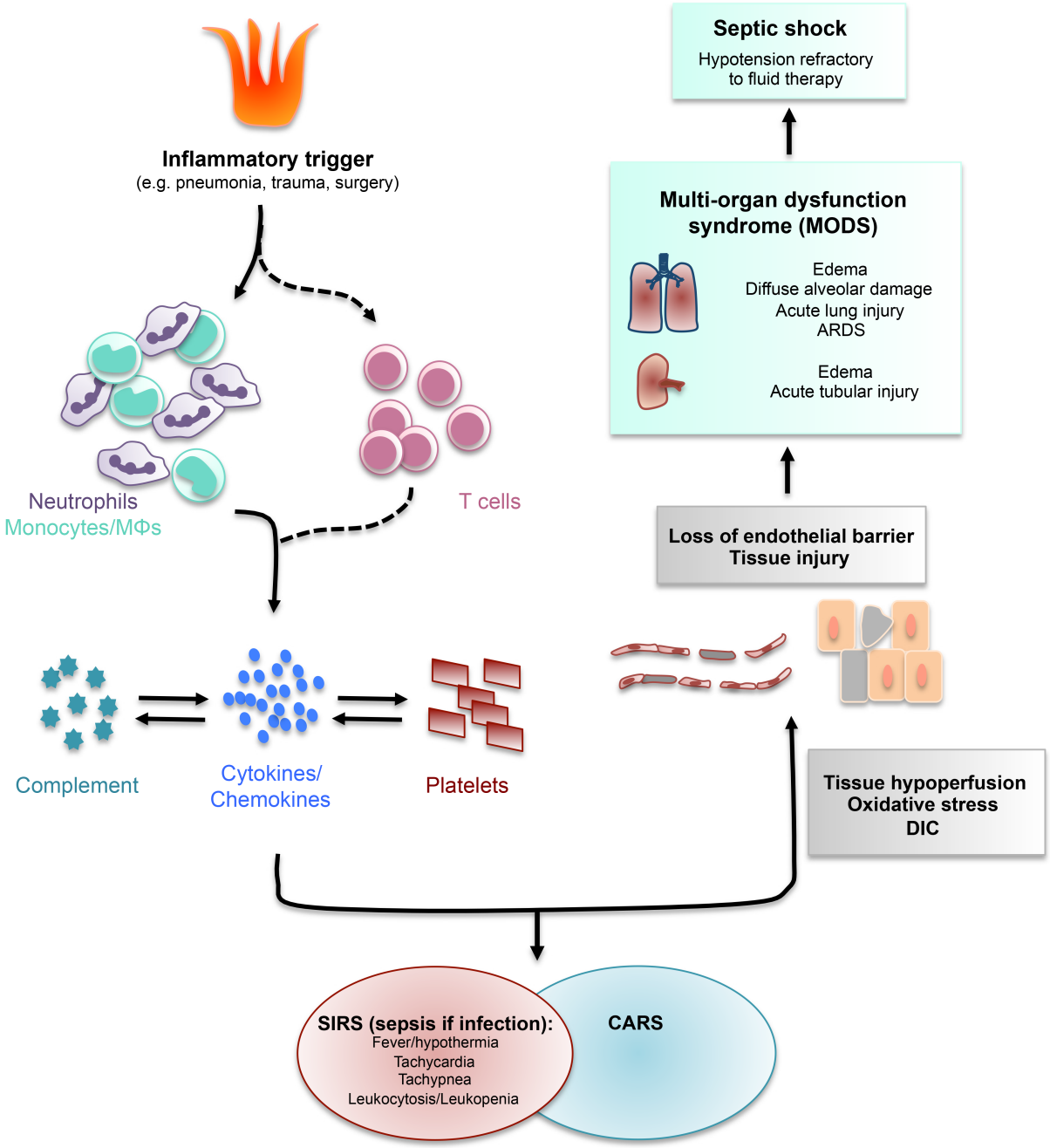

FIGURE 1.1: Diagram of general processes involved in sepsis. Sepsis can be triggered by a number of inflammatory stimuli, such as pneumonia, trauma, or surgery. The inflammatory trigger induces an overwhelming immune response (e.g. through pattern recognition receptors), particularly involving innate immune cells: neutrophils, monocytes and macrophages (MΦs).

Recent evidence suggests that T cells (particularly through superantigen-induced activation) may also play a critical role in the pathogenesis of sepsis. The activated immune cells release pro-inflammatory factors, cytokines and chemokines, which further activate platelets and the complement system. The resulting response triggers a state of hyperinflammation known as systemic inflammatory response syndrome (SIRS), which may be counterbalanced by a state of immunosuppression known as compensatory anti-inflammatory response syndrome (CARS). As a consequence of the increased inflammation, tissue and vasculature become injured due to oxidative stress, hypoperfusion, and disseminated intravascular coagulation (DIC). Multiple organs can be affected, including lung or kidney (multi-organ dysfunction syndrome; MODS). The vascular injury leads to hypotension, which if refractory to fluids is known as septic shock.

Group	Low affinity binding to α chain of MHC II	High affinity binding to β chain of MHC II	Presence of cystine loop	Representative superantigens
I	✔	✖	✖	TSST-1, SE-I X
II	✔	✖	✔	SEB, SEC, SEG, SE-I U, SE-I W, SPE A, SSA
III	✔	✔	✔	SEA, SED, SEE, SE-I H, SE-I J, SE-I N to SE-I P
IV	✔	✔	✖	SPE C, SPE G, SPE J, SMEZ
V	✔	✔	✖	SE-I I, SE-I K to SE-I M, SE-I Q to SE-I T, SE-I V, SPE H

TABLE 1.1: Categorization of superantigens. The table represents categorization of staphylococcal and streptococcal superantigens based on their structural properties. TSST-1 =

toxic shock syndrome toxin-1, SE = staphylococcal enterotoxin, SE-l = staphylococcal enterotoxin-like protein, SPE = streptococcal pyrogenic exotoxin, SSA = streptococcal superantigen, SMEZ = streptococcal mitogenic exotoxin Z. Adapted from Spaulding et al. (9).

Chapter 2: Materials and Methods

Mice

C57BL/6J (WT), MHC II$^{-/-}$, and TCR βδ$^{-/-}$ mice were obtained from Jackson Laboratory (Bar Harbor, Maine). CD169-DTR mice were a kind gift from Dr. Kamal M. Khanna (UConn Health, Department of Immunology, Farmington, CT). Mice were used between 1.5 and 4 months of age. All mice were kept in the Central Animal Facility at UConn Health in accordance with federal guidelines. All experimental procedures were approved by the Institutional Animal Care and Use Committee of UConn Health.

Toxin administration

To administer SEA, mice were anesthetized with isoflurane (Phoenix, St. Joseph, MO) in a vaporing chamber (Midmark, Versailles, OH). In most studies, 1 µg of SEA (Toxin Technology, Sarasota, FL) diluted in 50 µL of balanced salt solution (BSS) or BSS alone (vehicle) was pipetted on the nostrils (intranasal route – i.n.). In SEA titration experiments, 0.033 µg, 0.1 µg, 0.33 µg or 1 µg of SEA was administered i.n. as described before. The mice recovered from the anesthesia immediately after inhaling the toxin or vehicle control.

To ablate CD169^{+} cells in CD169-diphteria toxin receptor (DTR) mice, mice received 40 ng/g of body weight of diphtheria toxin (DT; Sigma-Aldrich) intraperitoneally (i.p.) 2 days before SEA or vehicle inhalation. Flow cytometry of the lung tissue was used to confirm cell depletion 2 days following DT injection.

Adoptive transfer

To adoptively transfer T cells, spleen and peripheral LNs (axillary, brachial, and inguinal) were collected from naïve WT mice. The tissue was passed through 100-µm strainer (Falcon/BD Biosciences) and RBCs were lysed with an ammonium chloride solution. The single cell

suspension was washed, re-suspended in 3 mL of BSS and then pipetted onto a nylon wool column. The column was then incubated at 37°C for 30 min. This step was repeated after pushing 3 mL of BSS through the column. The column was then flushed with BSS and the enriched cells were counted using Z1 particle counter (Beckman Coulter, Brea, CA). The purity of the cells was determined by flow cytometry (FACS LSRII; BD Biosciences). After anesthetizing mice with ketamine/xylazine solution (10 mg/mL of ketamine, 0.5 mg/mL of xylazine in PBS injected i.p. as 10μL/g of body weight), enriched T cells (~3.5×10^6 T cells) were adoptively transferred into TCR $\beta\delta^{-/-}$ recipient mice by retro-orbital injection as previously reported (30, 39).

In vivo antibody neutralization

For neutralization therapy experiments, mice received an i.p. injection of the following agents diluted in PBS:

TABLE 2-1: Antibodies used *in vivo.*

Antibody	Clone	Dose	Isotype control used	Source
Anti-4-1BBL	TKS-1	200 μg	Rat IgG_{2a}	BioXCell, Lebanon, NH
Anti-CD40L	MR1	500 μg	Hamster IgG	BioXCell
Anti-CD54	YN1/1.7.4	500 μg	Rat IgG	BioXCell
Anti-CD178	101626	250 μg	Rat IgG	R&D Systems, Minneapolis, MN
Anti-TNF	XT3.11	500 μg	Rat IgG	BioXCell
CTLA4-Ig*	N/A	200 μg	Mouse IgG	Dr. Robert Mittler (Department of Surgery and Emory Vaccine Center, Emory University, Atlanta, GA).
CTLA4-Ig**	N/A	250 μg	Rat IgG	Sigma-Aldrich, St. Louis, MO

* Used in experiments in chapter 1
** Used in experiments in chapter 2

Mouse IgG was from Sigma-Aldrich. Other isotype controls were obtained from BioXCell. All antibodies except anti-CD54 and anti-CD178 were administered 2 h prior to SEA inhalation. Anti-CD54 and anti-CD178 were given 36 h after SEA inhalation.

In vivo permeability assays

The *in vivo* permeability assays were performed using FITC-dextran similarly as described before (107, 108). To assess lung permeability from lung to blood, mice received 50 µL of FITC-dextran (3000 mW; 5 mg/mL; Life Technologies) i.n. and serum from tail blood was obtained 1 h later. For blood into lung permeability assay, mice received 100 µL of FITC-dextran i.v. through the retro-orbital route and BAL fluid was collected 1 h later. FITC fluorescence in the serum (1:70) or BAL fluid (undiluted) was determined by a plate reader (483-14/530-30; CLARIOstar, BMG LABTECH) and normalized either to the vehicle only-treated mice (Fig. 4-1) or the IgG-treated mice (Fig. 4-8).

Pan-caspase imaging

The amount of apoptosis in lung and spleen was detected by CAS-MAP™ near-infrared *in vivo* fluorescent imaging probe (Vergent Bioscience, Minneapolis, MN) according to the manufacturer's instructions. Briefly, the by CAS-MAP™ probe was i.v. injected 60-90 min prior to sacrifice. Lung and spleen were then imaged by Odyssey CLx Imager (LI-COR, Lincoln, NE).

Tissue harvest and processing

LNs and spleen

Airway-draining (mediastinal and cervical) and airway-non-draining LNs (axillary, brachial, inguinal and mesenteric) were harvested. LNs and spleen were crushed and passed through a 100-µm strainer (Falcon/BD Biosciences). RBCs were lysed with ammonium chloride solution.

BM

BM was flushed out with a 10 mL-syringe filled with BSS from one femur and tibia until no remaining tissue was observed. The tissue was passed through a 100-μm strainer and RBCs were lysed.

Peripheral blood

Mice were warmed up with a heat lamp for 3 min and peripheral blood was obtained by making a small incision on their tail. For serum, the blood was collected into serum separator tubes (BD Biosciences). For blood cells, 3-4 drops of blood were collected into BSS-heparin solution (0.411g/L; Sigma-Aldrich). The cells were washed and RBCs were lysed with ammonium chloride solution. This step was repeated to remove remaining RBCs.

Lung

Mice were sacrificed with an i.p. injection of ketamine. The lung tissue was perfused with PBS by inserting a butterfly needle through the heart. Alternatively, in experiments in which BAL fluid was collected, lung tissue was harvested without perfusion. The tissue was then dissected into small pieces, placed in a conical flask containing 20 mL of collagenase solution (150 U/mL collagenase (Sigma-Aldrich), 60 U/mL DNAse I (Sigma-Aldrich), 2% FBS, 1 mM Ca_2Cl, 1 mM Mg_2Cl), and left spinning at 230 rpm for 30 min at 37°C. The tissue was passed through a 100-μm strainer and RBCs were lysed with ammonium chloride solution and counted.

BAL fluid

The mice were sacrificed with an i.p. injection of ketamine. The thoracic cavity was exposed and a small incision was made into the upper portion of the trachea. A syringe containing 2 mL of PBS attached to polyethylene tubing (0.58x0.97 mm; Instech Laboratories, Inc., Plymouth Meeting, PA) was inserted into the trachea and secured with a thread. The lungs were then gently lavaged by injecting PBS into the tissue until fully expanded. The lavage was repeated 2-3 more times.

Flow cytometry

Surface staining for flow cytometry was performed as described previously (30). Single cell suspensions were counted with Z1 particle counter (Beckman Coulter, Brea, CA). Unspecific binding was blocked with FcR blocking solution (culture supernatant from 2.4.G.2 hybridoma, 5% mouse serum (Sigma-Aldrich), 10 µg/mL human IgG (Sigma-Aldrich), 0.1% sodium azide) and stained with antibodies and LIVE/DEAD® Fixable Blue Dead Cell Stain (Life Technologies, Grand Island, NY) for 30-45 min on ice. For intracellular staining, cells were cultured with brefeldin A (1 µg/mL; Calbiochem, San Diego, CA) and with or without PMA (50 ng/mL, Calbiochem)/ ionomycin (1 µg/mL, Fisher Scientific) for 5 h. The cells were stained with surface antibodies, fixed in 2% formaldehyde, permeabilized with 0.25% saponin and stained with intracellular antibodies overnight at 4°C. Flow cytometry was performed using a FACS-LSRII (BD Biosciences) and the data was analyzed with FlowJo software (Tree Star, Ashland, OR). Antibody-stained positive cells were determined with corresponding isotype controls. Fluorochrome-conjugated antibodies were obtained from BD Biosciences (San Jose, CA), eBioscience (San Diego, CA), or BioLegend (San Diego, CA). The following fluorochrome-conjugated antibodies were used:

TABLE 2-2: Flow cytometry antibodies and the clones.

Antibody	Clone
anti-CD3	145-2C11 or 17A2
anti-CD19	1D3
anti-CD8a	53-6.7
anti-B220	RA3-6B2
anti-NK1.1	PK136
anti-CD49b	DX5
anti-Ly6G	1A8
anti-Ly6C	HK1.4
anti-CD11c	HL3 or N418
anti-Vβ3	KJ25

anti-Vβ14	14-2
anti-CD25	PC61
anti-CD69	H1.2F3
anti-MHC II	M5/114.15.2
anti-F4/80	BM8
anti-CD103	2E7
anti-CD11b	M1/70
ant-CD45.2 (shown as CD45)	104
anti-CD31	390
anti-CD54	YN1/1.7.4

anti-granzyme B	NGZB
anti-CD95	Jo2
anti-CD11a	H155-78
anti-IFN-γ	XMG1.2
anti-SIGLEC F	E50-2440
anti-CD169	SER-4

Staining for SEA was performed with polyclonal anti-SEA antibody produced in rabbit (whole antiserum; Sigma-Aldrich) followed by secondary rabbit IgG Alexa Fluor 488 (Life Technologies).

Cell sorting

For T cell sorting, LNs (cervical, mediastinal, axillary, brachial, inguinal, and mesenteric) were collected and processed as described above. For sorting of dendritic cells (DCs), the LN tissue was digested with collagenase solution (150 U/mL collagenase (Sigma-Aldrich), 2% FBS in MEM) for 30 min at 37°C and 5% CO_2. After tissue digestion, 100 µL of 0.1M EDTA in PBS per 1 mL of collagenase solution was added. The tissue was then passed through a 100-µm strainer and washed in 5 mM EDTA and 2% FBS Ca^{2+}/Mg^{2+} free BSS. For endothelial cell sorting, lung tissue was prepared as described above. After FcR blocking and antibody staining, cells were sorted with FACS Aria (BD Biosciences).

CyTOF

Lungs were obtained from mice 14 or 40 h after SEA or vehicle inhalation, digested with collagenase/DNAse solution and purified using Lympholyte M (Cedarlane Labs, Burlington, NC). Each one of the 4 samples was labeled with Cell-ID™ Cisplatin to identify live and dead cells and subsequently barcoded with Cell-ID™ Pd Barcoding kit (all CyTOF reagents are from Fluidigm, San Francisco, CA). The 4 samples were pooled together, permeabilized with methanol, and incubated with Fc receptor blocking solution and 24 heavy metal-conjugated antibodies, including 7 signaling markers. DNA was labeled using Cell-ID™ Intercalator-Ir. The pooled sample was spiked with normalization beads and analyzed by a mass cytometer (Helios, Fluidigm). The data were de-barcoded using the Fluidigm Debarcoder v1.04. A single cell and live cell gate were obtained from each sample. The samples were further sub-gated to include the same number of cells per sample and merged to create ViSNE maps (MATLAB, MathWorks, Natick, MA) using only the non-

signaling markers. Histograms comparing the expression of signaling and activation markers were generated using MATLAB. Median intensity values were obtained by FlowJo software.

Co-culture assays

To obtain naïve T cells, spleen and LNs were harvested from a naïve mouse and processed as described above. To enrich the population of $V\beta3^+$ T cells, the cells were depleted using anti-B220 clone RA3-6B2, anti-NK1.1 clone PK136, anti-Vβ2 clone B20.6, anti-Vβ4 clone KT-4, anti-Vβ5.1,5.2 clone MR9-4, anti-V6β clone RR4-7 and anti-Vβ8 clone F23.1 biotin-conjugated antibodies (eBioscience and BD Biosciences) and anti-biotin magnetic beads (Miltenyi Biotec Inc, Auburn, CA). For co-culture of T cells with serum or blood cells, tail blood was obtained 10 or 30 min after SEA or vehicle inhalation into either heparin-containing BSS or serum separator tubes (BD Biosciences). Blood cells were processed as described above. Next, the enriched T cells (100,000/well) were incubated with either cells derived from the blood (25,000/well) or the isolated serum (diluted 1:4 in culture medium) overnight at 37°C and 5% CO_2. For co-culture of T cells with DC subpopulations, LNs (mediastinal, cervical, axillary, brachial, inguinal) were collected 40 min after SEA or vehicle inhalation and processed as described above. The cells were enriched for DCs by depleting $B220^+$ and $Thy1.2^+$ cells using Dynabeads (Life Technologies), stained and sorted. The sorted DC subpopulations (5,000/well) were incubated with naïve enriched T cells (20,000/well) overnight at 37°C and 5% CO_2. After the culture, supernatants were collected to measure IL-2 concentration by ELISA (BD Biosciences) and the cells were washed and stained for flow cytometry as described above.

ELISA and multiplex assays

Serum was obtained from tail blood by using the serum separator tubes (BD Biosciences). BAL fluid was collected as described above. The isolated serum and BAL fluid were stored at −80°C. ELISAs for albumin (Bethyl Laboratories, Montgomery, TX), CD54, angiopoietin-2,

receptor for advanced glycation end products (RAGE), granzyme B (R&D Systems) and cytokine ELISAs for IL-6, TNF and IFN-γ (BD Biosciences) were performed according to the manufacturer's instructions.

For the multiplex assay of LN lysates (see chapter 3), LNs were isolated from mice 4 or 16 h after SEA or vehicle exposure. The tissue was placed in MagNA Lyser green beads tubes (Roche, Basel, Switzerland) filled with 400 µL PBS containing Protease Inhibitor Cocktail (Sigma-Aldrich) and lysed using MagNA Lyser Instrument (Roche) at 6,000 rpm for 1 min. The lysates were stored in −80°C. Chemokine and cytokine expressions were measured with customized Luminex® -based multiplex assay (EMD Millipore, Billerica, MA). The expression of individual chemokines and cytokines was normalized to the protein concentration measured by the Pierce BCA protein assay kit (Thermo Scientific, Rockford, IL). Bio-Plex Pro™ Mouse Cytokine 23-plex Assay (Biorad) was used to measure the time course of cytokine and chemokine release in serum and BAL fluid (see chapter 4).

Quantitative real-time PCR and RNA sequencing

For quantitative real-time PCR (qRT-PCR) analyses of the whole tissue, LNs from SEA or vehicle-exposed mice were removed, frozen on dry ice and stored at −80°C. To acquire RNA, the whole tissue was snap-frozen in liquid nitrogen and crushed into powder. The total RNA was isolated from the LN tissue or sorted cells with RNeasy Mini Kit (Qiagen, Valencia, CA) and converted to cDNA using iScript cDNA Synthesis Kit (Biorad, Hercules, CA). mRNA expression level of target genes and the endogenous control gene *β-actin* or *Gapdh* were assessed by real-time PCR using Taqman primers (Life Technologies) and a CFX96 Real-Time PCR instrument (Biorad). Each sample was run in duplicate and the gene expression was normalized to *β-actin* or *Gapdh* using the standard curve method.

For RNA sequencing, total LN cells (isolated from cervical, mediastinal, axillary, brachial, inguinal, and mesenteric LNs) were collected 40 min after SEA or vehicle inhalation. The

cells were sorted and mRNA was acquired as described above. Total RNA was sequenced (Otogenetics, Norcross, GA) and transcriptomes from SEA Vβ3$^+$ T cells were compared to transcriptomes from vehicle Vβ3$^+$ T cells and SEA Vβ14$^+$ T cells (control groups). Genes in SEA Vβ3$^+$ cells that were downregulated ($\log_2$ fold change ≤ −1.5) or upregulated ($\log_2$ fold change ≥ +1.5) were compared to control groups in all three experiments were selected. The selected list of genes was further examined and any genes with inconsistent or close to zero expressions removed. Gene expressions patterns in the selected genes were analyzed using Gene set enrichment analysis (GSEA, Broad Institute, Cambridge, MA). The following gene set databases were used: h.all.v5.0.symbols.gmt and c5.all.v5.0.symbols.gmt (http://www.broadinstitute.org/gsea/msigdb/index.jsp). To construct heat maps, gene expressions were corrected to $\log_2$ and processed using GENE-E software (Broad Institute). The RNA sequencing data can be viewed online (http://www.ncbi.nlm.nih.gov/geo/; accession number: GSE76190).

Confocal microscopy

Whole cervical LNs or lung was fixed in periodate-lysine-paraformaldehyde (PLP) solution (1 μM sodium periodate, 75 mM L-lysine, 1% paraformaldehyde in phosphate buffer) at 4°C overnight. The tissue was washed in phosphate buffer, left in 30% sucrose at 4°C overnight, frozen in OCT and stored at −80°C. The frozen tissue was cut into 20 μm-thick sections with LEICA CM1850 cryostat (Leica Biosystems, Buffalo Grove, IL) and the sections were stored at −20°C. For antibody staining, the sections were firstly blocked for unspecific binding using a staining buffer (either 2% FBS in PBS or 2% FBS, 2% goat serum, 0.5% FcR blocking solution, 0.05% Tween-20, 0.3% Tritone-X100 in PBS) for 1 h at RT and then stained with primary antibodies diluted in the staining buffer for 1 h at RT. The sections were examined with Zeiss LSM780 confocal microscope mounted on an inverted Axio Observer Z1 (Zeiss, Oberkochen, Germany). Immunofluorescent staining was performed with the following antibodies: DyLight 488-conjugated anti-Ly6B.2 clone 7/4 (labeled as 7/4; Novus

Biologicals, Littleton, CO), V450-conjugated anti-CD11b clone M1/70, PE-conjugated anti-Vβ3 clone KJ25, allophycocyanin-conjugated anti-CD11c clone HL3, PE-conjugated anti-active caspase-3 clone C92-605 (all from BD Biosciences), eFlour 660-conjugated anti-CD169 clone SER-4, allophycocyanin-conjugated MHC II clone M5/114.15.2 (both from eBioscience). SEA staining was performed with polyclonal anti-SEA antibody (whole rabbit antiserum; Sigma-Aldrich) followed by Alexa Flour 488-conjugated anti-rabbit IgG staining. B cell follicles in LNs were determined with Pacitic Orange-conjugated anti-B220 clone RA3-6B2 (not shown in images; Life Technologies). The images represent confocal z-stack projections, which were acquired using 20×/0.8 numerical aperture objective. Image analysis, including adjustment for contrast and brightness and cellular quantification, was done with Imaris software (Bitplane, Zurich, Switzerland). The number of active caspase-3^+ cells in the SEA-exposed mice was only determined in loci of increased inflammation (areas with an increased number of inflammatory cells). No such areas were found in the vehicle control. Colocalization studies that measured the percentage of cells positive for multiple markers were completed by Imaris with threshold value for colocalization set to 7.

Statistical analysis

The following tests were used to determine statistical significance ($p<0.05$): one-way ANOVA (with Dunnett's or Tukey's multiple comparisons tests), two-way ANOVA (with Sidak's multiple comparisons test), two-tailed Student's unpaired *t* test or paired *t* test. All statistical tests were performed using Prism-GraphPad (La Jolla, CA) and Microsoft Excel.

Chapter 3: Systemic Inflammatory Response Following *S. aureus* Enterotoxin A Inhalation

This work was published in the *Journal of Immunology*, vol. 196, issue 11, pp. 4510-4521, June 1, 2016 under the title "TNF and CD28 Signaling Play Unique but Complementary Roles in the Systemic Recruitment of Innate Immune Cells after *Staphylococcus aureus* Enterotoxin A Inhalation" and was authored by: Julia Svedova, Naomi Tsurutani, Wenhai Liu, Kamal M. Khanna, and Anthony T. Vella.
Some modifications to the original text were done to accommodate additional figures and tables used to supplement this chapter.

Abstract

Staphylococcus aureus enterotoxins cause debilitating systemic inflammatory responses, but how they spread systemically and trigger inflammatory cascade is unclear. Here, we showed in mice that after inhalation, *Staphylococcus aureus* enterotoxin A rapidly entered the bloodstream and induced T cells to orchestrate systemic recruitment of inflammatory monocytes and neutrophils. To study the mechanism used by specific T cells that mediate this process, a systems approach revealed inducible and non-inducible pathways as potential targets. It was found that TNF caused neutrophil entry into the peripheral blood, while CD28 signaling, but not TNF, was needed for chemotaxis of inflammatory monocytes into blood and lymphoid tissue. However, both pathways triggered local recruitment of neutrophils into lymph nodes. Thus, our findings revealed a dual mechanism of monocyte and neutrophil recruitment by T cells relying on overlapping and non-overlapping roles for the non-inducible costimulatory receptor CD28 and the inflammatory cytokine TNF. During

sepsis, there might be clinical value in inhibiting CD28 signaling to decrease T cell-mediated inflammation and recruitment of innate cells while retaining bioactive TNF to foster neutrophil circulation.

Introduction

Staphylococcus aureus (*S. aureus*) is a part of normal human flora colonizing skin, nasopharynx and most commonly the anterior nares of the nose in almost 30% of the general population (11). A recent epidemiological study showed that Gram-positive bacteria were found in 47% of intensive care unit patients with an infection, with *S. aureus* present in 20% of positive cultures (77). Infection and related sepsis are one of the leading causes of death in the United States (3). Sepsis, characterized as systemic inflammatory response syndrome (SIRS) with a known or suspected infection, is a result of a dysregulated immune response, commonly accompanied by an uncontrolled release of cytokines that can lead to systemic tissue injury, shock and even death (7). Methicillin-resistant *S. aureus* is particularly well spread in hospital settings and is associated with key virulence factors that may contribute to the severity and rapidity of sepsis (13). One such virulence factor is superantigens, such as *S. aureus* enterotoxins. These are heat resistant proteins that bypass classical antigen processing and presentation to mediate powerful oligoclonal T cell receptor Vβ chain-specific responses (110, 111) leading to toxic shock syndrome and potentially death (32, 112-114).

A recent study showed that the presence of an enterotoxin was essential for the lethality of *S. aureus*-induced sepsis in rabbits (85). In addition, superantigens can synergize with TLR4 or TLR2 agonists and enhance the inflammatory response and the induction of lethal shock in mice (115, 116). Superantigens have been found in blood of septic patients and their prevalence, in particular prevalence of *S. aureus* enterotoxin A (SEA), was correlated with severity of infection (79, 80, 117). Therefore, it is likely that the presence of

S. aureus enterotoxins drives or at least significantly exacerbates the inflammatory response in septic patients. It is still unclear, however, how *S. aureus* enterotoxins spread systemically especially in cases of an unknown entry point and how they trigger both adaptive and innate immunity to propagate systemic inflammation.

Mice exposed to *S. aureus* enterotoxins reproduce several important hallmarks of SIRS/sepsis in humans, including a rapid-onset immune response with a robust cytokine release (10, 111) and an immunosuppression/anergy phase (52, 118, 119) similar to the compensatory anti-inflammatory response syndrome (CARS) that often occurs in septic patients (120). Furthermore, SEA inhalation also recapitulates a common complication in sepsis, acute lung injury. The lungs of exposed mice show elevated proteins, presence of red blood cells and increased levels of cytokines (39, 106). Using the SEA model of SIRS, we sought to study systemic immune responses occurring immediately after SEA administration. The pulmonary SEA challenge resulted in a rapid release of monocytes and neutrophils to blood and their accumulation in lymphoid tissues. Remarkably, this inflammatory innate cell migration was dependent on the presence of T cells. In particular, the systemic recruitment of monocytes and neutrophils was dually regulated by T-cell based CD28 signaling and the inflammatory cytokine TNF.

Results

Systemic recruitment of monocytes and neutrophils is observed rapidly after SEA inhalation

SEA inhalation results in alveolitis characterized by increased protein content, presence of RBCs, secretion of cytokines, and accumulation of monocytes and neutrophils (30, 39). The local lung response is coincident with an expansion of SEA-specific T cells in all lymphoid tissues (39). To understand how SEA inhalation causes a systemic response, serum and blood cells were isolated immediately after SEA or vehicle challenge and

incubated with enriched naïve T cells. Cells derived from blood after SEA or vehicle inhalation and serum from vehicle mice did not affect T cell activation (Fig. 3-1, A and B; data not shown). However, serum obtained only 10 min after SEA inhalation was able to activate SEA-specific $V\beta3^+$ T cells to express CD69 and CD25 while having little effect on bystander $V\beta14^+$ T cells (Fig. 3-1, A and B). The same type of response was observed when the naïve T cells were incubated with SEA (Fig. 3-2). Finally, only T cells co-cultured with serum from SEA mice produced IL-2 (Fig. 3-1, C). To estimate the amount of SEA that was found in the serum upon inhalation, enriched naïve T cells were co-cultured with increasing concentrations of SEA overnight and the level of T cell activation was assessed by flow cytometry. Fig. 3-2 represents titration curves of CD69 and CD25 expression on SEA-specific $V\beta3^+$ T cells and bystander $V\beta14^+$ T cells. The titration curves were then used to extrapolate the concentration of SEA in the serum of mice 10 min after SEA inhalation (dotted line – value obtained from Fig. 1A and B). Because the serum was diluted 1:4 when added to culture, the concentration of SEA in the serum was estimated to be between ~12 and 28 ng/mL of blood (Fig. 3-2; red arrow values multiplied by 4). Interestingly, this concentration was only a fraction of the amount administered i.n. to each mouse (1 µg). Thus, SEA can rapidly enter the bloodstream after inhalation in small but sufficient quantities to activate T cells.

The rapid spread of the enterotoxin after inhalation through blood posed the question of whether the systemic inflammatory response to SEA was accompanied by a common hallmark of SIRS and sepsis, blood leukocytosis (7). To test if SEA inhalation mediates systemic circulation of innate immune cells, mice were challenged with SEA or vehicle alone and then the peripheral blood cells were analyzed for the presence of monocytes or neutrophils. Inflammatory monocytes were identified as $CD3^-CD19^-CD11b^+Ly6G^-Ly6C^{hi}$ while neutrophils were identified as $CD3^-CD19^-CD11b^+Ly6G^+Ly6C^+$ (Fig. 3-3, A). The percent of neutrophils in blood increased 6.4-fold 2 h after SEA challenge compared to vehicle while there was no relative increase in monocytes (Fig. 3-3, B). Nevertheless, both

populations were increased 4 h after SEA inhalation. SEA-based inflammation is dependent on T cells, which are found in lymphoid tissues (39). Therefore, it was hypothesized that the circulating inflammatory innate cells would migrate to the LNs and spleen. Indeed, the percent of inflammatory monocytes and neutrophils at 4 h after SEA inhalation was increased in spleen, mediastinal, cervical, and non-draining LNs compared to vehicle control (Fig. 3-3, C). Inflammatory monocytes remained elevated at 12 h whereas the percent of neutrophils decreased to the level of vehicle-treated mice. Like percentages, the same trends were observed when assessing the absolute numbers of inflammatory monocytes and neutrophils (data not shown). The recruited monocytes likely originated from the BM because there was a depletion of BM inflammatory monocytes reaching over 50% reduction compared to the vehicle control by 4 h after SEA inhalation (Fig. 3-3, D). Interestingly, SEA challenge caused only a small decline in the number of BM neutrophils. In sum, SEA inhalation resulted in rapid systemic recruitment of monocytes and neutrophils to blood and lymphoid tissues.

The recruitment of innate immune cells after SEA inhalation is guided by T cells to the T cell zone of the LNs

SEA inhalation induces monocyte and neutrophil migration to lungs in a T cell dependent manner (30). To determine the role of T cells in the systemic recruitment of innate immune cells to blood and LNs, TCR $\beta\delta^{-/-}$ mice, that lack both αβ and γδ T cells, received C57BL/6J T cells or nothing and subsequently, they were i.n. challenged with SEA or vehicle. In the absence of T cell transfer, cervical LNs and blood from SEA-treated mice showed no difference in accumulation of monocytes or neutrophils compared to the vehicle group (Fig. 3-4). However, SEA-challenged TCR $\beta\delta^{-/-}$ mice that received T cells had significant increases in the percent of both monocytes and neutrophils compared to vehicle alone (Fig. 3-4). Thus, T cells were required to trigger the systemic recruitment of inflammatory innate immune cells to blood and LNs after inhalation of SEA.

Migration of neutrophils and monocytes to LNs was previously reported (121-127). However, while some studies showed that following an infection or antigen challenge, neutrophils were recruited to the subcapsular sinus (121, 124), others found innate immune cells in the T cell zone (125, 127). To determine where the recruited cells accumulated, cervical LNs were collected 1, 2, and 4 h after SEA inhalation and examined by confocal microscopy. Inflammatory innate immune cells ($CD11b^+7/4^+$) were detected in the LNs as early as 2 h after SEA but not in the vehicle control (Fig. 3-5, A). By 4 h, the quantity of inflammatory innate immune cells increased even further, which was confirmed by enumerating $7/4^+$ cells per field (Fig. 3-5, B). Importantly, the recruited cells were primarily in the T cell zone of the LNs whereas the few inflammatory cells in the vehicle alone mice were mostly located in the subcapsular sinus and B cell follicles (Fig. 3-5, C). These findings demonstrate that SEA inhalation induced recruitment of monocytes and neutrophils particularly to the T cell zone in the LNs where the SEA-specific T cells become activated.

SEA inhalation triggers a rapid release of specific chemokines by both T cells and dendritic cells

Monocyte and neutrophil migration can be driven by a number of chemokines (128-130). To understand which chemotactic factors might play a role in the systemic recruitment of monocytes and neutrophils, total RNA was isolated from draining LNs (cervical and mediastinal) to assess the expression of various chemokine genes. Compared to vehicle, expression of multiple chemotactic factors increased as early as 1 h after SEA inhalation (Suppl. Fig. 2A). Interestingly, mRNA levels of chemokines particularly important for the recruitment of neutrophils and monocytes – *Cxcl1*, *Cxcl2*, *Ccl2*, *Ccl3*, *Ccl4*, and *Ccl7* (128, 130) showed a rapid increase in expression peaking at 2 h (Fig. 3-6, A; clear bar graphs). To validate these findings, LN lysates were examined for the protein levels of these chemokines by a multiplex assay. Multiple chemokines were significantly elevated 4 h after SEA inhalation, including 38-fold for CXCL1, 792-fold for CXCL2, 53-fold for CCL2, 46-fold

for CCL3 and 92-fold for CCL4 (Fig. 3-6. B). Nevertheless, the increased chemokine levels were transient because by 16 h after SEA challenge, they were already decreasing. In addition, the expression of chemotactic factors was systemic as SEA challenge caused a similar increase in chemokine levels in draining LNs, peripheral LNs, and mesenteric LNs (data not shown). We previously showed that SEA-activated αβ T cells directed γδ T cells to release IL-17, which contributed to the recruitment of neutrophils to lungs after SEA inhalation (30). Therefore, we assayed for IL-17, but only a small increase was detected in the LN lysates of the SEA group compared to vehicle (Fig. 3-6, B, bottom panel).

Because SEA can directly crosslink MHC class II (MHC II) molecules on antigen-presenting cells and Vβ chains of the TCR (22), we hypothesized that DCs and T cells were an important source of chemokines recruiting monocytes and neutrophils. Therefore, $Lin^{-}CD11c^{+}MHC\ II^{+}$ DCs were sorted and the relative expression of chemokines was determined. DCs from SEA-challenged mice upregulated *Cxcl1* and *Cxcl2* mRNA levels but not *Ccl3* and *Ccl4* compared to DCs from the vehicle group (Fig. 3-7, A). Interestingly, SEA-activated $Vβ3^{+}$ T cells but not bystander $Vβ14^{+}$ T cells substantially expressed *Ccl3* and *Ccl4*, in particular, 680-fold and 738-fold increases compared to vehicle, respectively (Fig. 3-7, B). DCs are heterogeneous and thus, to understand if a specific subset was critical, $CD11c^{low}MHC\ II^{hi}$ migratory DCs and $CD11c^{hi}MHC\ II^{low}$ resident DCs (131, 132) were sorted (Fig. 3-7, C). Migratory DCs expressed more *Cxcl1* and *Cxcl2* as normalized to *β-actin* expression than the resident DCs (Fig. 3-7, D). To summarize, SEA inhalation induced rapid production of chemokines by SEA-activated T cells and DCs (predominatly migratory DCs).

To see if the differential chemokine expression in the DC subpopulations was due to their ability to present SEA, we tested if either migratory DC ($Lin^{-}CD11c^{low}MHC\ II^{hi}$) or resident DC ($Lin^{-}CD11c^{hi}MHC\ II^{low}$) subpopulations were preferentially stimulating the SEA-specific T cells. In particular, four distinct DC subpopulations were sorted from either SEA or vehicle-immunized mice (Fig. 3-8, A) and without adding SEA, the sorted DC subpopulations were cultured with naïve T cells. Both $CD11b^{+}$ and $CD103^{+}$ migratory DCs

from the SEA-immunized mice, but not resident DCs, activated Vβ3$^+$ T cells to upregulate CD69 (Fig. 3-8, B). There was no difference in CD69 expression on the bystander Vβ14$^+$ T cells when cultured with DCs from SEA-immunized mice compared to the vehicle control. These findings show that that only migratory DCs presented SEA *ex vivo* to naïve SEA-specific T cells.

Mechanism of T cell guided innate cell recruitment

To determine the mechanism of how SEA-activated T cells promote chemokine production by DCs, SEA-specific Vβ3$^+$ and bystander Vβ14$^+$ T cells were sorted 40 min after SEA or vehicle inhalation and RNA was isolated for transcriptome analysis (Fig. 3-9, A). Comparing RNA from SEA Vβ3$^+$ T cells to vehicle Vβ3$^+$ or SEA Vβ14$^+$ control groups, many genes were found to be upregulated in the SEA-specific Vβ3$^+$ T cells (Fig. 3-9, B; Table 3-1). Gene expression increases were predominantly associated with cell development, proliferation, and regulation of metabolic processes. However, GSEA also revealed a significant association with apoptosis and negative regulation of cells (Fig. 3-9. C). In addition, both pro- (*Tnf*, *Il2*, *Ifng*) and anti-inflammatory cytokines (*Il10*) were upregulated in Vβ3$^+$ T cells from the SEA-treated group suggesting a role for T cell costimulation (Fig. 3-9, D).

The expression of inducible as well as constitutively expressed costimulatory molecules were compared. While there was no difference in the expression of constitutively expressed costimulatory molecules, five inducible costimulatory molecules were significantly upregulated in SEA Vβ3$^+$ T cells, including 4-1BBL (*Tnfsf9*), LIGHT (*Tnfsf14*), CD40L (*Cd40lg*), SLAM (*Slamf1*), and TWEAK receptor (*Tnfrsf12a*) (Fig. 3-9, E and F). Interestingly, inducible coinhibitory molecules, particularly PD-L1 (*Cd274*), PD-L2 (*Pdcd1lg2*), and PD1 (*Pdcd1*), were also upregulated in SEA Vβ3$^+$ T cells compared to the control groups (Fig. 3-9, G and H), further confirming the dual capacity of T cells to promote and suppress inflammation immediately after SEA inhalation.

Previous studies found that 4-1BB-4-1BBL and CD40-CD40L pathways can enhance the recruitment of innate immune cells (133, 134). Furthermore, 4-1BBL and CD40L expression on Vβ3$^+$ T cells was validated by flow cytometry (data not shown). Therefore, it was hypothesized that the systemic migration of innate immune cells might be dependent on the expression of inducible costimulatory molecules. To determine whether 4-1BBL and CD40L play a role in the migration of monocytes and neutrophils, mice were pre-treated with anti-4-1BBL, anti-CD40L or the corresponding IgG control and then i.n. challenged with SEA. Neither 4-1BBL nor CD40L blockade impeded migration of monocytes or neutrophils to blood and LNs (Fig. 3-10, A and B), suggesting other mechanisms were involved.

One possibility is that a constitutively expressed costimulatory molecule, such as CD28, might be responsible for this recruitment. The membrane receptor CD28 engages its ligands CD80 and CD86 on DCs and potently enhances TCR-induced cytokine release and proliferation of naïve T cells (135, 136). In addition, CD28 engagement is needed for optimal superantigen-induced T cell expansion (137). Consistent with this previous work, genes associated with CD28 signaling (138-140) were upregulated in Vβ3$^+$ T cells after SEA inhalation (Table 3-2). Secondly, cytokines like TNF and IL-2 are major factors released by enterotoxin-specific T cells (32, 141) and our data show that *Tnf* is promptly synthesized by SEA-specific Vβ3$^+$ T cells (Fig. 3-9. D). Furthermore, GSEA of the hallmark pathways demonstrated a significant enrichment in the pathway of TNF signaling via NFκB in the SEA-specific Vβ3$^+$ T cells (Fig. 3-11, A). Thus, it was hypothesized that CD28 costimulation and a cytokine played redundant or non-overlapping roles in innate cell recruitment in SEA-triggered acute inflammation.

To test this notion, CD28 and TNF were neutralized in SEA-treated mice with CTLA4-Ig or anti-TNF. First, we tested whether CD28 or TNF neutralization affected serum IL-6 levels since increased IL-6 correlates with decreased survival not only in models of sepsis but also in septic patients (142-145). Both, CTLA4-Ig and anti-TNF significantly reduced serum IL-6 compared to the IgG controls, with anti-TNF being even more effective

in decreasing IL-6 than CTLA4-Ig (Fig. 3-11, B). Thus, both treatments appeared to attenuate inflammation by reducing serum IL-6 levels.

To assess whether CD28 or TNF orchestrate monocyte and neutrophil chemotaxis after SEA inhalation, LN tissue from CTLA4-Ig or anti-TNF treated-mice was examined for the expression of chemokines. While CTLA4-Ig significantly reduced *Cxcl1*, *Cxcl2*, *Ccl2*, *Ccl3*, and *Ccl7* mRNA expression, anti-TNF only decreased *Cxcl2* expression and had no significant effect on the other chemokines (Fig. 3-11, C). These findings suggested that CTLA4-Ig would be more effective in blocking the systemic recruitment of monocytes and neutrophils compared to anti-TNF. Indeed, the percent of inflammatory monocytes in LNs and blood was significantly reduced after CTLA4-Ig treatment. In contrast, anti-TNF relatively increased the percent of monocytes in the blood but had no effect on their migration to LNs (Fig. 3-11, D). Nevertheless, both CD28 and TNF blockade significantly reduced the accumulation of neutrophils in LNs (Fig. 3-11, E, upper panels). Based on the results from Fig. 3-3, B, which demonstrated robust migration of neutrophils and monocytes into the bloodstream after SEA inhalation, it was tested if these pathways operated by preventing migration of innate cells into blood. CTLA4-Ig did not inhibit neutrophil circulation (Fig. 3-11, E, lower left panel), but interestingly, TNF blockade significantly inhibited recruitment of neutrophils into blood (Fig. 3-11, E, lower right panel). These findings posed the question of whether the reduction of neutrophils in the LNs after anti-TNF treatment was due to the decreased circulation of blood neutrophils (Fig 1-11, E, lower panels) or reduced *Cxcl2* expression (Fig. 3-11, C). In TNF blocked mice, there was no correlation between the percentage of neutrophils in the blood versus the LNs (Fig. 3-11, F). However, mRNA *Cxcl2* expression positively correlated with the percentage of neutrophils in the LNs suggesting that migration into LNs was dependent on a chemokine gradient rather than the amount of circulating cells (Fig. 3-11, G). Thus, the systemic recruitment of monocytes and neutrophils after SEA inhalation is orchestrated by a non-inducible CD28 signal with overlapping and non-overlapping roles for TNF.

Discussion

Staphylococcus aureus enterotoxins have been implicated in the pathology of toxic shock, sepsis as well as a number of pulmonary and autoimmune diseases due to their ability to elicit a massive and systemic cytokine storm (10, 78, 95, 146). However, it is unclear how *S. aureus* enterotoxins enter the periphery to instigate these effects since the lungs and airways are usually impermeable to inhaled antigens. In fact, antigens are typically cleared from these tissues by a number of mechanisms, including mucociliary transport, innate defense molecules and resident phagocytes (147, 148). Alternatively, inhaled antigens can be carried by migratory DCs to the draining LNs where they are presented to antigen-specific T cells, a process that occurs over hours (147, 149). Unlike most antigens, we demonstrate in this report that inhaled SEA enters the blood circulation within minutes and can be recovered in the serum rather than associated with cells (Fig. 3-1). This ability to enter the bloodstream while maintaining its full bioactivity accounts for the rapid systemic response observed after *S. aureus* enterotoxin pulmonary exposure (30, 39).

From a biomedical perspective, our study showed that just as seen in many patients with SIRS/sepsis (150), SEA inhalation induced leukocytosis since the pulmonary SEA challenge initiated rapid recruitment of innate immune cells to blood followed by their migration to lymphoid tissues (Fig. 3-3). During inflammation, innate immune cells are often assumed to originate from BM. While the pool of inflammatory monocytes in the BM was markedly depleted, there was only a small decrease in BM neutrophils after SEA inhalation (Fig. 3-3, C). A second neutrophil reservoir is the marginated pool where the egress of neutrophils is much faster than the BM peaking at 2 h after an injection of a stimulant (151). The large increase in circulating neutrophils 2 h after SEA inhalation suggests that many of the recruited neutrophils originated from the marginated pool rather than BM.

Activation and expansion of T cells has been considered the core of *S. aureus* enterotoxin-induced inflammation (10). Nevertheless, several studies reported that an inflammatory response could occur even in the absence of T cells (152, 153). In the inhaled SEA model of SIRS, TCR $\beta\delta^{-/-}$ mice were unable to recruit monocytes and neutrophils to blood and LNs whereas only a small transfer of T cells induced a rapid mobilization of the innate cells (Fig. 3-4). The recruited cells localized to the T cell zone of the LNs (Fig. 3-5). This specific location in the LNs renders an opportunity to modulate adaptive immunity. Previous studies showed that after recruitment to LNs, inflammatory monocytes differentiate into DCs and are capable of antigen presentation, including cross-presentation, resulting in enhanced Th1 responses via IL-12 (126, 127). Similarly, neutrophil migration to LNs has been associated with several different functions, including carrying bacteria to LNs via the lymphatic system, augmenting lymphocyte proliferation, and downregulating CD4 T cell responses by decreasing antigen presentation by antigen-presenting cells (122, 124, 154). Thus, it will be important to determine if the migration of inflammatory monocytes and neutrophils to the T cell zone of LNs affects the function of T cells and the overall inflammatory response after pulmonary *S. aureus* enterotoxin challenge.

To test whether the recruitment of innate immune cells was caused by mediators directly released by T cells, we examined T cells for chemokine expression and found that upon activation, T cells expressed chemokines but also induced chemokine expression in DCs (Fig. 3-7). This was coincident with increases in inducible costimulatory pathways rapidly after SEA inhalation that included *Tnfsf9* (4-1BBL) and *Cd40lg* (CD40L) (Fig. 3-9, E and F). However, while inducible costimulation was not involved in the monocyte and neutrophil chemotaxis (Fig. 3-10), blocking non-inducible CD28 costimulation significantly reduced the migration of inflammatory monocytes (Fig. 3-11). In contrast, neutrophil recruitment was driven by two T cell-dependent signals. Firstly, TNF triggered a rapid release of neutrophils into blood, which we postulate is derived from the marginated pool. Secondly, a chemokine axis induced by both the CD28 and TNF pathways directed

neutrophils to LNs (Fig. 3-11, E). In particular, the inhibition of neutrophil migration to LNs was coincident with reduced expression of *Cxcl2* (Fig. 3-11, C and D) and it was previously reported that the migration of neutrophils into tumor-draining LNs via high endothelial venules was dependent on CXCL2 but not on CXCL1 (125). Therefore, we hypothesize that CXCL2 may be the key chemokine driving the neutrophil migration into LNs from blood after pulmonary challenge with *S. aureus* enterotoxins or during Gram-positive sepsis. Finally, we showed that T cells were essential for the systemic recruitment of neutrophils and monocytes after SEA inhalation (Fig. 3-4). However, because TNF can be produced by many cell types (155) and CD28 expression was reported on immune cells other than T cells (156, 157), it is possible that blocking with CTLA4-Ig and anti-TNF affected other cell populations that could also contribute to the reduced migration of innate cells.

Despite decades of research, there is currently no approved drug treatment for SIRS/sepsis patients (7). Because of the central role TNF plays in the pathology of SIRS/sepsis, anti-TNF therapies were previously thought to be an excellent therapeutic target (158). However, clinical studies failed to find improvements in the outcomes of patients with sepsis receiving anti-TNF treatment (159-161). Moreover, rheumatoid arthritis patients on anti-TNF therapy gained a higher likelihood of developing serious infections (162). Our results show that although TNF blockade attenuated inflammation by reducing serum IL-6 (Fig. 3-11, B), it also significantly depleted the pool of circulating blood neutrophils (Fig. 3-11, E). The capacity of neutrophils to mount a rapid microbicidal response makes them a crucial component of the immune system during sepsis. In fact, the relative resistance to *S. aureus* in C57BL/6 mice was recently attributed to increased chemokine secretion and subsequent neutrophil recruitment compared to other mouse strains (163). In addition, reduced levels of circulating neutrophils may be associated with a decreased likelihood of survival in sepsis (142, 164). The suppressed neutrophil levels in blood could potentially compromise the immune system's capacity to kill off bacteria in the bloodstream. Therefore, it is possible that the failure of anti-TNF therapies to ameliorate

outcomes in sepsis is partially due to the reduced neutrophil count in blood leading to increased bacteremia.

Costimulatory molecules represent another group of potential therapeutic targets in SIRS/sepsis. In particular, CD28 may play an important role in the propagation of inflammation during the course of the disease. A clinical trial using a monoclonal superagonist anti-CD28 resulted in a life-threatening SIRS with clinical signs and symptoms similar to sepsis (165). In contrast, blocking CD28 signaling, especially in cases of superantigen-induced toxic shock, showed attenuation of the disease in mice (166, 167). Here we showed that blocking CD28 reduced IL-6 levels and chemokine expression, while impeding migration of monocytes and neutrophils to LNs without affecting neutrophilia in blood (Fig. 3-11). Therefore, targeting CD28, especially in cases of Gram-positive sepsis in which *S. aureus* enterotoxins may drive the pathology, merits further investigation.

Lastly, not only costimulatory but also coinhibitory molecules, particularly *Cd274* (PD-L1), *Pdcd1lg2* (PD-L2) and *Pdcd1* (PD1), were upregulated after SEA inhalation (Fig. 3-9). Similarly, both pro- and anti-inflammatory cytokines were upregulated as were the processes of cell activation and apoptosis (Fig. 3-9). In patients with sepsis, the acute SIRS phase characterized by a hyperinflammatory state and the release of pro-inflammatory cytokines was thought to be frequently followed by an immunosuppressive CARS phase and presence of anti-inflammatory cytokines (168). However, recent evidence suggests that both pro- and anti-inflammatory responses occur simultaneously from the onset of sepsis with one prevailing over the other during the course of the disease (7, 169, 170). Similarly, we showed that both inflammatory and immunosuppressive processes are triggered simultaneously in T cells immediately after SEA inhalation, confirming the relevance of *S. aureus* enterotoxins in the pathology of sepsis.

In sum, our study demonstrated that inhaled SEA rapidly enters the bloodstream and triggers systemic inflammation by forming an inflammatory cell network comprised of both the innate and adaptive immune system. In particular, our findings revealed a dual

mechanism of monocyte and neutrophil recruitment by SEA-specific T cells relying on overlapping and non-overlapping roles of the non-inducible costimulatory receptor CD28 and the inflammatory cytokine TNF. Treatments for SIRS/sepsis may benefit by targeting disease initiation rather than treating the consequent symptoms.

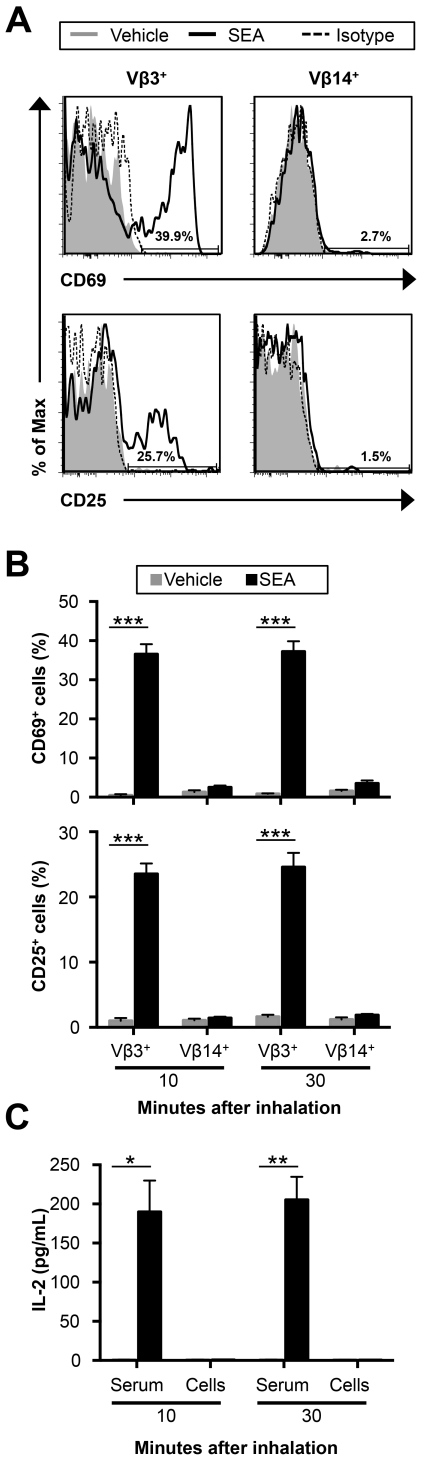

FIGURE 3-1: After inhalation, SEA circulates systemically via blood. Tail blood was collected 10 or 30 min after SEA or vehicle inhalation and the serum or blood cells were incubated overnight with enriched naïve T cells. The expression of activation markers CD69 and CD25 was measured on SEA-activated $CD3^+V\beta3^+$ T cells and on bystander $CD3^+V\beta14^+$

T cells by flow cytometry. A) Representative histograms of $CD69^+$ and $CD25^+$ cells in $CD3^+V\beta3^+$ and $CD3^+V\beta14^+$ populations after a co-culture of naïve T cells with serum from SEA or vehicle mice. B) Percent of $CD69^+$ and $CD25^+$ cells in $CD3^+V\beta3^+$ and $CD3^+V\beta14^+$ populations after a co-culture of naïve T cells with serum from SEA or vehicle mice. C) Concentration of IL-2 in the supernatants from a co-culture between naïve T cells and serum or cells from blood harvested from SEA or vehicle mice. Data were combined from 3 independent experiments with n=3 in vehicle group and n=6 in SEA group. Data are shown as mean ± SEM. Statistical significance was determined by two-tailed Student's t-tests (*P<0.05; **P<0.01; ***P<0.001).

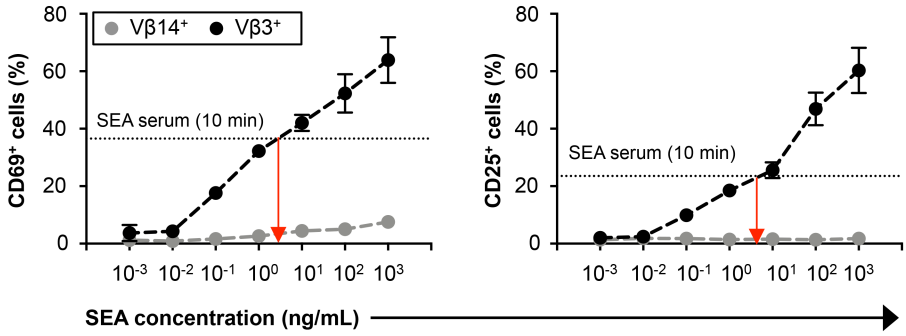

Figure 3-2: Estimation of SEA levels in serum immediately after inhalation. Naïve enriched T cells were incubated overnight with increasing concentrations of SEA. The percentages of $CD69^+$ and $CD25^+$ cells in $CD3^+V\beta3^+$ and $CD3^+V\beta14^+$ was detected by flow cytometry. The dashed horizontal line represents the average percent of $CD69^+$ or $CD25^+$ cells in $CD3^+V\beta3^+$ T cells after a co-culture with serum (1:4 diluted in culture medium) from mice 10 min after SEA inhalation (see Fig. 3-1). Data were combined from 3 independent experiments with n=3.

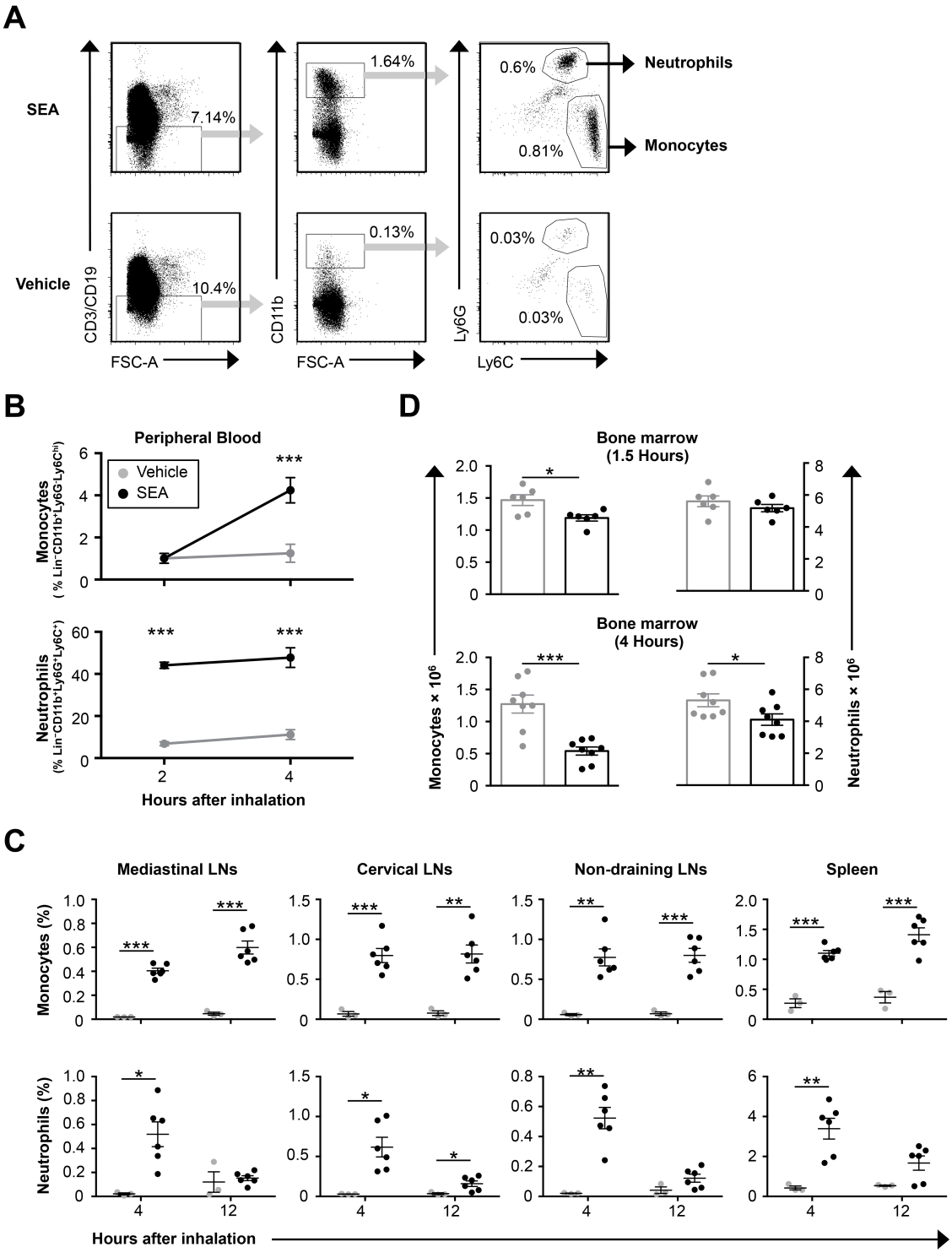

FIGURE 3-3: SEA inhalation induces systemic migration of inflammatory monocytes and neutrophils. Peripheral blood, BM, LNs and spleen were collected after SEA or vehicle

inhalation. A) Representative plots of cervical LN cells 4 h after SEA or vehicle challenge to identify $Lin^{-}(CD3/CD19^{-})CD11b^{+}Ly6G^{-}Ly6C^{hi}$ inflammatory monocytes and $Lin^{-}CD11b^{+}Ly6G^{+}Ly6C^{+}$ neutrophils. The percent is relative to live cell gate. B) Percent of monocytes and neutrophils in peripheral blood 2 and 4 h after SEA or vehicle challenge. Data were combined from 3 independent experiments with n=8 per group. C) Percent of inflammatory monocytes and neutrophils in LNs and spleen 4 and 12 h after SEA or vehicle challenge. Non-draining LNs = axillary, brachial, inguinal, and mesenteric LNs. Data were combined from 3 independent experiments with n=3 for vehicle group and n=6 for SEA group. D) Absolute number of inflammatory monocytes and neutrophils in BM from one femur and tibia 1.5 and 4 h after SEA or vehicle challenge. Data were combined from at least 3 independent experiments with n=6-8 per group. Data are shown as mean ± SEM. Statistical significance was determined by two-tailed Student's t-tests (*P<0.05; **P<0.01; ***P<0.001).

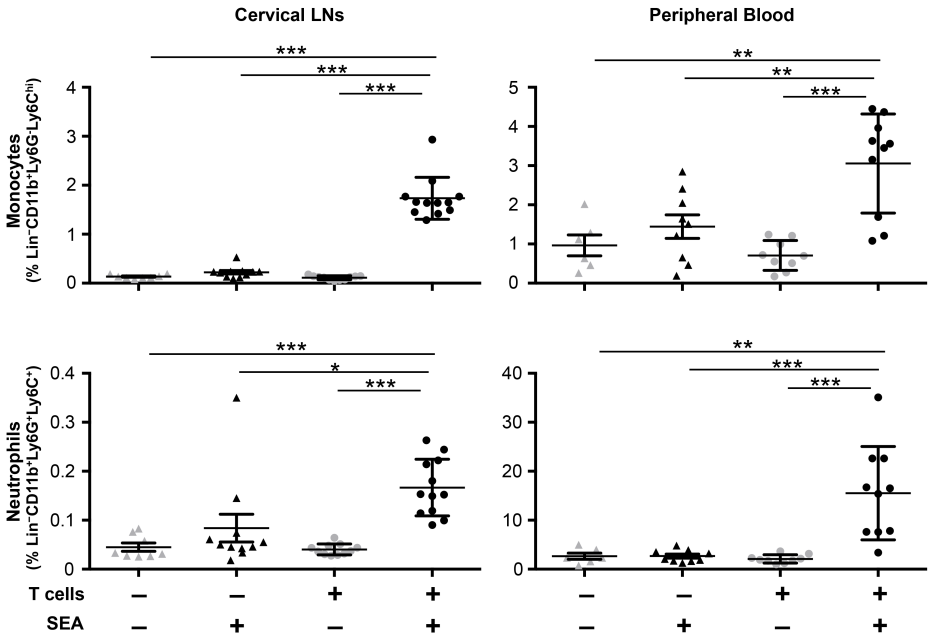

FIGURE 3-4: T cells are required for the systemic recruitment of inflammatory monocytes and neutrophils after SEA inhalation. TCR $\beta\delta^{-/-}$ mice received C57BL/6J T

cells or nothing. On the next day, they were challenged with SEA or vehicle and cervical LNs and peripheral blood were collected 6 h after the challenge to identify $Lin^{-}(CD3/CD19^{-})CD11b^{+}Ly6G^{-}Ly6C^{hi}$ inflammatory monocytes and $Lin^{-}CD11b^{+}Ly6G^{+}Ly6C^{+}$ neutrophils. For cervical LNs, data were combined from at least 4 independent experiments with n = 8-12 per group. For peripheral blood, data were combined from at least 3 independent experiments with n = 6-10 per group. Data are shown as mean ± SEM. Statistical significance was determined by two-tailed Student's t-tests (*P<0.05; **P<0.01; ***P<0.001).

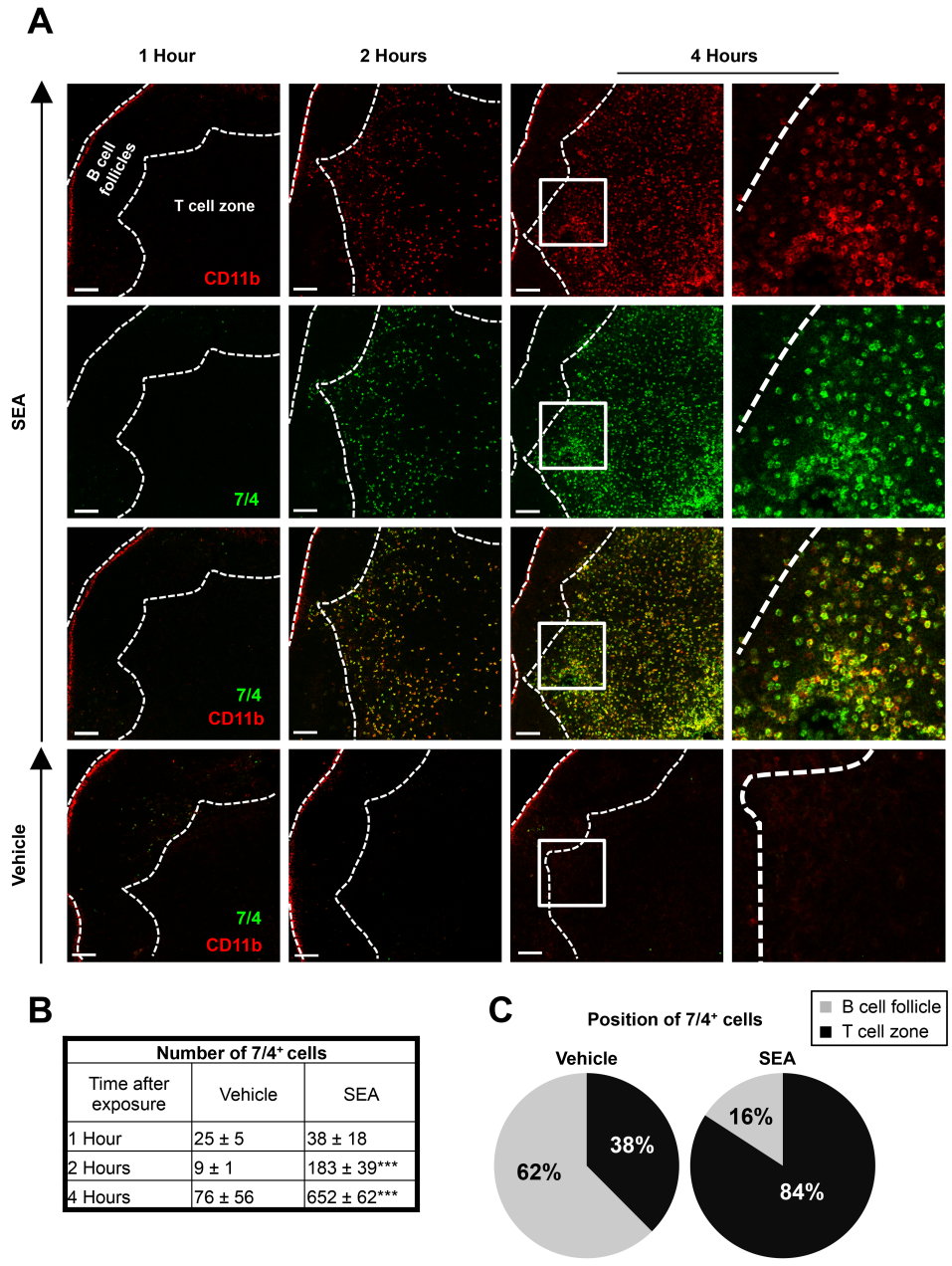

Number of 7/4⁺ cells		
Time after exposure	Vehicle	SEA
1 Hour	25 ± 5	38 ± 18
2 Hours	9 ± 1	183 ± 39***
4 Hours	76 ± 56	652 ± 62***

FIGURE 3-5: Inflammatory innate immune cells migrate to the T cell zone of the LNs after SEA inhalation. A) Representative confocal microscopy images of frozen sections from cervical LNs 1, 2 and 4 h after SEA or vehicle challenge. Inflammatory innate immune cells (monocytes and neutrophils) were labeled with anti-CD11b and anti-7/4 antibodies. The white dashed line marks B cell follicles and was determined by anti-B220 staining (not shown). The vertical panel on the right represents an enlarged image of the area in the white square. The displayed images are projections of confocal z stacks taken using 20×

magnification/0.8 numerical aperture objective and Zeiss LSM780 confocal microscope. Scale bar = 80 μm. B) Number of 7/4$^+$ cells. The amount of 7/4$^+$ cells per field was determined from 3 images per mouse by Imaris (Bitplane). Statistical significance was assessed by two-tailed Student's t-tests (***P<0.001). C) Position of 7/4$^+$ cells in LNs. The number of 7/4$^+$ cells in B cell follicles vs. T cell zone was determined from 3 images per mouse by Imaris. The data are representative of least 3 independent experiments with n=3-5 per group.

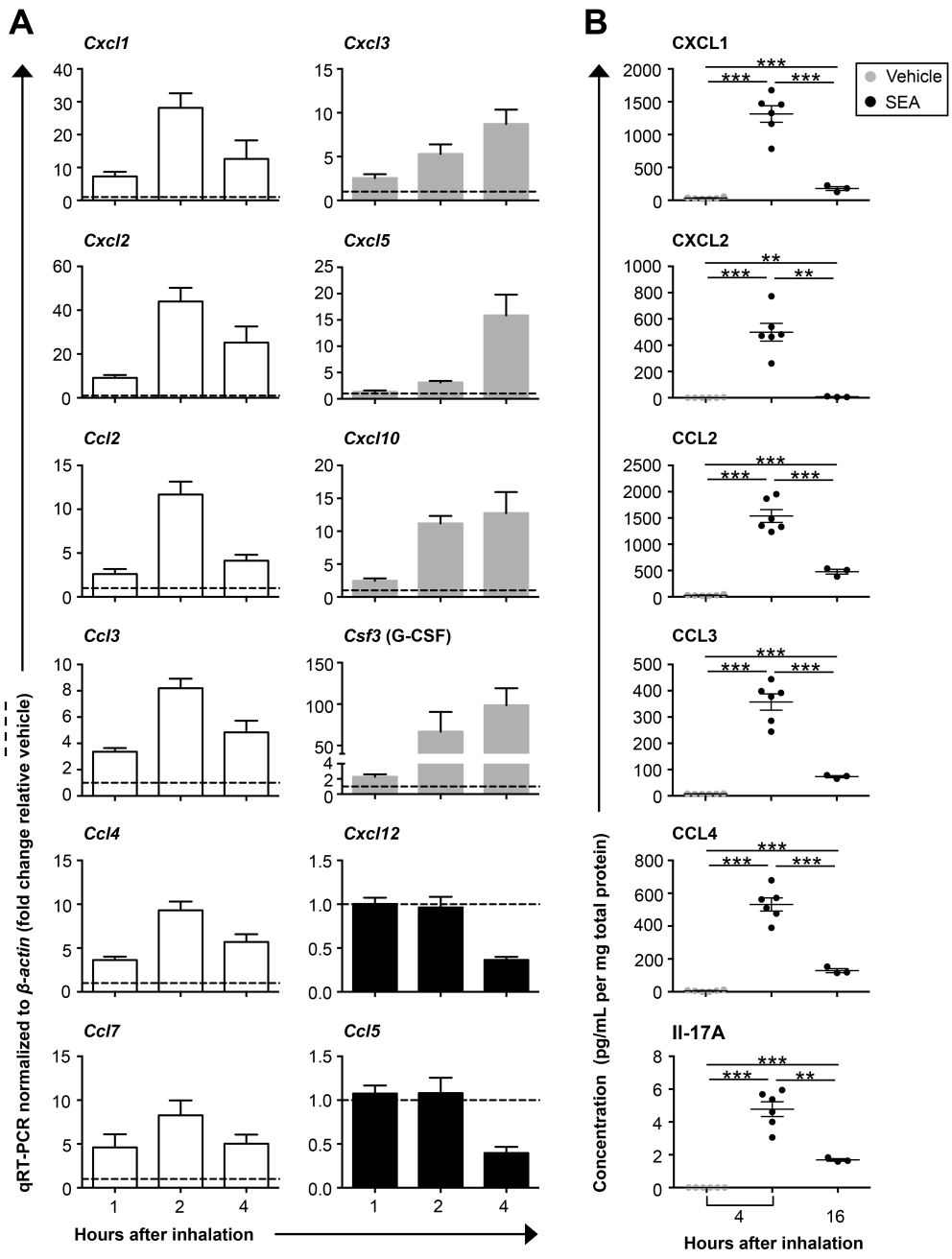

FIGURE 3-6: SEA inhalation causes an increased expression of monocyte and neutrophil chemotactic factors in LNs. A) Changes in chemokine gene expressions after SEA inhalation. Draining LNs (cervical and mediastinal) were collected 1, 2 or 4 h after SEA or vehicle inhalation and lysed to isolate RNA. qRT-PCR expression was normalized to *β-actin* and is represented as a fold change relative to vehicle-treated group (dashed line set as 1). Individual chemokine expressions were divided into 3 groups based on their

expression patterns (early increase in expression: □; late increase in expression: ■; late decrease in expression: ■). Data were combined from 3 independent experiments with n = 7 per group. Data are shown as mean + SEM. B) Changes in chemokine protein levels after SEA inhalation. Draining LNs were collected 4 or 16 h after SEA or vehicle exposure. Whole tissue was lysed with magnetic beads and chemokine expressions were measured with a multiplex assay. Data were combined from three independent experiments with n = 6 (4 h exposure) or n = 3 (16 h exposure). Data are shown as mean ± SEM. Statistical significance was determined by two-tailed Student's t-tests (*p<0.05; **p<0.01; ***p<0.001).

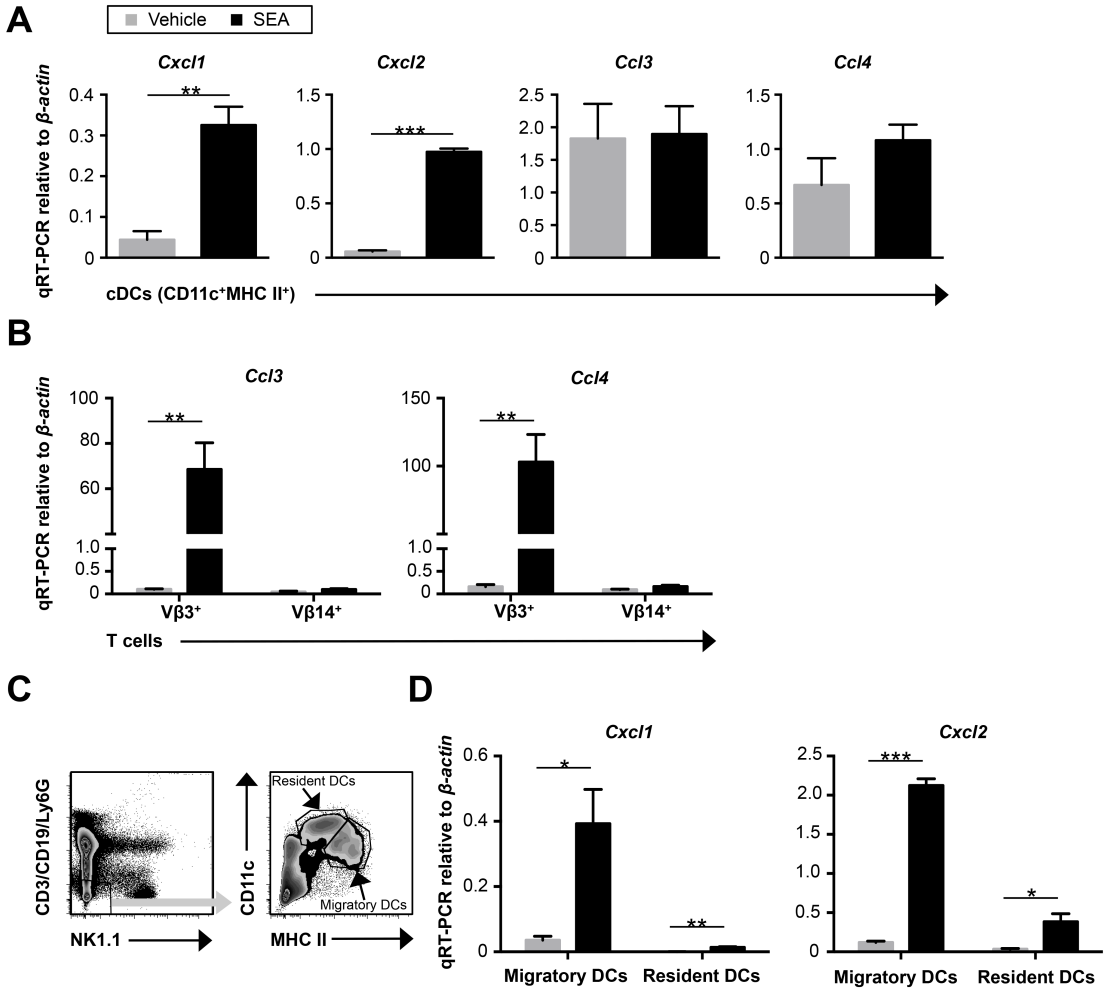

FIGURE 3-7: T cells and DCs express chemokines after SEA inhalation. LNs (axillary, brachial, inguinal, mesenteric, cervical and mediastinal) were collected 2 h after SEA or vehicle challenge and cells were stained to sort for specific populations. RNA isolated from the sorted populations was used for qRT-PCR analysis. A) Expression of *Cxcl1*, *Cxcl2*, *Ccl3* and *Ccl4* in $CD3^{-}CD19^{-}$(or $B220^{-}$)$NK1.1^{-}DX5^{-}MHC\ II^{+}CD11c^{+}$ conventional DCs (cDCs). B) Expression of *Ccl3* and *Ccl4* in $V\beta3^{+}$ and $V\beta14^{+}$ T cells. C) Gating strategy to isolate migratory and resident DCs. D) Expression of *Cxcl1* and *Cxcl2* in migratory and resident DCs. Expression of chemokines is shown relative to *β-actin*. Data are displayed as mean + SEM. Data are representative of 3 independent experiments with n=3 per group. Statistical significance was determined by two-tailed Student's t-tests (**P*<0.05; ***P*<0.01; ****P*<0.001).

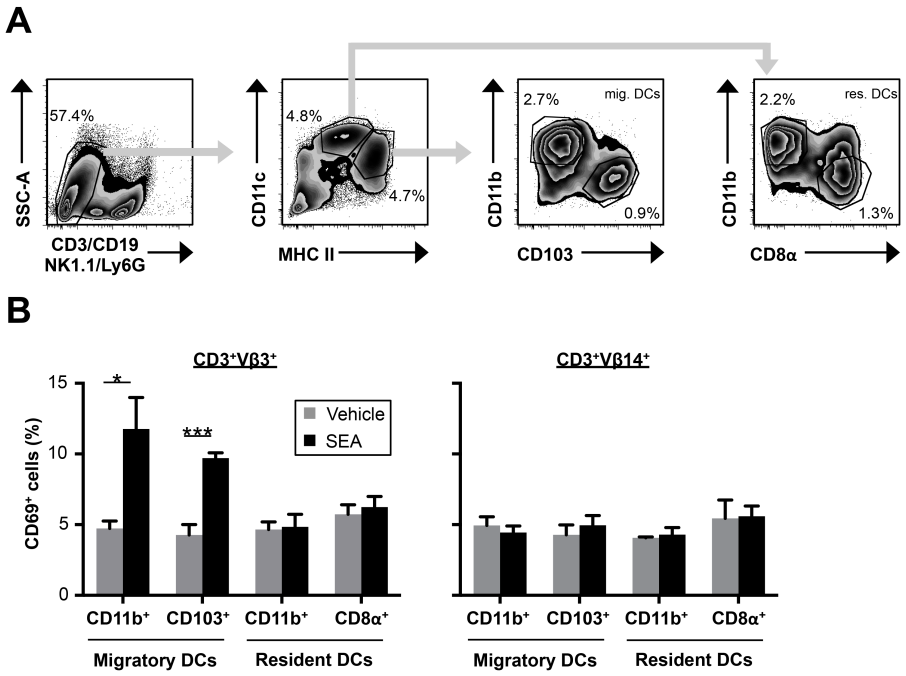

FIGURE 3-8: Migratory DCs present SEA to T cells. A) Gating strategy used to sort for DC subpopulations. B) CD69 expression on T cells after co-culture with *ex vivo* derived DCs. LNs were harvested 40 min after SEA or vehicle inhalation and the sorted DC subpopulations were co-cultured with naïve T cells. The expression of CD69 was measured on SEA-activated $CD3^{+}V\beta3^{+}$ T cells and on bystander $CD3^{+}V\beta14^{+}$ T cells by flow cytometry.

Data are displayed as mean ± SEM and are representative of 4 independent experiments with n=4 per group. Statistical significance was determined by two-tailed Student's t-tests (*P<0.05; **P<0.01; ***P<0.001).

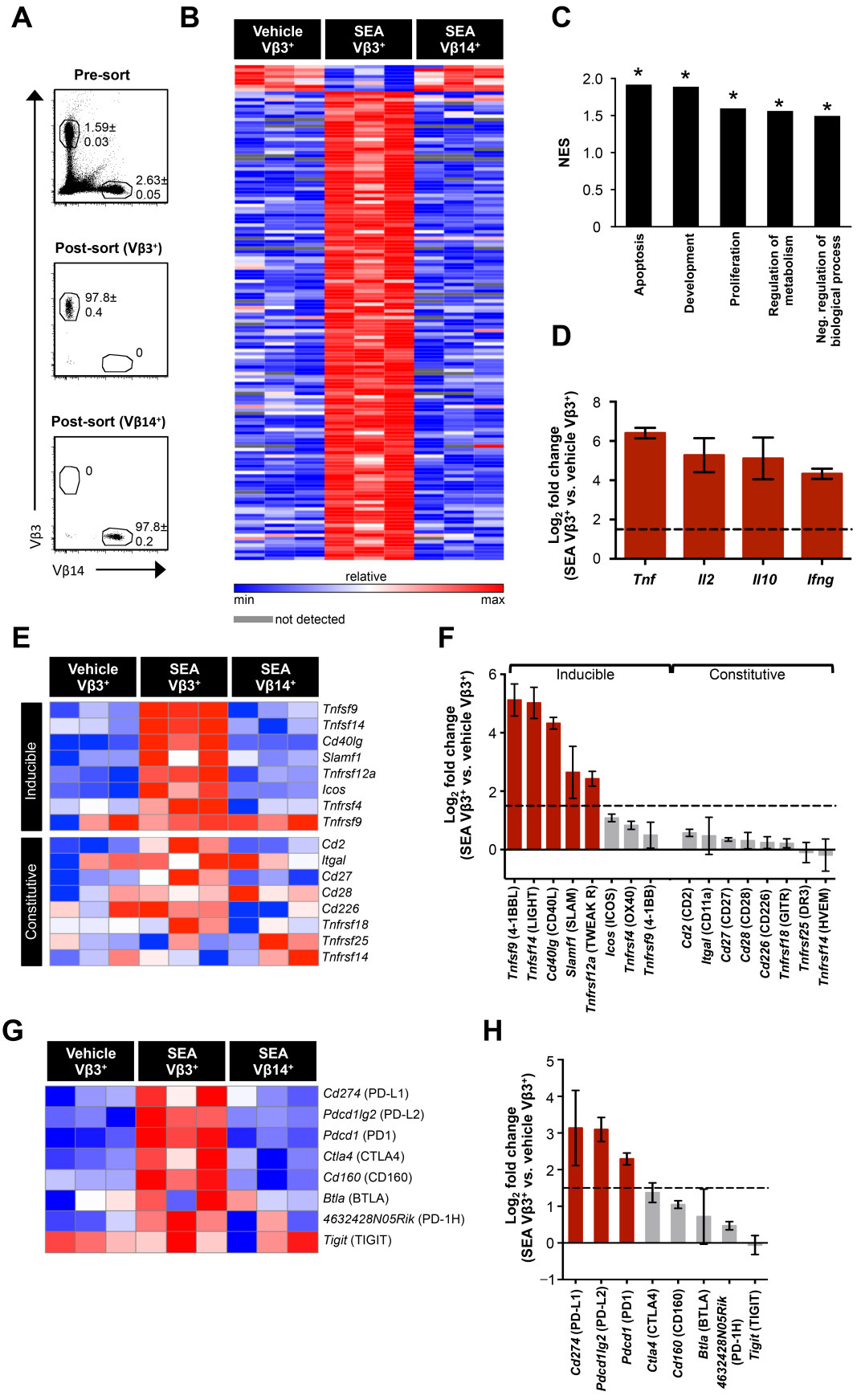
A
Pre-sort
1.59±
0.03
2.63±
0.05
Post-sort (Vβ3+)
97.8±
0.4
0
Post-sort (Vβ14+)
0
97.8±
0.2
Vβ3
Vβ14
B
Vehicle Vβ3+
SEA Vβ3+
SEA Vβ14+
relative
min
max
not detected
C
NES
2.0
1.5
1.0
0.5
0
Apoptosis
Development
Proliferation
Regulation of metabolism
Neg. regulation of biological process
D
Log2 fold change (SEA Vβ3+ vs. vehicle Vβ3+)
8
6
4
2
0
Tnf
Il2
Il10
Ifng
E
Vehicle Vβ3+
SEA Vβ3+
SEA Vβ14+
Inducible
Constitutive
Tnfsf9
Tnfsf14
Cd40lg
Slamf1
Tnfrsf12a
Icos
Tnfrsf4
Tnfrsf9
Cd2
Itgal
Cd27
Cd28
Cd226
Tnfrsf18
Tnfrsf25
Tnfrsf14
F
Inducible
Constitutive
Log2 fold change (SEA Vβ3+ vs. vehicle Vβ3+)
6
4
2
0
Tnfsf9 (4-1BBL)
Tnfsf14 (LIGHT)
Cd40lg (CD40L)
Slamf1 (SLAM)
Tnfrsf12a (TWEAK R)
Icos (ICOS)
Tnfrsf4 (OX40)
Tnfrsf9 (4-1BB)
Cd2 (CD2)
Itgal (CD11a)
Cd27 (CD27)
Cd28 (CD28)
Cd226 (CD226)
Tnfrsf18 (GITR)
Tnfrsf25 (DR3)
Tnfrsf14 (HVEM)
G
Vehicle Vβ3+
SEA Vβ3+
SEA Vβ14+
Cd274 (PD-L1)
Pdcd1lg2 (PD-L2)
Pdcd1 (PD1)
Ctla4 (CTLA4)
Cd160 (CD160)
Btla (BTLA)
4632428N05Rik (PD-1H)
Tigit (TIGIT)
H
Log2 fold change (SEA Vβ3+ vs. vehicle Vβ3+)
5
4
3
2
1
0
−1
Cd274 (PD-L1)
Pdcd1lg2 (PD-L2)
Pdcd1 (PD1)
Ctla4 (CTLA4)
Cd160 (CD160)
Btla (BTLA)
4632428N05Rik (PD-1H)
Tigit (TIGIT)

FIGURE 3-9: SEA simultaneously activates and suppresses T cells. LNs were removed 40 min after SEA or vehicle inhalation. The total RNA from the sorted Vβ3$^+$ and Vβ14$^+$ T cells was used for genomic sequencing. A) Purity of Vβ3$^+$ cells and Vβ14$^+$ cells. The percent is relative to live cell gate. B) Heat map of the most downregulated and upregulated genes in SEA-activated Vβ3$^+$ T cells compared to vehicle Vβ3$^+$ T cells and SEA Vβ14$^+$ T cells (control groups). Genes that had a significantly altered expression (log_2 fold change ≤ −1.5 or ≥ +1.5) in SEA-activated Vβ3$^+$ cells compared to either vehicle Vβ3$^+$ T cells or SEA Vβ14$^+$ T cells in all 3 experiments were selected. C) Net enrichment score (NES) for gene ontology clusters upregulated in SEA-activated Vβ3$^+$ cells compared to control groups (GSEA; *P<0.01). D) Log_2 fold change in the expression of cytokines in SEA-activated Vβ3$^+$ T cells compared to vehicle Vβ3$^+$ T cells. Significant difference is represented by a dashed line (≥1.5). Data are shown as mean ± SEM. E) Heat map showing expression of inducible and constitutively expressed costimulatory molecules in SEA Vβ3$^+$ T cells and control groups (vehicle Vβ3$^+$ and SEA Vβ14$^+$ T cells) 40 min after SEA or vehicle inhalation. F) Log_2 fold change in the expression of costimulatory molecules in SEA-activated Vβ3$^+$ T cells compared to vehicle Vβ3$^+$ T cells. Significant difference is represented by a dashed line (≥1.5). Data are displayed as mean ± SEM. G) Heat map of coinhibitory molecules in SEA-activated Vβ3$^+$ T cells and vehicle Vβ3$^+$ and SEA Vβ14$^+$ control groups. H) Log_2 fold change in the expression of coinhibitory molecules in SEA Vβ3$^+$ T cells compared to vehicle Vβ3$^+$ T cells. Significant difference is represented by a dashed line (≥1.5). Data are displayed as mean ± SEM. Data are representative of 3 independent experiments with n=3 per group.

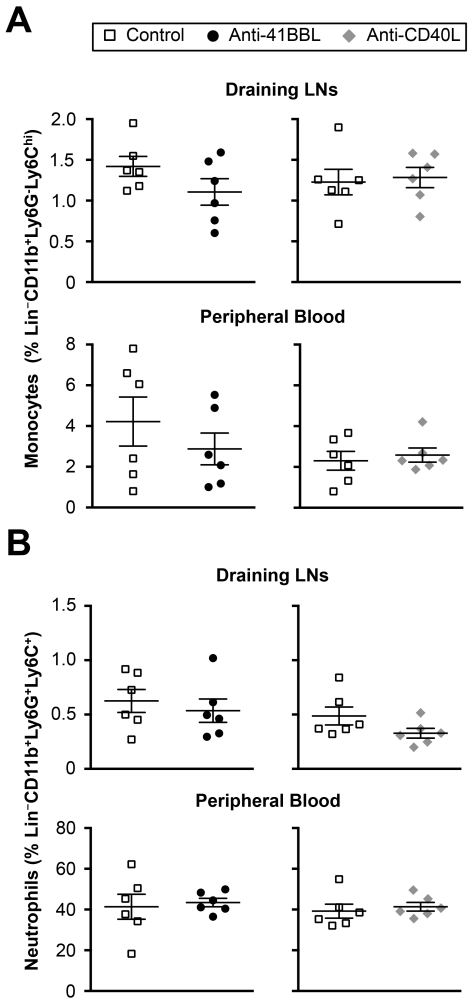

FIGURE 3-10: Inducible costimulatory molecules 41BBL and CD40L are not involved in the recruitment of monocytes and neutrophils after SEA inhalation. A) and B) Percent of Lin^{-}(CD3/CD19/NK1.1^{-})$CD11b^{+}Ly6G^{-}Ly6C^{hi}$ monocytes (A) and $Lin^{-}CD11b^{+}Ly6G^{+}Ly6C^{+}$ neutrophils (B) in draining LNs (cervical and mediastinal) and blood in mice treated with anti-4-1BBL or anti-CD40L prior to SEA challenge. Two hours prior to SEA inhalation, mice were treated with anti-4-1BBL or anti-CD40L or the respective IgG control i.p. Blood and draining LNs were removed 4 hours after the SEA challenge. Data were combined from 2 independent experiments with n=6 per group. Data are shown as mean ± SEM. Statistical significance was determined by two-tailed Student's t-tests.

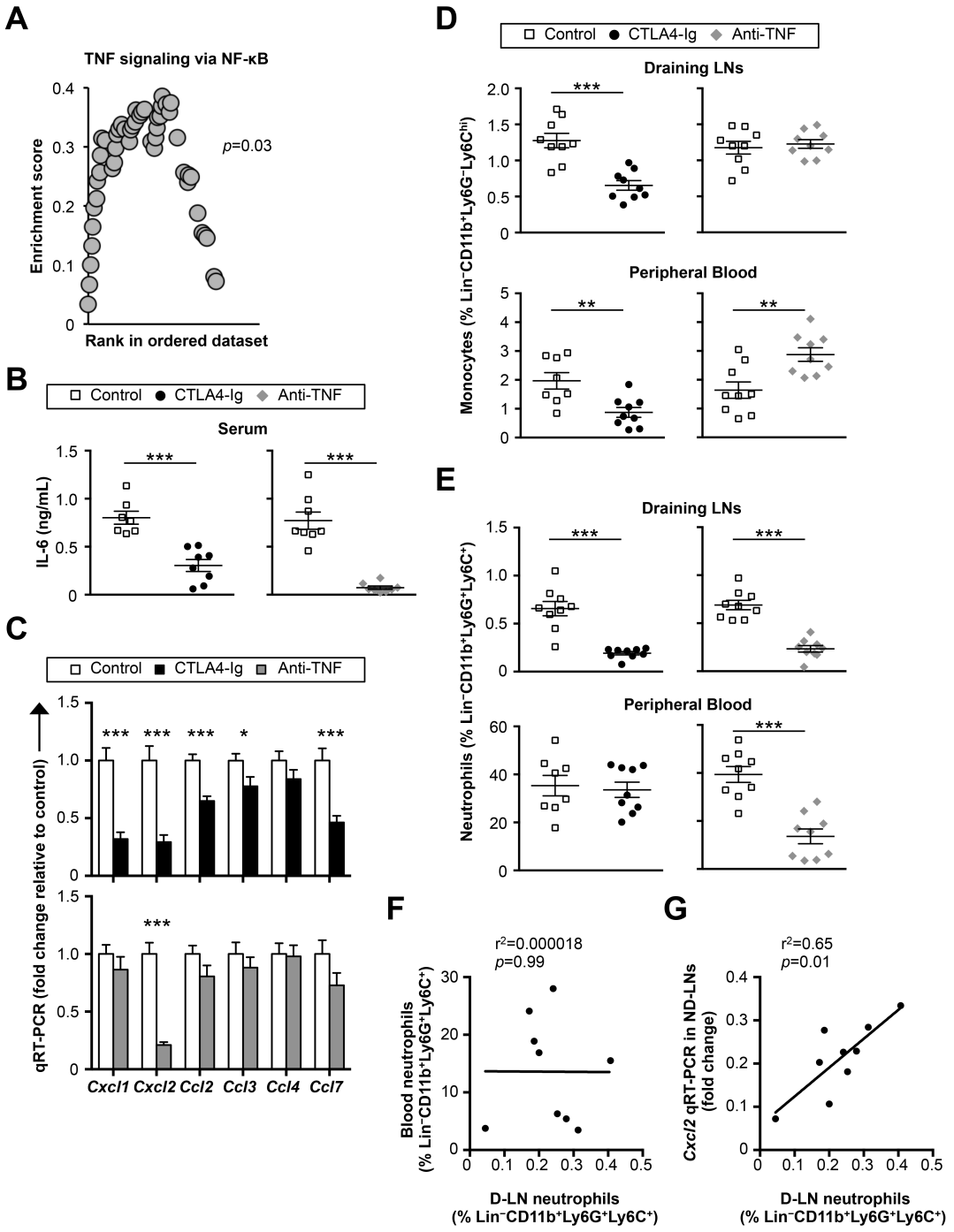

FIGURE 3-11: The migration of monocytes and neutrophils after SEA inhalation is dependent on CD28 and TNF. A) The NFκB signaling via TNF is upregulated in SEA-activated Vβ3$^+$ T cells 40 min after SEA inhalation. GSEA was used to evaluate significantly enriched pathways in SEA-activated Vβ3$^+$ cells compared to the control groups (vehicle Vβ3$^+$ cells and SEA Vβ14$^+$ cells). Data are representative of 3 independent experiments with

n=3 per group. B) Concentration of serum IL-6 in mice treated with CTLA4-Ig or anti-TNF prior to i.n. SEA challenge. Two hours prior to SEA inhalation, mice were treated with CTLA4-Ig or anti-TNF antibody or the respective IgG control i.p. Serum was collected 4 hours after SEA challenge. C) Chemokine expressions in non-draining LNs (mesenteric, axillary, brachial, inguinal) from mice that were treated with either CTLA4-Ig or anti-TNF and the respective IgG control prior pulmonary SEA challenge. Tissue was collected 4 hours after the SEA challenge. The qRT-PCR expression was normalized to *β-actin* and it is expressed as a fold change relative to the IgG-treated group. D) and E) Percent of Lin^{-}(CD3/CD19/$NK1.1^{-}$)$CD11b^{+}Ly6G^{-}Ly6C^{hi}$ monocytes (D) and $Lin^{-}CD11b^{+}Ly6G^{+}Ly6C^{+}$ neutrophils (E) in draining LNs (cervical and mediastinal) and blood in mice treated with CTLA4-Ig or anti-TNF prior to SEA inhalation. Tail blood and draining LNs were collected 4 h after SEA challenge. Data were combined from 3 independent experiments with n=7-9 per group. Data are shown as mean ± SEM. Statistical significance was determined by two-tailed Student's t-tests (**P*<0.05; ***P*<0.01; ****P*<0.001). F) and G) Correlating the percent of D-LNs (draining LNs) neutrophils with the percent of neutrophils in blood (F) and ND-LNs (non-draining LNs) *Cxcl2* expression (G). Data are representative of 3 independent experiments with n=9 per group. The *P* value of the linear regression fit curve is calculated from F test.

Change in Expression	Gene Symbol	Name
Downregulated in SEA Vβ3$^+$ cells	*0610012G03Rik*	RIKEN cDNA 0610012G03 gene
	Apol9a	apolipoprotein L 9b; apolipoprotein L 9a
	Ddit4	DNA-damage-inducible transcript 4
	Gm10640	predicted gene 10640
	Ppp1r35	protein phosphatase 1, regulatory subunit 35
	Thap11	THAP domain containing 11
	Tsc22d3	TSC22 domain family, member 3
	Txnip	thioredoxin interacting protein
Upregulated in SEA Vβ3$^+$ cells	*1190002H23Rik*	RIKEN cDNA 1190002H23 gene
	1700102P08Rik	RIKEN cDNA 1700102P08 gene
	1700106N22Rik	RIKEN cDNA 1700106N22 gene
	2010002N04Rik	RIKEN cDNA 2010002N04 gene
	2310010J17Rik	RIKEN cDNA 2310010J17 gene
	A930024E05Rik	RIKEN cDNA A930024E05 gene
	Aif1	allograft inflammatory factor 1
	Arc	activity regulated cytoskeletal-associated protein
	Areg	amphiregulin
	Arl5b	ADP-ribosylation factor-like 5B
	Atf3	activating transcription factor 3
	Bcl2a1a	B-cell leukemia/lymphoma 2 related protein A1a
	Bcl2a1b	B-cell leukemia/lymphoma 2 related protein A1b
	Bcl2a1d	B-cell leukemia/lymphoma 2 related protein A1d
	Bhlhe40	basic helix-loop-helix family, member e40
	Btg2	B-cell translocation gene 2, anti-proliferative
	C130039O16Rik	RIKEN cDNA C130039O16 gene
	Car7	carbonic anhydrase 7
	Ccl1	chemokine (C-C motif) ligand 1
	Ccl20	chemokine (C-C motif) ligand 20
	Ccl3	chemokine (C-C motif) ligand 3
	Ccl4	chemokine (C-C motif) ligand 4
	Ccnl1	cyclin L1
	Ccr8	chemokine (C-C motif) receptor 8
	Cd40lg	CD40 ligand
	Cd69	CD69 antigen
	Cdkn1a	cyclin-dependent kinase inhibitor 1A (P21)
	Cish	cytokine inducible SH2-containing protein
	Coq10b	hypothetical protein LOC675736; coenzyme Q10 homolog B (S. cerevisiae); predicted gene 4899
	Crem	cAMP responsive element modulator
	Csrnp1	cysteine-serine-rich nuclear protein 1
	Cxcl10	chemokine (C-X-C motif) ligand 10; similar to Small inducible cytokine B10 precursor (CXCL10) (Interferon-gamma-induced protein CRG-2) (Gamma-IP10) (IP-10) (C7)
	Dnajb1	DnaJ (Hsp40) homolog, subfamily B, member 1
	Dnajb4	DnaJ (Hsp40) homolog, subfamily B, member 4
	Dusp1	dual specificity phosphatase 1
	Dusp2	dual specificity phosphatase 2
	Dusp5	dual specificity phosphatase 5
	Egr1	early growth response 1
	Egr2	early growth response 2
	Egr3	early growth response 3
	Ehd1	EH-domain containing 1
	Evi2a	ecotropic viral integration site 2a
	F2r	coagulation factor II (thrombin) receptor
	Fasl	Fas ligand (TNF superfamily, member 6)
	Fggy	FGGY carbohydrate kinase domain containing
	Fos	FBJ osteosarcoma oncogene
	Fosb	FBJ osteosarcoma oncogene B
	Fosl1	fos-like antigen 1
	Fosl2	similar to fos-like antigen 2; fos-like antigen 2
	Gadd45b	growth arrest and DNA-damage-inducible 45 beta
	Gch1	GTP cyclohydrolase 1

Change in Expression	Gene Symbol	Name
Upregulated in SEA Vβ3^{+} cells	*Gem*	GTP binding protein (gene overexpressed in skeletal muscle)
	Gm11974	predicted gene 11974
	Gm7334	predicted gene 7334; B-cell translocation gene 3; similar to BTG3
	Gpr171	G protein-coupled receptor 171
	Hspa5	heat shock protein 5
	Icam1	intercellular adhesion molecule 1
	Ier2	immediate early response 2
	Ier3	immediate early response 3
	Ier5	immediate early response 5
	Ifng	interferon gamma
	Il10	interleukin 10
	Il2	interleukin 2; similar to Interleukin-2 precursor (IL-2) (T-cell growth factor) (TCGF)
	Il4	interleukin 4
	Irf4	interferon regulatory factor 4
	Jun	Jun oncogene
	Junb	Jun-B oncogene
	Kdm6b	KDM1 lysine (K)-specific demethylase 6B
	Klre1	killer cell lectin-like receptor family E member 1
	Lgals7	lectin, galactose binding, soluble 7
	Lif	leukemia inhibitory factor
	Lta	lymphotoxin A
	Lyz1	lysozyme 1
	Maff	v-maf musculoaponeurotic fibrosarcoma oncogene family, protein F (avian)
	Map3k8	mitogen-activated protein kinase kinase kinase 8
	Marcksl1	MARCKS-like 1; predicted gene 9106
	Mir17hg	MiR-17-92 cluster host gene
	Myc	myelocytomatosis oncogene
	Nab2	Ngfi-A binding protein 2
	Nfkbia	nuclear factor of kappa light polypeptide gene enhancer in B-cells inhibitor, alpha
	Nfkbib	nuclear factor of kappa light polypeptide gene enhancer in B-cells inhibitor, beta
	Nfkbid	nuclear factor of kappa light polypeptide gene enhancer in B-cells inhibitor, delta
	Nfkbiz	nuclear factor of kappa light polypeptide gene enhancer in B-cells inhibitor, zeta
	Nr4a1	nuclear receptor subfamily 4, group A, member 1
	Nr4a2	nuclear receptor subfamily 4, group A, member 2
	Nr4a3	nuclear receptor subfamily 4, group A, member 3
	Orai1	ORAI calcium release-activated calcium modulator 1
	P2ry14	purinergic receptor P2Y, G-protein coupled, 14
	Pdcd1	programmed cell death 1
	Pdcd1lg2	programmed cell death 1 ligand 2
	Per1	period homolog 1 (Drosophila)
	Pex11a	peroxisomal biogenesis factor 11 alpha
	Phf6	PHD finger protein 6
	Pim1	proviral integration site 1
	Pim3	proviral integration site 3
	Pla2g2d	phospholipase A2, group IID
	Plaur	plasminogen activator, urokinase receptor
	Plk2	polo-like kinase 2 (Drosophila)
	Plk3	polo-like kinase 3 (Drosophila)
	Ppp1r10	protein phosphatase 1, regulatory subunit 10
	Ppp1r11	protein phosphatase 1, regulatory (inhibitor) subunit 11
	Ppp1r15a	protein phosphatase 1, regulatory (inhibitor) subunit 15A; myeloid differentiation primary response gene 116

Change in Expression	Gene Symbol	Name
Upregulated in SEA Vβ3$^+$ cells	*Prkab2*	protein kinase, AMP-activated, beta 2 non-catalytic subunit
	Rasgef1b	RasGEF domain family, member 1B; hypothetical protein LOC100044232
	Rel	reticuloendotheliosis oncogene
	Rheb	Ras homolog enriched in brain; similar to RAS-homolog enriched in brain
	Rilpl2	Rab interacting lysosomal protein-like 2
	Rnaset2	ribonuclease T2
	Rrad	Ras-related associated with diabetes
	Sertad1	SERTA domain containing 1
	Siah2	seven in absentia 2
	Skil	SKI-like
	Slamf7	SLAM family member 7
	Slc41a1	solute carrier family 41, member 1
	Spry1	sprouty homolog 1 (Drosophila); similar to sprouty 1
	Srf	serum response factor
	Srgn	serglycin
	Sult2b1	sulfotransferase family, cytosolic, 2B, member 1
	Tagap	similar to T-cell activation Rho GTPase-activating protein; T-cell activation Rho GTPase-activating protein; T-cell activation GTPase activating protein 1
	Tgif1	TGFB-induced factor homeobox 1
	Tgif2	TGFB-induced factor homeobox 2; predicted gene, OTTMUSG00000007704; similar to TGFB-induced factor 2
	Tgoln2	trans-golgi network protein 2; trans-golgi network protein
	Tmem88	transmembrane protein 88
	Tnf	tumor necrosis factor
	Tnfaip3	tumor necrosis factor, alpha-induced protein 3
	Tnfrsf12a	tumor necrosis factor receptor superfamily, member 12a
	Tnfsf11	tumor necrosis factor (ligand) superfamily, member 11
	Tnfsf14	tumor necrosis factor (ligand) superfamily, member 14
	Tnfsf9	tumor necrosis factor (ligand) superfamily, member 9
	Tob2	transducer of ERBB2, 2
	Trib1	tribbles homolog 1 (Drosophila)
	Trim36	tripartite motif-containing 36
	Tsc22d2	TSC22 domain family, member 2
	Tuba1c	tubulin, alpha 1C; predicted gene 6682
	Uprt	uracil phosphoribosyltransferase (FUR1) homolog (S. cerevisiae)
	Utf1	undifferentiated embryonic cell transcription factor 1
	Wsb1	WD repeat and SOCS box-containing 1
	Xcl1	chemokine (C motif) ligand 1
	Zc3h12a	zinc finger CCCH type containing 12A
	Zfp36	zinc finger protein 36
	Zfp36l1	zinc finger protein 36, C3H type-like 1
	Zswim4	zinc finger, SWIM domain containing 4

TABLE 3-1: SEA inhalation rapidly alters expression of multiple genes in Vβ3$^+$ T cells. Mice were challenged with SEA or vehicle and LNs were removed 40 min after the challenge. The cells were sorted for Vβ3$^+$ and Vβ14$^+$ cells and the total RNA from the sorted cells was used for transcriptome sequencing analysis. Expression of genes from SEA-activated Vβ3$^+$ T cells was compared to the expression in vehicle Vβ3$^+$ and SEA Vβ14$^+$ control groups. Genes that had a significantly decreased ($\log_2$ fold change ≤ −1.5) or increased ($\log_2$ fold change ≥ +1.5) expression in SEA-activated Vβ3$^+$ T cells compared to either vehicle Vβ3$^+$ or SEA Vβ14$^+$ T cells in all 3 experiments were selected. The table lists

genes (symbols and names) with decreased (blue) or increased (red) expression in SEA-activated Vβ3$^+$ cells compared to the controls. Data are representative of 3 independent experiments with n=3 per group.

Gene Symbol	Name	Average Log_2 Fold Change
Ccl3	chemokine (C-C motif) ligand 3	N/A
Il4	interleukin 4	N/A
Nr4a1	nuclear receptor subfamily 4, group A, member 1	7.3981
Egr3	early growth response 3	6.7289
Tnf	tumor necrosis factor	6.4014
Egr2	early growth response 2	6.3678
Egr1	early growth response 1	5.4819
Il2	interleukin 2	5.2735
Cd69	CD69 Antigen	4.5872
Ifng	interferon gamma	4.3299
Irf4	interferon regulatory factor 4	3.7978
Tnfaip3	Tumor necrosis factor, alpha-induced protein 3	3.1533
Nfkb1a	nuclear factor of kappa light polypeptide gene enhancer in B-cells inhibitor, alpha	2.5560

TABLE 3-2: Genes enhanced by CD28 signaling are upregulated by T cells after SEA inhalation. The table shows genes with increased expression in SEA Vβ3$^+$ T cells compared to the vehicle Vβ3$^+$ control group that were previously shown to be enhanced by CD28 signaling (138-140). The log_2 fold change is an average of log_2 fold changes in SEA-activated Vβ3$^+$ T cells vs. vehicle Vβ3$^+$ T cells from 3 independent experiments. For some of the genes, log_2 fold change could not be calculated as the expression of these genes was not detected in one or more of the samples in the vehicle Vβ3$^+$ group (labeled N/A). Data are representative of 3 independent experiments with n=3 per group.

Chapter 4: Pulmonary Response Following *S. aureus* Enterotoxin A Inhalation

This work was published in the *American Journal of Physiology – Lung Cellular and Molecular Physiology*, vol. 313, issue 1, pp. 177-191, July 1, 2017 under the title "Therapeutic blockade of CD54 attenuates pulmonary barrier damage in T cell-induced acute lung injury" and was authored by: Julia Svedova, Antoine Ménoret, Payal Mittal, Joseph M. Ryan, James A. Buturla, and Anthony T. Vella.

Abstract

Acute respiratory distress syndrome (ARDS) is a serious, often fatal condition without available pharmacotherapy. While the role of innate cells in ARDS has been studied extensively, emerging evidence suggests that T cells may be involved in disease etiology. *Staphylococcus aureus* enterotoxins are potent T cell mitogens capable of triggering life-threatening shock. We demonstrate that 2 days after inhalation of *S. aureus* enterotoxin A, mice developed T cell-mediated increases in vascular permeability, as well as expression of injury markers and caspases in the lung. Pulmonary endothelial cells underwent sequential phenotypic changes marked by rapid activation coinciding with inflammatory events secondary to T cell priming, followed by reductions in endothelial cell number juxtaposing simultaneous T cell expansion and cytotoxic differentiation. Although initial T cell activation influenced the extent of lung injury, CD54 (ICAM-1) blocking antibody administered well beyond enterotoxin exposure substantially attenuated pulmonary barrier damage. Thus, CD54-targeted therapy may be a promising candidate for further exploration into its potential utility in treating ARDS patients.

Introduction

Despite decades of research, acute lung injury (ALI)/acute respiratory distress syndrome (ARDS) remains an underdiagnosed and undertreated life-threatening condition and accounts for over 10% of all intensive care unit admissions (87). ALI/ARDS is a syndrome of acute lung inflammation that presents with bilateral lung infiltrates, pulmonary edema, and hypoxemia (88). The mechanism of ALI/ARDS involves a pulmonary or extrapulmonary insult such as pneumonia, aspiration, sepsis or major surgery, leading to a recruitment of leukocytes and platelets, release of pro-inflammatory factors, and injury to the endothelial and epithelial layers. Disruption of the pulmonary endothelial barrier ultimately precipitates the characteristic pathophysiological changes of increased vascular permeability, accumulation of protein-rich fluid, and impaired gas exchange (88, 171).

The two most frequent underlying causes are pneumonia and sepsis, with most patients developing ALI/ARDS secondary to an established bacterial, viral or fungal infection (88). Both Gram-positive and Gram-negative bacteria can be involved (172, 173), but previous studies have preferentially focused on Gram-negative bacteria and, more specifically, the effects of their bacterial-derived LPS (174). Importantly, however, there are many cases of ALI/ARDS that are likely associated with Gram-positive bacteria, and *Staphylococcus aureus* in particular, which is a major contributor to morbidity and mortality resulting from serious infections (12, 175). One of the critical virulence factors of *S. aureus* capable of inducing massive inflammation are enterotoxins (10, 176). These superantigens bypass classical antigen presentation processes and instead induce oligoclonal expansion of T cells by bridging MHC II with a specific T cell receptor Vβ chain (10). Superantigens are known for their extreme potency; unlike conventional antigens activating $1/10^4$-10^6 T cells, superantigens can activate up to 1/4 T cells (22). The resultant T cell-induced inflammatory response and cytokine storm (most notably, IL-2, IFNγ and TNF) can have disastrous consequences leading to toxic shock, tissue damage, organ dysfunction and even death (9,

10). Most *S. aureus* strains produce superantigen toxins and recent evidence suggests that they may be involved in a number of serious illnesses, including pneumonia, sepsis, and endocarditis (9, 16). *S. aureus* enterotoxin A (SEA) has been found in patients with sepsis, and its prevalence correlated with infection severity (79, 80). In animal studies, organ damage and lethality caused by S. *aureus* induced bacteremia or necrotizing pneumonia were shown to be superantigen-dependent (85, 96, 177). Furthermore, it was demonstrated that $CD4^+$ T cell activation significantly exacerbated murine lung pathology and impaired bacterial clearance in pneumonia caused by an enterotoxin-producing *S. aureus* strain (178). Thus, *S. aureus* enterotoxins likely play a crucial role in the severity of sepsis, pneumonia, and the associated ALI/ARDS.

Previous studies showed that administration of *S. aureus* enterotoxin in animal models resulted in acute pulmonary inflammation (34, 179-181) and this response appeared to be mediated by T cells (30, 39, 182). In particular, inhalation of *S. aureus* enterotoxin firstly induced a systemic inflammatory response characterized by rapid T cell activation, cytokine and chemokine release, and a T cell-orchestrated recruitment of innate immune cells into the circulation, lymphoid tissues and lung (30, 34, 183, 184). This early response occurring within several hours of *S. aureus* enterotoxin exposure was followed by development of considerable lung pathology at 48 h after inhalation, which was marked by a massive T cell expansion in lymphoid tissues and lung (34, 39). Importantly, no lung pathology was found in the absence of T cells, in particular $CD8^+$ T cells (39). The pulmonary response presented with perivascular and peribronchial inflammation, disruption of terminal vessels and accumulation of proteins, red blood cells and leukocytes in the airways (34, 39, 105, 106). These pathological features strongly resemble the histological findings in ALI/ARDS patients (88, 171), suggesting that *S. aureus* enterotoxin-activated T cells may be capable of inducing ALI/ARDS. Although T cells were previously found to orchestrate both the early inflammatory responses and the subsequent lung inflammation

(30, 39, 183), the mechanism driving the development of vascular permeability is not fully understood.

The goal of the this work was to define how SEA inhalation alters the pulmonary barrier over time and to establish the main molecular players involved in the development of lung injury, in order to identify clinically translatable therapeutic targets. We show that *S. aureus* enterotoxin inhalation caused increased vascular permeability, elevated expression of endothelial and epithelial injury markers, increased caspase expression in lung, and a temporal differential cytokine/chemokine profile distinguishing intrapulmonary and systemic responses. Mechanistically, *S. aureus* enterotoxin triggered rapid activation of pulmonary endothelial cells in the early phase of inflammation, which was followed by significant reductions in endothelial cell number during the late phase of inflammation, marked by massive T cell expansion and cytotoxic differentiation. The early inflammatory responses due to *S. aureus* enterotoxin-induced T cell activation in part determined the extent of pulmonary barrier damage. However, remarkably, lung injury could be mitigated by therapeutic blockade of CD54, also known as intercellular adhesion molecule-1 (ICAM-1), when administered 36 h after initiation of inflammation. Thus, our data show that ALI/ARDS may be treatable with immunotherapeutic agents given hours, or perhaps even days, beyond the onset of inflammatory response.

Results

S. aureus Enterotoxin Inhalation Induces Lung Injury Marked By Cell Death

We have previously shown that upon local inhalation, SEA was detectable in serum within minutes and triggered systemic activation of T cells. This systemic inflammatory response was marked by cytokine and chemokine release, as well as innate cell migration into the circulation and lymphatic tissue (183). Furthermore, activation of SEA-specific αβ T cells induced IL-17 release by γδ T cells, which further aided recruitment of neutrophils into

lung (30). Despite these rapid inflammatory responses occurring within the first 8 h, lung alveolitis manifested only 2 days after SEA inhalation (39). These data suggested that in the time period between the first minutes of systemic T cell activation and the appearance of extensive lung histopathology at 48 h, a communication web was formed between the systemic response and the lung mucosa, ultimately resulting in deterioration of the pulmonary barrier function.

In line with this hypothesis, we tested for increased lung permeability and the appearance of cellular injury markers and cell death following SEA inhalation. Lung permeability was assessed by administering FITC-dextran, i.n. or i.v., and then measuring fluorescence in the serum (lung-to-blood) or in the BAL fluid (blood-to-lung), respectively. While there was no difference in permeability at 24 h in the SEA-treated mice compared to vehicle, permeability was significantly increased by 48 h after SEA (Fig. 4-1, A). Importantly, albumin was also increased in BAL fluid at 48 h (Fig. 4-1, B).

It was previously shown that after *S. aureus* enterotoxin inhalation acute alveolitis correlated with increased T cell and innate immune cell presence in the BAL fluid and lung (30, 34, 39, 105, 180). Here, it is shown that 48 h after SEA inhalation, clusters of SEA-specific $V\beta3^+$ T cells were concentrated at the interstitial areas surrounding bronchioles and perivascular regions (Fig. 4-1, C). Additionally, these specific $V\beta3^+$ T cells co-localized with $CD11b^+7/4^+$ inflammatory innate cells, and this area of inflammation was further characterized by the presence of enlarged $CD169^+$ lung macrophages (Fig. 4-1, C). The dramatic changes in the inflammatory cell number and lung permeability suggested that SEA inhalation could induce injury to pulmonary epithelial and endothelial cells. Indeed, CD54, RAGE, and angiopoietin-2, which are established markers of epithelial and endothelial cell injury in ALI/ARDS (185), were significantly increased in BAL fluid 48 h after SEA inhalation but not at 24 h post-SEA (Fig. 4-1, D).

In a previous report, it was shown that mice lacking T cells (TCR $\beta\delta^{-/-}$ mice) did not develop any lung pathology following SEA inhalation. Furthermore, CD4-depleted WT mice

showed a partial abrogation of the inflammatory response whereas CD8-depleted mice had an almost complete abrogation of pulmonary inflammation (39). These findings suggested that the inflammatory response to SEA could not occur in the absence of T cells. Nevertheless, T cell-independent responses to a *S. aureus* enterotoxin have been reported (153). Therefore, to further establish the role of T cells in SEA-induced pulmonary injury, WT and TCR $\beta\delta^{-/-}$ mice were exposed to SEA or vehicle and BAL fluid was collected 48 h after inhalation. Unlike WT mice, SEA-exposed TCR $\beta\delta^{-/-}$ mice did no show any differences in the total number of BAL fluid cells, albumin concentration as well as the endothelial injury marker angiopoietin-2 (186), when compared to the vehicle control (Fig. 4-2, A), confirming the critical role of T cells in inducing lung injury after SEA inhalation.

It was next hypothesized that the increased number of inflammatory cells and the presence of injury markers in BAL fluid were associated with apoptosis, particularly occurring in tissues with significant T cell expansion, i.e. lung and spleen (39). To test this, SEA- or vehicle-exposed mice received a pan-caspase-binding fluorescent probe prior to sacrifice and the relative fluorescence levels in lung and spleen were measured. Both lung and spleen from SEA-treated mice showed significantly greater fluorescence than control, indicating an increase in cell death in tissues with expanded T cell population (Figs. 4-2, B and C). To confirm that T cells were mediating the observed increase in caspase expression in the lung and spleen, the study was repeated using TCR $\beta\delta^{-/-}$ mice. No differences in relative fluorescence between the tissues were found, demonstrating that T cells are required for the induction of caspases in the lung (Figs. 4-2, B and C). To further validate these findings, lung tissue sections were examined for the presence of active caspase-3, an irreversible marker of cell death (187). Lungs from SEA-treated mice had a greater number of active caspase-3^{+} cells relative to vehicle control (Fig. 4-2, D and E). Thus, SEA inhalation caused clustering of inflammatory cells to the interstitial bronchioles and perivascular regions, expression of epithelial and endothelial injury markers, and an increase in cell death, ultimately giving rise to increased pulmonary permeability.

***S. aureus* Enterotoxin Triggers Early And Delayed Inflammation Which Activates and Subsequently Reduces the Number of Lung Endothelial Cells**

Previous studies showed that development of pulmonary inflammation at 48 h was preceded by a rapid systemic inflammatory response in the first several hours after *S. aureus* enterotoxin inhalation. This response involved activation of enterotoxin-specific T cells, robust cytokine and chemokine release, and a recruitment of innate immune cells into circulation, lymphoid tissues, and lung (30, 34, 183). Our findings in Fig. 4-1, however, suggested that there was no pulmonary injury or change in lung permeability at 24 h. In order to better understand the relationship between the early inflammatory events and development of lung injury at 48 h, we performed a multiplex assay on mouse serum and BAL fluid obtained 4, 14, 24 or 48 h after SEA inhalation. As predicted, SEA induced massive increases in serum cytokines and chemokines 4 h after inhalation (Fig. 4-3). These levels dropped off by 14 h and were not different from the vehicle control by 24 h. In sharp contrast, the proinflammatory cytokines/chemokines in BAL fluid were increased only at 48 h, with the exceptions of CXCL1 and IL-12p40 (Fig. 4-3). The early presence of CXCL1 and IL-12p40 in BAL fluid could not be due to leakage from systemic circulation because, like CXCL1 and IL12-p40, IL-6, G-CSF and CCL2 were markedly elevated in blood at 4 h, but were not found in BAL fluid at the early time points. Therefore, we concluded that CXCL1 and IL-12p40 were likely produced locally rather than permeated from blood to BAL fluid. This finding was consistent with our previous report showing that IL-17 release by pulmonary γδ T cells promotes recruitment of neutrophils to the lung by 8 h after SEA inhalation (30).

To further study pulmonary response diversity prior to the onset of injury, lung cells were obtained from mice 14 or 40 h after SEA or vehicle inhalation, barcoded, stained with heavy metal-conjugated antibodies and analyzed by cytometry by time-of-flight (CyTOF), also known as mass cytometry. The high-dimensional cytometry data were visualized as

colorimetric 2-dimensional ViSNE maps (188), which cluster single-cell data based on similarity in marker expression patterns. Furthermore, because the individual samples were barcoded, pooled, and acquired simultaneously by CyTOF, each map represents all four samples (14 h vehicle, 14 h SEA, 40 h vehicle, 40 h SEA). Using combinations of lineage markers, we identified various lung cell populations to discern which cells were stimulated after SEA inhalation (Fig. 4-4). We first looked at SEA-specific $V\beta3^+$ T cells; however, insufficient numbers of specific T cells could be collected at 14 h, likely due to activation-induced increased adherence to the tissue (189). Nevertheless, $CD8^+V\beta3^+$ and $CD4^+V\beta3^+$ T cells (Fig. 4-5, A) isolated 40 h after SEA inhalation showed upregulation of pSTAT5 and DNA content (Fig. 4-5, B), consistent with activation and proliferation. Interestingly, even non-responding bystander $CD4^+V\beta14^+$ T cells showed some increase in STAT phosphorylation (Figs. 4-5, A and B) but not to the extent of SEA-specific T cells. These findings confirmed that CyTOF could be used to identify changes in cell signaling. $CD11c^+$MHC II^+ dendritic cells (Fig. 4-5, C) were slightly activated at 14 h but more robustly at 40 h as indicated by increased pSTAT3 (Fig. 4-5, D). Notably, $CD45^-CD31^+CD54^+$ endothelial cells (Fig. 4-5, E) had upregulated pSTAT1 and MHC II and some downregulation of IκB as early as 14 h after SEA inhalation (Fig. 4-5, F). These results were replicated in 3 additional independent experiments (Fig. 4-5, G-I). Finally, STAT phosphorylation in other lung cell populations trended with their lineages (Fig. 4-5, J and K). Overall, these data suggest that endothelial cells became activated early but were able to maintain their function as there were no changes in pulmonary permeability or injury markers at 24 h (Fig. 4-1).

To study endothelial cell activation, lung cells were collected 14, 24 or 40 h after SEA or vehicle inhalation, sorted for $CD45^-CD31^+CD54^+$ endothelial cells and then analyzed for gene expression. Sorted cells displayed a number of dynamic changes in response to SEA (Fig. 4-6, A). Expression of integrin *Vcam1* were increased at 14 h (Fig. 4-6, A), likely signifying early activation. Interestingly, the expression of *Nos3* (endothelial nitric oxide

synthase), an enzyme essential to endothelial cell homeostasis (190, 191) was firstly upregulated at 24 h and then downregulated at 40 h (Fig. 4-6, A). Finally, *Icam1* (CD54) expression was increased two-fold over vehicle at 40 h post-SEA inhalation (Fig. 4-6, A). In addition to these sequential phenotype changes in pulmonary endothelial cells, there was a significant reduction in their numbers at 48 h after SEA (Fig. 4-6, B), and endothelial cell percentage inversely correlated with percentage of SEA-specific $V\beta3^+$ T cells in the lung (Fig. 4-6, C). Endothelial cells from SEA-exposed mice also showed increased CD54 and CD95 (Fas) expressions (Fig. 4-6, D), and similarly, SEA-specific $V\beta3^+$ T cells had greater expression levels of CD11a (receptor for CD54) and CD95 (Fig. 4-6, E). Granzyme B was also measured since it was found to increase in cases of septic ALI/ARDS patients (192). Indeed, SEA-specific $V\beta3^+$ T cells were found to have upregulated granzyme B expression (Fig. 4-6, E), but, most importantly, robust levels of granzyme B were detected in BAL fluid at 48 h (Fig. 4-6, F). Thus, as lung permeability manifested at time points beyond 24 h (Fig. 4-1, A), there were coincident increases in markers of cytotoxicity and cell death, particularly granzyme B and CD95.

S. aureus Enterotoxin-Induced Lung Injury Is Dependent on T Cell Costimulation, But Therapy Is Possible Through CD54 Interference

It was previously demonstrated that systemic recruitment of neutrophils and monocytes after *S. aureus* enterotoxin-induced T cell activation was uniquely regulated by TNF and CD28 costimulation (183). Thus, it was hypothesized that preventing early inflammation with CD28 or TNF blockade would minimize the increase in pulmonary permeability. Mice were pre-treated with the CD28 signaling inhibitor CTLA4-Ig, anti-TNF antibody or IgG control 2 h prior to SEA inhalation and at 48 h post-SEA BAL fluid and lung were harvested (Fig. 4-7, A). CTLA4-Ig and anti-TNF pre-treatment significantly reduced BAL fluid cell numbers (Fig. 4-7, B), whereas CTLA4-Ig, but not anti-TNF, decreased the overall proportion of T cells and inflammatory innate cells in the BAL fluid (Fig. 4-7, C;

p=0.043 for CTLA4-Ig and *p*=0.12 for anti-TNF). Importantly, anti-TNF and CTLA4-Ig significantly reduced the presence of albumin and some of the injury and inflammation markers, but CTLA4-Ig was more potent overall at attenuating the lung injury (Fig. 4-7, D). Additionally, CTLA4-Ig decreased the total number of monocytes in lung (Fig. 4-7, E). Thus, early inflammatory responses define in part the severity of *S. aureus* enterotoxin-mediated lung injury.

Despite the role played by early inflammatory responses in influencing the extent of lung injury, therapeutic strategies to block them have limited translational relevance when taking into consideration the typical disease progression and time scales involved, as well as the logistics of diagnosing and treating patients in the hospital. Alternatively, we investigated later events in the SEA-induced response, during which time entry and accumulation of lung T cells is evident. Pulmonary tissue and endothelial cells in particular, can be injured in a number of ways, including mechanisms involving cytokines and direct death pathways such as CD95 signaling (191, 193, 194). Additionally, CD54 was previously shown to enhance leukocyte transmigration and promote cytotoxic T cell function (195-197). Thus, CD95 and CD54 (Fig. 4-6, D) could be essential mediators of pulmonary barrier damage occurring later in the SEA response progression.

We therefore hypothesized that CD95 and/or CD54 blockade would prevent pulmonary barrier leakiness at clinically relevant time points beyond the initiation of inflammation. Thus, 36 h after SEA inhalation mice were treated with anti-CD178 (ligand for CD95; FasL), anti-CD54 or IgG control, and BAL fluid and lung were collected at 48 h (Fig. 4-8, A). While anti-CD178 showed no change in total cell number, anti-CD54 significantly reduced the total number of cells in BAL fluid (Fig. 4-8, B) and also decreased the overall proportion of T cells and inflammatory innate cells present (*p*=0.0012, Fig. 4-8, C). Importantly, anti-CD54 therapy potently decreased the measured injury markers (CD54 and RAGE), inflammatory markers (granzyme B, IFNγ and IL-6), and albumin in BAL fluid (Fig. 4-8, D). Paradoxically, BAL fluid TNF levels were increased with anti-CD54 treatment (Fig.

4-8, D). This overall reduction in inflammation was not limited to soluble factors, since CD54 blockade also reduced the total numbers of SEA-specific Vβ3$^+$ T cells lung (Fig. 4-8, E). Interestingly, anti-CD178 treatment only increased the number of neutrophils in the lung while having no effect on measures of lung injury (Fig. 4-8, D and E). To validate the effect of anti-CD54 on preserving lung barrier integrity, mice were treated with anti-CD54 or IgG control 36 h after SEA inhalation, and lung permeability was measured with FITC-dextran (as described previously) at 48 h. Indeed, the anti-CD54-treated mice showed significantly lower levels of FITC fluorescence in BAL fluid relative to IgG-treated mice, but not statistically different from vehicle control (p=0.27; Fig. 4-8, F). While CD54 blockade reduced total numbers of SEA-specific T cells in the lung by 45% (Fig. 4-8, E), we also observed substantial decreases in BAL fluid IFNγ and granzyme B levels (73% and 76%, respectively) in the treated mice (Fig. 4-8, D). These findings suggest that anti-CD54 therapy might directly diminish T cell cytotoxic potential, in addition to reducing pulmonary T cell infiltration. However, there was no difference in IFNγ and granzyme B expressions by SEA-specific CD8$^+$ T cells (Fig. 4-8, G), suggesting that the synthesis of cytotoxic molecules was not markedly impacted by the therapy. In sum, these findings demonstrate that anti-CD54 therapy significantly attenuates *S. aureus* enterotoxin-mediated lung injury well after the initiation of inflammation.

Discussion

ALI/ARDS is a life-threatening condition that affects approximately 200,000 people in the United States annually, but despite recent advances in supportive care, the mortality rates remain unacceptably high (87, 88, 171). Although many clinical studies investigated various pharmacotherapies for ALI/ARDS, results have been mostly disappointing (8, 171). Thus, there is an urgent need to better understand the mechanisms of tissue injury in order

to design novel treatments for ALI/ARDS, and we propose CD54 as a promising immunotherapeutic target.

While the role of innate cells, particularly neutrophils and macrophages, has been studied extensively in ALI/ARDS (129, 198), the involvement of adaptive immunity, T cells, in particular, is only now beginning to emerge (90). Prior studies showed that ALI/ARDS patients present with greater numbers of lymphocytes in circulation (91) and in BAL fluid (92). Furthermore, the T cell growth factor IL-2 was found to be elevated in BAL fluid of ARDS patients and was strongly associated with increased mortality (93, 94). ARDS alveolar T cells also showed significant increases in activation, proliferation, and cytokine secretion (199). In mouse models of ALI, Th17 cells were shown to be pathogenic (92), while Tregs were essential for recovery (200). Nevertheless, the mechanism of T cell-based pulmonary injury is unclear. Similar to LPS and bleomycin inhalation in mice (201), SEA models acute lung injury but with greater emphasis on the role of T cells. It is important to note that enterotoxins, including SEA, have been detected in the circulation of intensive care unit patients (79), and also in *S. aureus* isolates from individuals with complications from pneumonia (177, 202). This only suggests an association of *S. aureus* enterotoxins with ARDS, but non-human primates exposed to aerosolized enterotoxin exhibited severe pulmonary lesions with lethality in some subjects (98). Thus, there is a critical need to attempt to identify *S. aureus* enterotoxin protein in BAL fluid of ALI/ARDS patients.

To explore the mechanisms governing the development of ALI following *S. aureus* enterotoxin inhalation, we first defined the inflammatory changes that take place in the lung in terms of two distinct phases. The initial response is caused by rapid, oligoclonal T cell activation leading to robust cytokine and chemokine release (Fig. 4-3), and recruitment of neutrophils and monocytes into circulation followed by their appearance in the lung (30, 183). This phase of the response occurs within hours after SEA inhalation. Here we found that the early inflammatory responses were accompanied by changes in cell signaling and the appearance of activation markers of endothelial cells. Upregulation of pSTAT1 and MHC

II (potentially in response to IFNγ stimulation (203, 204)) and changes in mRNA expression levels of integrin *Vcam1* was evident (Figs. 4-5, F and 4-6, A). However, there were no changes in lung permeability or signs of damage noted (Fig. 4-1) and the barrier was also impermeable even to the high levels of circulating cytokines found in the serum at 4 h (Fig. 4-3).

Lung permeability was clearly increased at 48 h (Fig. 4-1, A), which coincides with the second phase of the inflammatory response marked by robust T cell expansion in the lung (39). This occurs just prior to peripheral T cell deletion and anergy, which is a noted outcome of enterotoxin T cell response (43, 44). The change in lung permeability was further accompanied by increased levels of soluble CD54, angiopoietin-2 and RAGE (Fig. 4-1, D), increased expression of caspases (Fig. 4-2) and elevated cytokines and chemokines in BAL fluid (Fig. 4-3). At 40 h after SEA inhalation, the onset of the second phase was marked by changes in signaling events and activation of different pulmonary cell populations (Fig. 4-5). In particular, pSTAT5 expression was increased in T cells and NK cells (Fig. 4-5, G and J), whereas pSTAT3 expression was increased in dendritic cells and alveolar macrophages (Fig. 4-5, H and K). We posit that STAT5 phosphorylation is in response to T cell release of IL-2, while IL-6 release from innate cells promotes STAT3 phosphorylation (203). On the other hand, endothelial cells upregulated *Icam-1* and downregulated *Nos3* transcription (Fig. 4-6, A), suggesting a loss of homeostatic mechanisms and polarization toward a more activated phenotype (190, 205). Finally, this later effect likely portended the reduction of endothelial cells, which also coincided with increased CD54 and CD95 expression (Figs. 2-6, B and D). Thus, lung endothelial cells became activated and later began to disappear, probably by a death process, as *S. aureus* enterotoxin induced T cell activation and expansion.

Taken together, these findings suggested a two-hit mechanism of endothelial cell injury: firstly, pulmonary endothelial cells became activated (Figs. 4-5, F and 4-6, A) due to early inflammatory responses occurring systemically or locally, but the endothelial barrier

remained intact throughout this phase (Fig. 4-1). More specifically, the massive levels of serum cytokines detected at 4 h (Fig. 4-3) or the transiently recruited neutrophils in the lung (30) could activate the endothelial cells without invoking their injury or death. A second hit, coinciding with the systemic and intrapulmonary expansion of SEA-specific T cells, induced the endothelial cells to downregulate homeostatic factors and acquire a more activated and death-prone phenotype, eventually leading to cellular dysfunction and death. Recently, it was proposed that sequential hits to the lung from various insults, such as pneumonia, sepsis, or mechanical ventilation may cause the severe pathology of ARDS. This proposed model for disease etiology and progression is known as the “multiple hit theory” (8). Similarly, animal models of ALI that consist of two inflammatory insults to the lung may better mimic the clinical scenario (206).

To unravel the mechanism responsible for the observed increase in pulmonary permeability, we designed our experimental strategy based on recent data showing that the early inflammatory responses were differentially affected by blocking TNF or CD28 costimulation (183). In the current report, we demonstrate that TNF or CD28 blockade elicited a profound reduction of albumin in BAL fluid as well as diminished inflammation and expression of injury markers in the lung (Fig. 4-7). Thus, although there were no changes in pulmonary permeability initially (Fig. 4-1), early blockade of T cell activation reduced the subsequent lung injury. Consistent with the two-hit injury model, these findings suggested that the activation of endothelial cells due to an initial inflammatory stimulus may not necessarily induce their injury and death but may increase their sensitivity to secondary injury.

Understanding that the initial T cell activation influences lung injury at later time points is undoubtedly important; however, it may be difficult to translate these findings into clinical care, since delivering early therapy during the initial insult is often not possible. Previous studies attempting to reduce the inflammatory response after *S. aureus* enterotoxin inhalation administered therapy prophylactically or immediately after toxin exposure (207-

210). Alternatively, we sought a therapeutic approach to reduce *S. aureus* enterotoxin-induced lung injury in a scenario mimicking a clinical setting wherein enterotoxin inhalation preceded initiation of therapy by many hours. Because CD95 and CD54 were upregulated on endothelial cells after SEA inhalation (Fig. 4-6, D), we administered blocking antibodies targeting CD178 and CD54 at 36 h post-SEA. Previous studies found that both CD95 and CD178 were elevated in BAL fluid of ALI/ARDS, and the CD95/CD178 pathway may be critical for inducing epithelial cell injury (86, 192, 211, 212). However, with the exception of increasing lung neutrophil numbers (Fig. 4-8, E), blocking CD178 had no effect on lung injury measures in our model (Fig. 4-8, B-D). In sharp contrast, CD54 blockade profoundly reduced pulmonary injury, by means of decreasing BAL fluid cell number, preventing increases in proinflammatory cytokine release, minimizing expression of markers of endothelial and epithelial cell damage, and reducing lung permeability (Fig. 4-8). Being a costimulatory molecule, CD54 is expected to inhibit T cell activation at the time of antigen presentation (213-216), but our results show that many hours after SEA-induced activation, CD54 plays an active role in shaping T cell responses. In particular, specific T cell numbers were significantly reduced after CD54 therapy (Fig. 4-8, E). In addition to reducing T cell expansion in lung, another proposed mechanism by which CD54 blockade might maintain the lung barrier is based on data showing that CD54 was important for enhancing cytotoxic function of lymphocytes (194, 217, 218). Similarly, we observed substantial reductions in granzyme B and IFNγ in the BAL fluid of anti-CD54-treated mice (Fig 2-8, D). Intriguingly, there was no difference in the cytotoxic potential of SEA-specific $CD8^+$ T cells after CD54 therapy (Fig. 4-8, G), suggesting effector T cell differentiation was not markedly impaired. Rather than the synthesis, anti-CD54 therapy could be involved in regulating the release of cytotoxic and inflammatory molecules (196). Finally, although SEA-induced lung injury is T cell-dependent (Fig. 4-2), other cell populations, including inflammatory innate cells are recruited to lung (Fig. 4-1, C). Therefore, anti-CD54 could also ameliorate the SEA-induced lung injury by affecting other cell types, such as neutrophils and monocytes. Although

recruitment of neutrophils and monocytes to lung was no affected by anti-CD54 (Fig. 4-2, E), the treatment could affect the function of these cells, such as reactive oxygen species production (219). CD54-targeted therapy was previously shown to attenuate pulmonary damage in two models of neutrophil-dependent lung injury (220, 221) and anti-CD54 antibody (enlimomab) has already been tested in several clinical trials (e.g. transplantation, burn injuries and refractory rheumatoid arthritis) (222-224). Therefore, anti-CD54 may be a potential therapeutic target for ALI/ARDS worthy of further investigation. Finally, taking into account the role of CD54 in leukocyte migration during injury or infection (197), it will be important to accurately define therapeutic windows for CD54-blocking therapies given to ALI/ARDS patients. Furthermore, determining the molecular players downstream of CD54 engagement may also enable development of more targeted treatment options.

The utility of CD54 therapy is well matched to a typical ALI clinical scenario. A patient suffering from a severe pneumonia or trauma may experience over-activation of the immune system and/or direct damage to the tissue, resulting in impaired lung barrier defenses. This deficit may predispose the patient to additional insults such as toxins and danger- and pathogen-associated molecular patterns that can give rise to systemic inflammatory response syndrome and/or ALI with T cells likely playing a crucial role (225). An excellent example is the appreciation of *S. aureus* enterotoxins in septic patients (79-81). Here, *S. aureus* enterotoxin inhalation was found to induce sequential changes in the lung, defined by initial rapid endothelial cell activation coinciding with inflammatory responses due to T cell priming followed by pulmonary injury and cell death coinciding with T cell expansion in the lung. Importantly, even when administered therapeutically at time points well beyond the inciting inflammatory trigger, anti-CD54 effectively reduced all measures of lung inflammation and injury and restored pulmonary barrier integrity. Thus, an immunotherapeutic agent targeting CD54 pathway may be a suitable treatment option for ALI/ARDS patients, especially in suspected cases of T cell-induced inflammation.

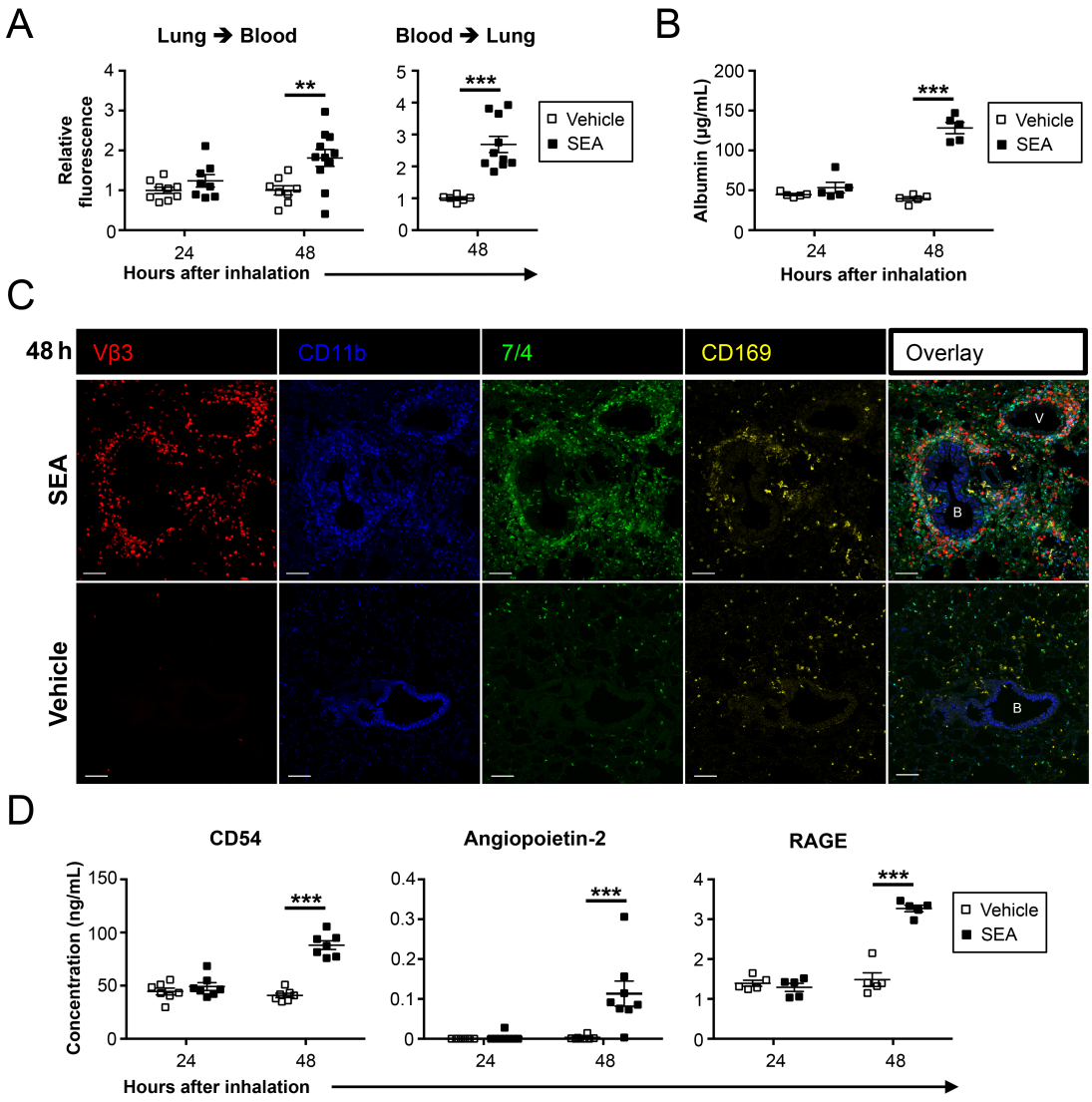

FIGURE 4-1: SEA increases pulmonary permeability, cellular recruitment and expression of epithelial and endothelial markers of injury 2 days after inhalation. *A*) Permeability in the lung was measured by FITC-dextran fluorescence assay. In the left panel, FITC-dextran was administered i.n. and serum was obtained 1 h later (24 and 48 h after SEA or vehicle inhalation). FITC fluorescence was measured in serum and normalized to the vehicle control. At least 3 independent experiments with n=8-11 per group. In the right panel, FITC-dextran was administered i.v. and BAL fluid was obtained 1 h later (48 h after SEA or vehicle). FITC fluorescence was measured in BAL fluid and normalized to vehicle control. Two independent experiments with n=6-10 per group. *B*) Concentration of albumin

in BAL fluid 24 and 48 h after SEA or vehicle inhalation. Three independent experiments with n=5 per group. *C*) Representative confocal microscopy images of lung tissue showing clusters of recruited myeloid cells ($CD11b^+$ $7/4^+$) and SEA-specific T cells ($V\beta3^+$) in proximity to macrophages ($CD169^+$) 48 h after SEA inhalation. B = bronchiole, V = blood vessel. Scale bar = 80 µm. Images are representative of 3 independent experiments with n=4 for vehicle and n=6 for SEA. *D*) Concentration of the lung injury markers CD54, angiopoietin-2 and RAGE in BAL fluid 24 and 48 h after SEA or vehicle inhalation. Three experiments with n=5-8 per group. Data are shown as mean ± SEM. Two-way ANOVA with Sidak's test or unpaired *t* test (for Fig. 1*A*, right panel); $^{**}p<0.01$, $^{***}p<0.001$.

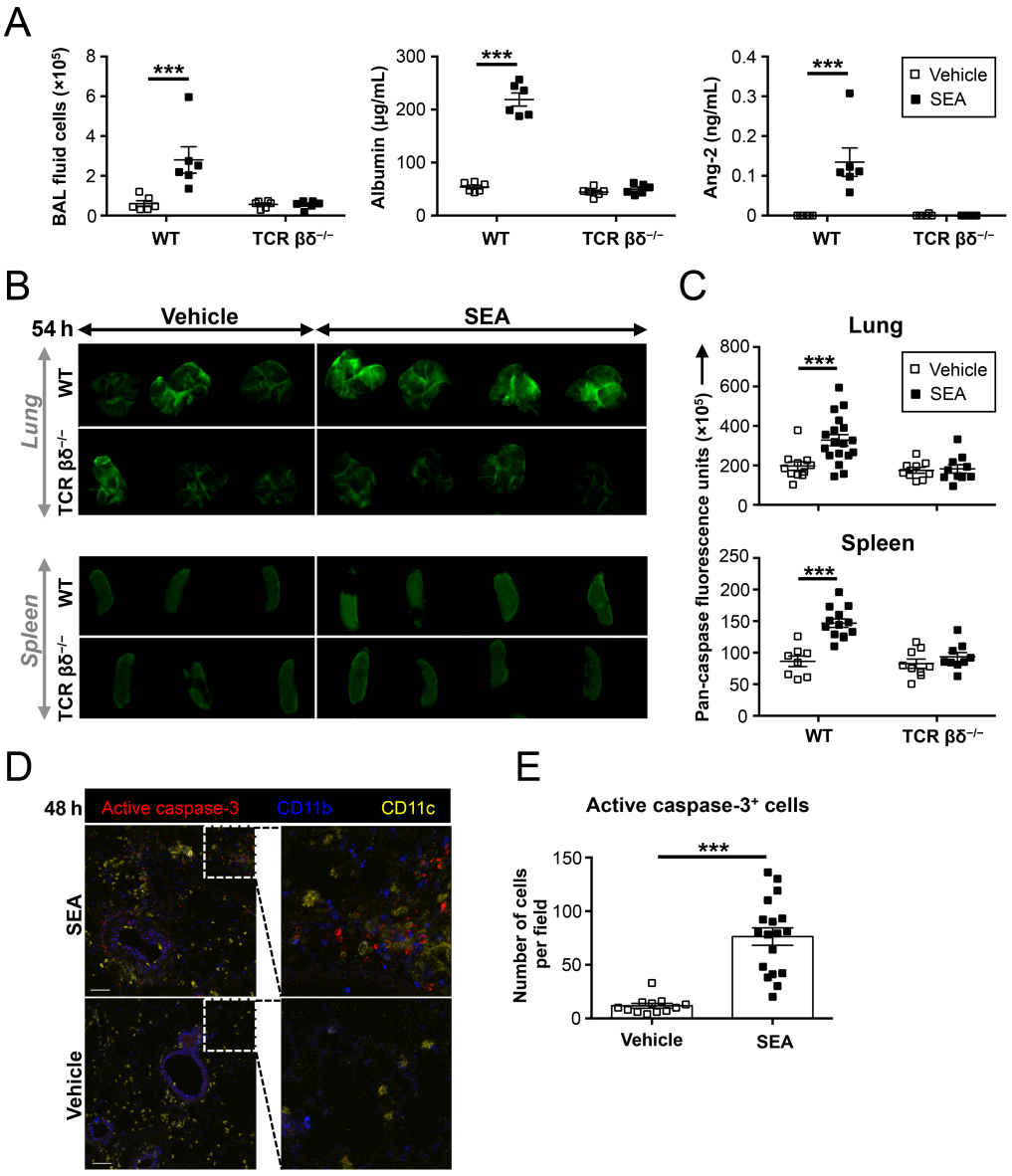

FIGURE 4-2: SEA induces apoptosis in the lung in a T cell-dependent manner. *A)* Number of BAL fluid cells and the concentration of albumin and angiopoietin-2 (ang-2) in BAL fluid 48 h after SEA or vehicle inhalation in WT and TCR $\beta\delta^{-/-}$ mice. Two independent experiments with total n=6 per group. *B*) Apoptosis in the lung and spleen of WT and TCR $\beta\delta^{-/-}$ mice 54 h after SEA or vehicle inhalation as measured by a pan-caspase-binding fluorescent probe. After injecting the probe i.v., tissue was removed and scanned by a fluorescence imager. *C*) Quantification of the pan-caspase-binding fluorescent probe in the

lung and spleen of WT and TCR $\beta\delta^{-/-}$ mice 54 h after SEA or vehicle inhalation. Three independent experiments with n=8-18 mice per group. *D*) Representative confocal microscopy images of lung tissue showing the presence of apoptotic cells (active caspase-3^{+}) 48 h after SEA inhalation. Scale bar = 80 μm. The right panels depict magnified images of the fields indicated in the left panels. *E*) Number of active caspase-3^{+} cells per field. The number of positive cells 48 h after SEA or vehicle inhalation was determined from 3 images per mouse using Imaris (Bitplane). Counts in the SEA mice were performed in areas of inflammation. Data are representative of 3 independent experiments with n=4 for vehicle and n=6 for SEA. Data are shown as mean ± SEM. Two-way ANOVA with Sidak's test or unpaired *t* test (for Fig. 2*E*); ***$p<0.001$.

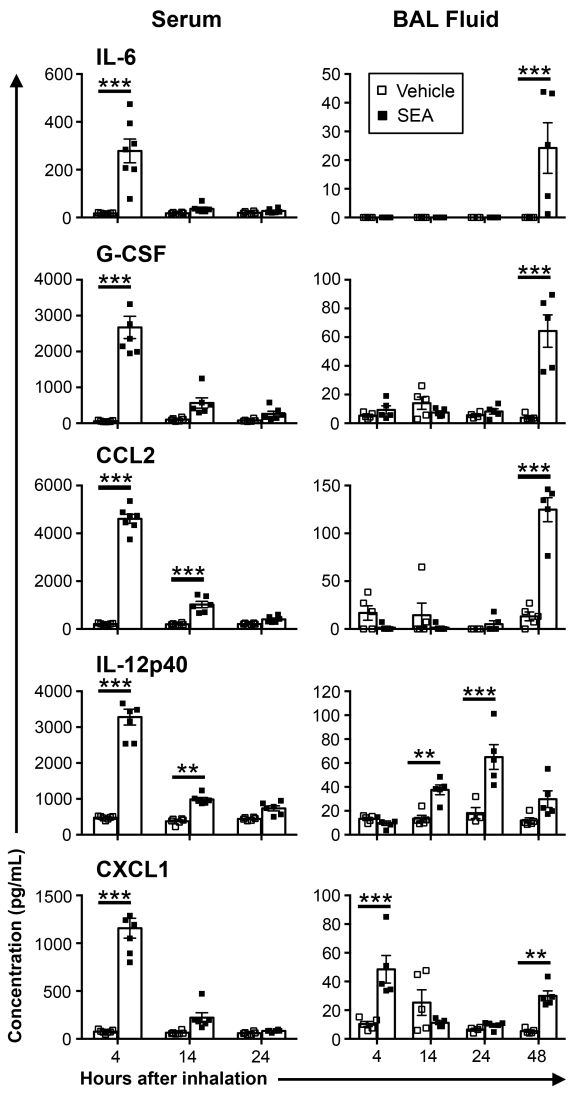

FIGURE 4-3: There are differential patterns of cytokine and chemokine release in BAL fluid vs. serum after SEA inhalation. BAL fluid and serum were collected 4, 14, 24 and 48 h after SEA or vehicle inhalation, and protein levels of various analytes were measured by multiplex immunoassay. Data were combined from 3 independent experiments with n=4-7 per group. Data are shown as mean ± SEM. Two-way ANOVA with Sidak's test; **p<0.01, ***p<0.001.

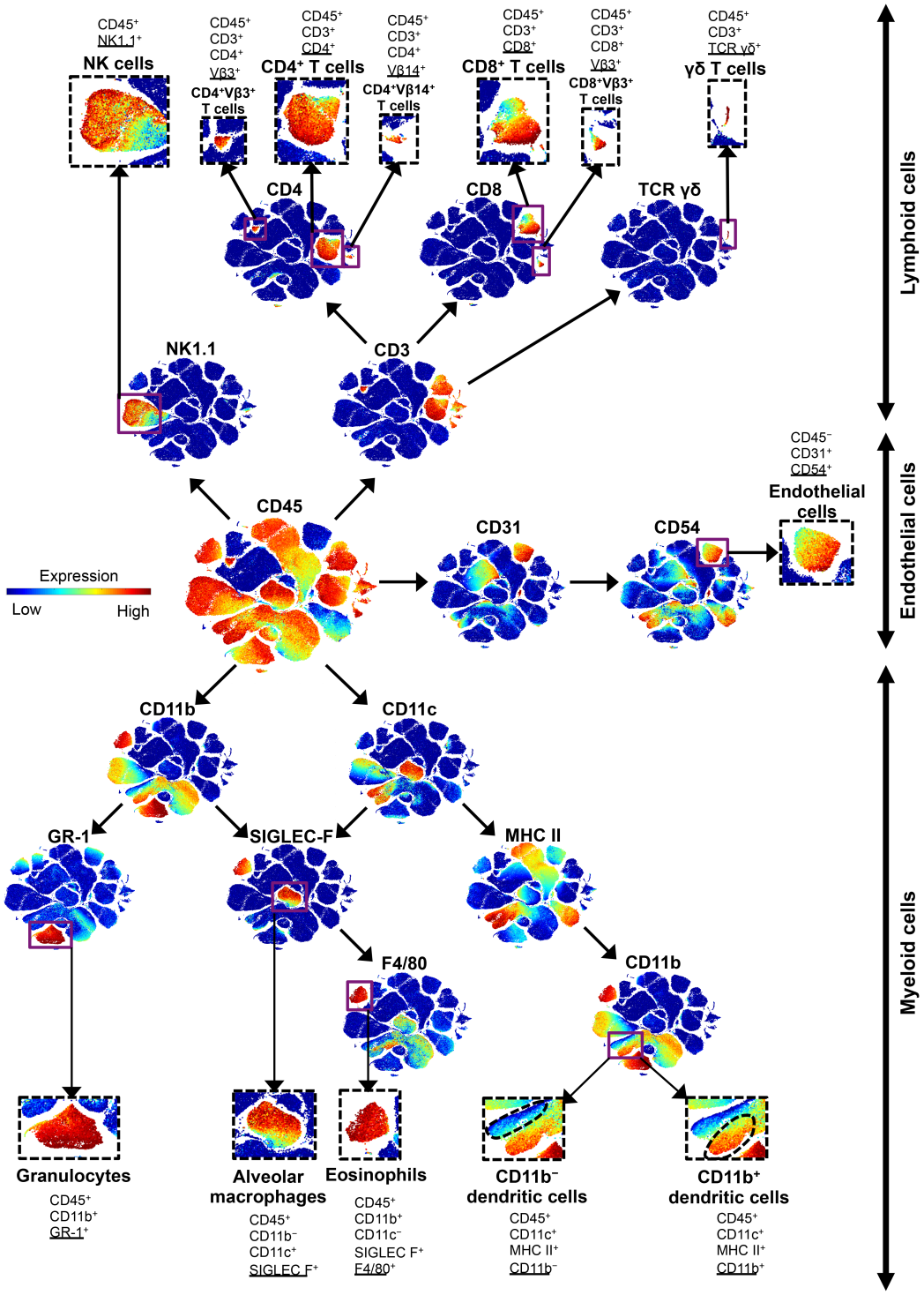

FIGURE 4-4: Gating strategy to identify lung cell populations using ViSNE maps.

Lungs were obtained from mice 14 or 40 h after SEA or vehicle inhalation. Each sample was barcoded, stained with heavy metal-conjugated antibodies and analyzed by mass cytometry

(Helios, Fluidigm). Data were debarcoded, and samples were further subgated to include 33,000 cells and merged to generated the ViSNE maps (Matlab). The VisNE maps identify clusters of cells that are generated according to marker expression patterns. Expression of each marker can be quantified based on the color gradient indicated on the left. The individual clusters in boxes in the periphery of figure 4 are phenotyped with known lineage markers and expression of the underlined marker is shown. The identity of each cluster is indicated in bold letters. Images are representative of 4 independent experiments.

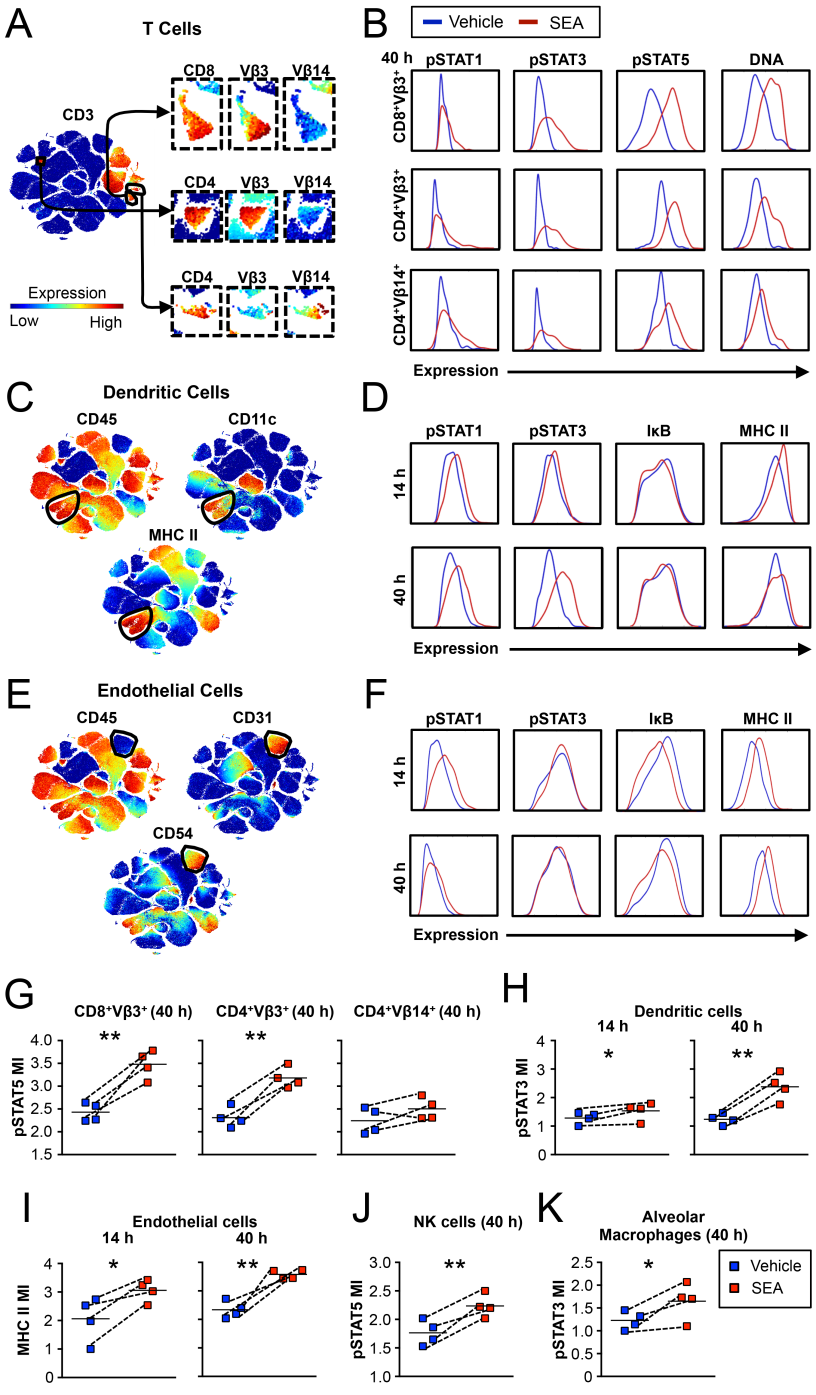

FIGURE 4-5: Endothelial cells become activated prior to the appearance of lung pathology. Lung tissue was obtained from mice 14 or 40 h after SEA or vehicle inhalation. Individual samples were barcoded, pooled and then stained with heavy metal-conjugated antibodies. The pooled sample was analyzed by mass cytometry (Helios, Fluidigm). ViSNE

maps generated using MATLAB were used to represent clusters of cells identified according to expression of markers used in the experiment. Expression of each marker can be visualized based on the color gradient indicated on the left. *A*) ViSNE maps to identify $CD3^+$ cells and subpopulations of $CD3^+$ cells (SEA-specific $CD45^+CD3^+CD8^+V\beta3^+$ and $CD45^+CD3^+CD4^+V\beta3^+$ T cells and bystander $CD45^+CD3^+CD4^+V\beta14^+$ T cells). *B*) Histograms showing the expression of signaling and activation markers in T cells 40 h after vehicle (blue) vs. SEA (red) inhalation. *C*) ViSNE maps identifying dendritic cells ($CD45^+CD11c^+$MHC II^+). *D*) Histograms showing the expression of signaling and activation markers in dendritic cells 14 (top panel) or 40 h (bottom panel) after vehicle (blue) vs. SEA (red) inhalation. *E*) ViSNE maps identifying endothelial cells ($CD45^-CD31^+CD54^+$). *F*) Histograms showing the expression of signaling and activation markers in endothelial cells 14 (top panel) or 40 h (bottom panel) after vehicle (blue) vs. SEA (red) inhalation. *G*) pSTAT median intensity (MI) in T cell populations 40 h after SEA or vehicle inhalation. *H*) pSTAT3 median intensity in dendritic cells 14 or 40 h after SEA or vehicle inhalation. *I*) MHC II median intensity in endothelial cells 14 or 40 h after SEA or vehicle inhalation. *J*) pSTAT5 median intensity in $CD45^+NK1.1^+CD3^-$ NK cells 40 h after SEA or vehicle inhalation. *K*) pSTAT3 median intensity in $CD45^+CD11c^+$SIGLEC F^+ alveolar macrophages 40 h after SEA or vehicle inhalation. Each experiment is represented as a pair of connected symbols (blue square = vehicle; red square = SEA) with a mean shown as a horizontal line. Data are representative of 4 independent experiments with n=4 per group. Paired *t* test; *p<0.05, **p<0.01.

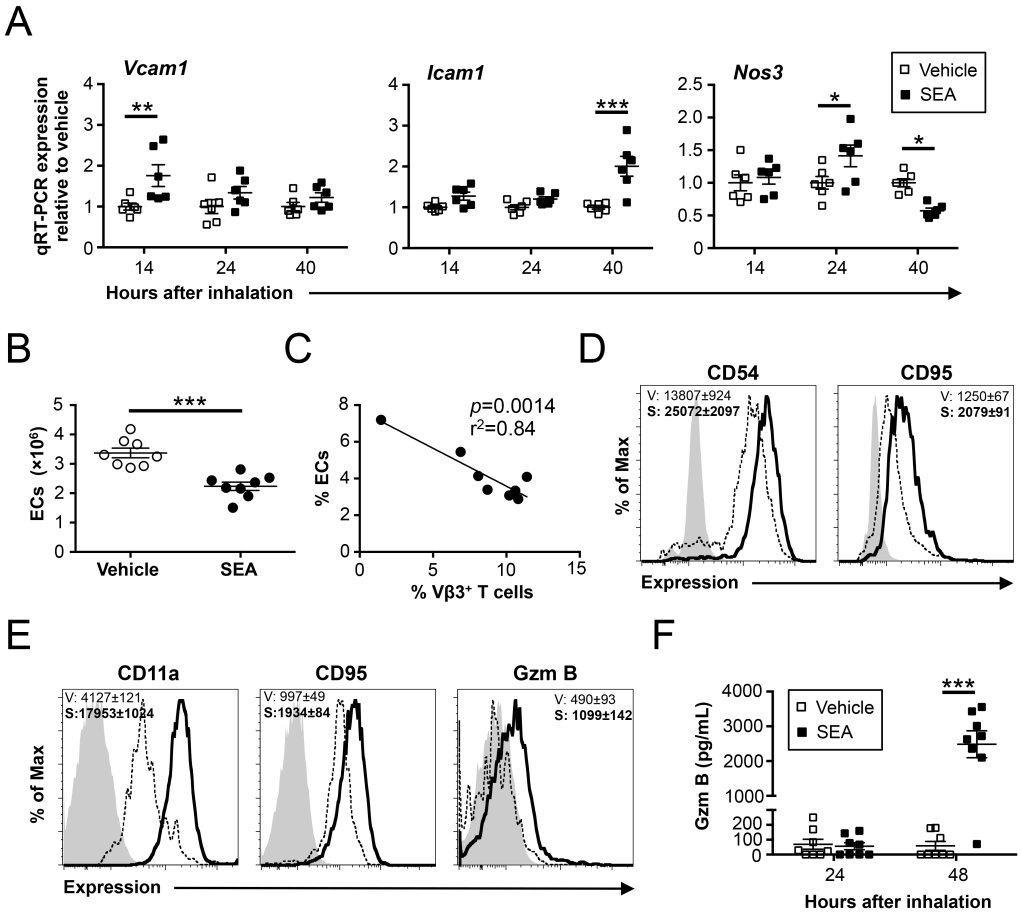

FIGURE 4-6: SEA inhalation causes both early and late changes in endothelial cells.

A) Endothelial cell gene expression 14, 24, or 40 h after vehicle or SEA inhalation. Endothelial cells ($CD45^-CD31^+CD54^+$) were then sorted from total lung cells and lysed to obtain RNA. Gene expression levels are normalized to *Gapdh* and shown relative to vehicle control (set to 1). Three independent experiments with n=6 per group. *B*) Number of lung endothelial cells (ECs; $CD45^-CD31^+$) 48 h after SEA or vehicle inhalation as measured by flow cytometry. *C*) Correlation between endothelial cell and $CD3^+V\beta3^+$ T cell percentages in the lung 48 h after SEA inhalation. Linear regression curve fit *p* value was calculated via F test. Two independent experiments with n=8 per group. *D*) Expression of surface CD54 and CD95 on endothelial cells ($CD45^-CD31^+$) 48 h after SEA or vehicle inhalation. *E*) Surface expression of CD11a and CD95 and intracellular expression of granzyme B (Gzm B) in

$CD3^+V\beta3^+$ T cells 48 h after SEA or vehicle inhalation. Histograms are representative of 2 independent experiments with n=8 per group. Median fluorescent intensities in the upper corner of each histogram are shown as average ± SD of 1 out of the 2 experiments. Isotype control (gray), vehicle = V (black dashed line), SEA = S (black thick line). *F*) Granzyme B concentration in BAL fluid of SEA or vehicle-treated mice 24 and 48 h after inhalation. Three independent experiments with n=8 per group. Data are represented as mean ± SEM. Two-way ANOVA with Sidak's test or unpaired *t* test (for Fig. 5*B)*; **p*<0.05, ***p*<0.01, ****p*<0.001.

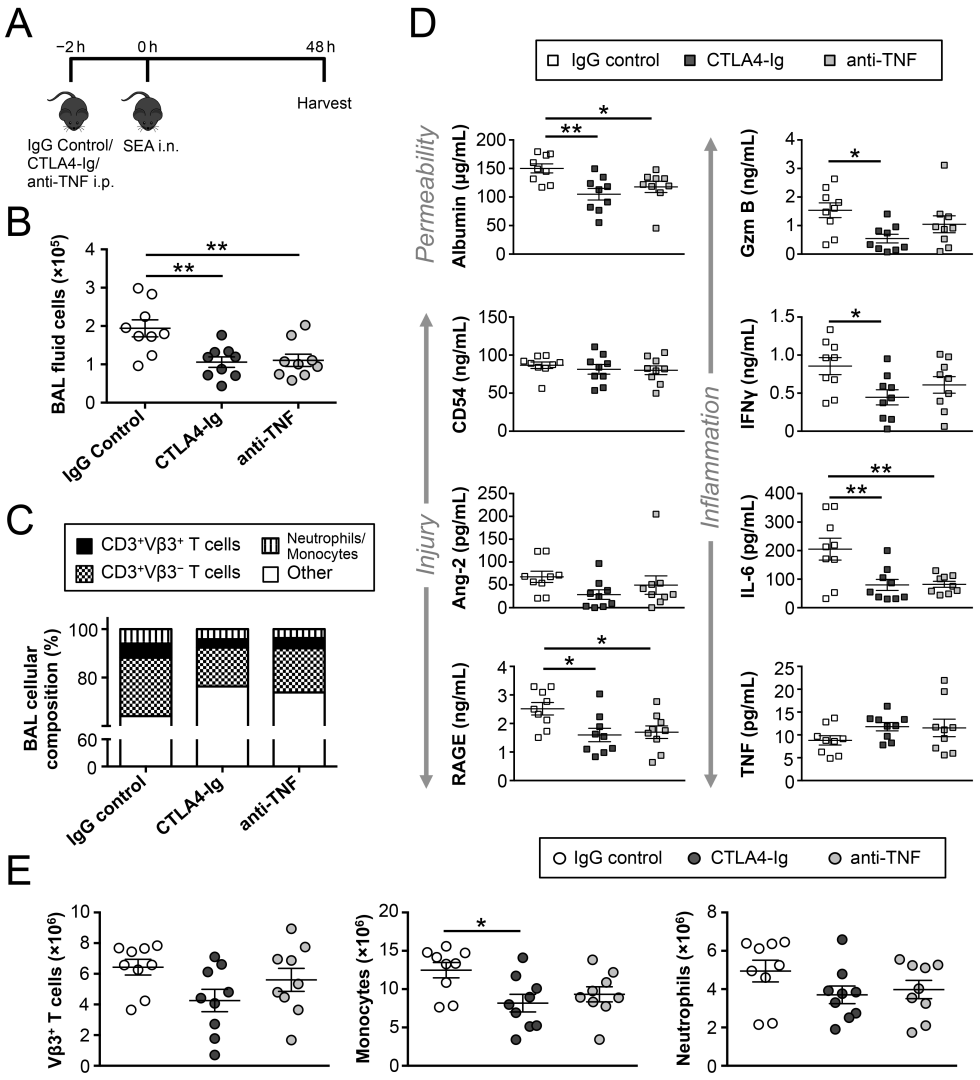

FIGURE 4-7: Blocking T cell activation with CTLA4-Ig or anti-TNF in part attenuates measures of lung permeability, cell injury and inflammation after SEA inhalation. *A*) Diagram of experimental set-up. Mice were treated with CTLA4-Ig, anti-TNF or IgG control 2 h prior to SEA inhalation. BAL fluid and lung tissue were obtained 48 h after SEA inhalation. *B*) Total number of BAL fluid cells pre-treated with IgG control, CTLA4-Ig, or anti-TNF as described in "*A*". *C*) Composition of cells within the BAL fluid following IgG control, CTLA4-Ig, or anti-TNF pre-treatment. Average percentages of $CD45^+CD3^+V\beta3^-$ T cells, $CD45^+CD3^+V\beta3^+$ T cells, neutrophils ($CD45^+CD11b^+Ly6C^+Ly6G^+$) and monocytes ($CD45^+CD11b^+Ly6C^+Ly6G^-$) in BAL fluid are represented by stacked bars. *D*) Concentrations of injury markers angiopoietin-2 (ang-2), RAGE, CD54), inflammatory markers granzyme B (gzm B), IFNγ, IL-6, and TNF, and albumin in BAL fluid from mice pre-treated with IgG control, CTLA4-Ig, or anti-TNF. *E*) Total number of $V\beta3^+$ T cells, monocytes and neutrophils in lung in mice pre-treated with IgG control, CTLA4-Ig, or anti-TNF. Data are represented as mean ± SEM. Three independent experiments with n=9 per group. One-way ANOVA with Dunnett's test; *p<0.05, **p<0.01, ***p<0.001.

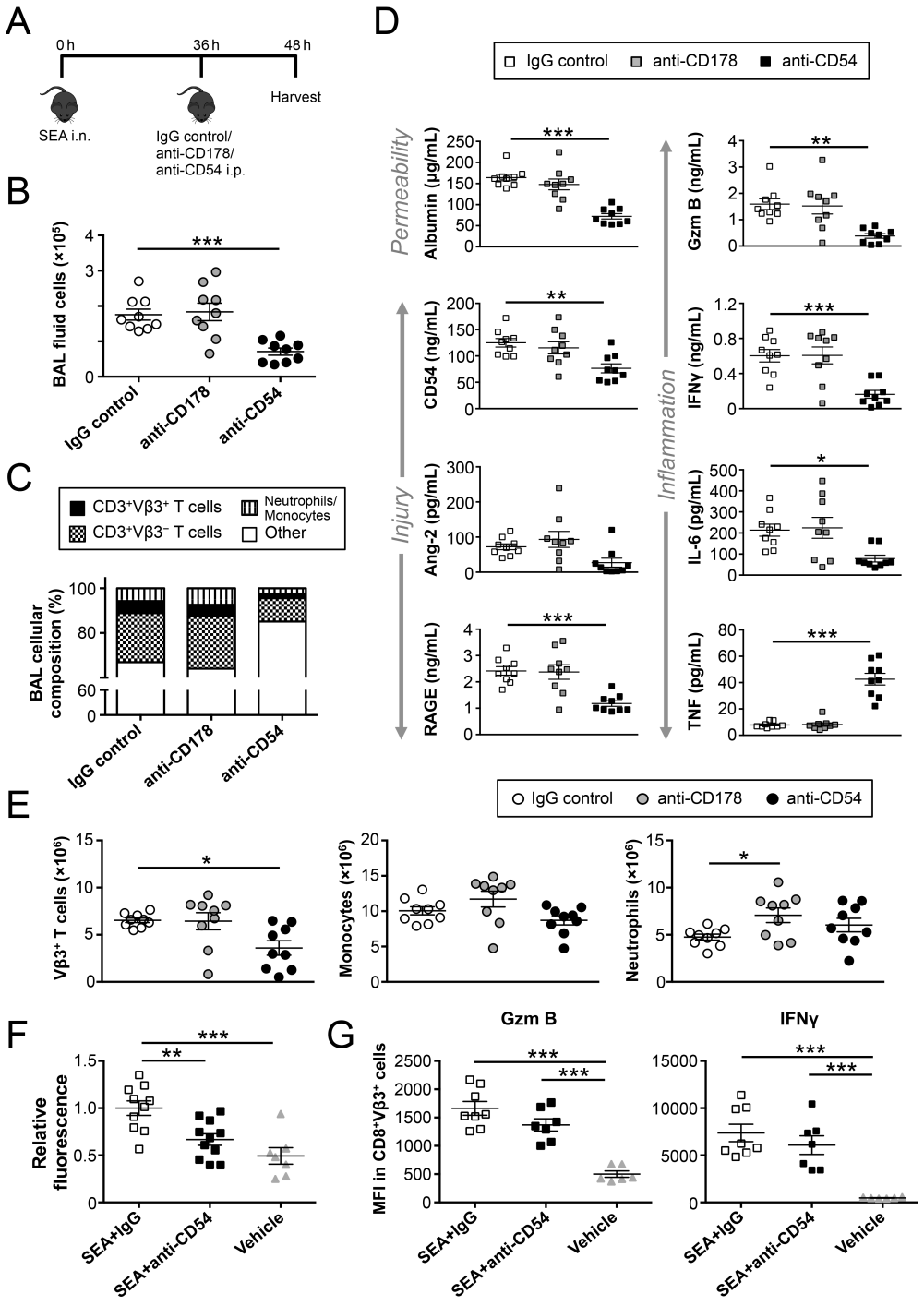

FIGURE 4-8: Delayed CD54 blockade substantially minimizes lung permeability, cell injury and inflammation after SEA inhalation. *A*) Diagram of experimental set-up. Mice were administered SEA i.n., then they were treated with IgG control, anti-CD178 or anti-CD54 i.p 36 h later. BAL fluid and tissue were obtained 48 h after SEA inhalation. *B*) Total

number of BAL fluid cells from mice treated with IgG control, anti-CD178, or anti-CD54 as described in "*A*". *C*) Composition of cells within the BAL fluid following IgG control, anti-CD178, or anti-CD54 treatment. Average percentages of $CD45^+CD3^+V\beta3^-$ T cells, $CD45^+CD3^+V\beta3^+$ T cells, neutrophils ($CD45^+CD11b^+Ly6C^+Ly6G^+$) and monocytes ($CD45^+CD11b^+Ly6C^+Ly6G^-$) in BAL fluid are represented by stacked bars. *D*) Concentrations of injury markers angiopoietin-2 (ang-2), RAGE, and CD54, inflammatory markers granzyme B (gzm B), IFNγ, IL-6, and TNF, and albumin in BAL fluid from mice treated with IgG control, anti-CD178, or anti-CD54. *E*) Total number of $V\beta3^+$ T cells, monocytes and neutrophils in lung in mice treated with IgG control, anti-CD178, or anti-CD54. Three independent experiments with n=9 per group. *F*) Lung permeability measured by FITC-dextran permeability assay. Mice were given SEA or vehicle i.n. and the SEA-exposed mice were treated with IgG control or anti-CD54 36 h later. FITC-dextran was administered i.v. 1 h prior to sacrifice. FITC fluorescence was measured in BAL fluid and normalized to IgG-treated mice. Data were combined from 3 independent experiments with n=7-11. *G*) The expression (median fluorescent intensity = MFI) of granzyme B and IFNγ in $CD8^+V\beta3^+$ T cells ($CD45^+CD3^+CD8^+V\beta3^+$). The lung cells were cultured with brefeldin A only (granzyme B) or brefeldin A + PMA/ionomycin (IFNγ) for 5 h and stained with antibodies. Two independent experiments with total n=6-8 per group. Data are shown as mean ± SEM. One-way ANOVA with Dunnett's test (for Fig. 4-8, *B*-*E*) or One-way ANOVA with Tukey's test (for Fig. 4-8, *F* and *G*); $*p<0.05$, $**p<0.01$, $***p<0.001$.

Chapter 5: Alveolar Macrophages in *S. aureus* Enterotoxin A-Mediated Inflammation

The findings of this chapter were published in *ImmunoHorizons*, vol. 1, issue 9, pp. 213-222, November 1, 2017 under the title "CD169^{+} macrophages restrain systemic inflammation induced by *Staphyloccocus aureus* enterotoxin A lung response." The article was written by Julia Svedova, Antoine Ménoret, Stephen T. Yeung, Masato Tanaka, Kamal M. Khanna, and Anthony T. Vella.

Abstract

Alveolar macrophages (AMs) are considered the first line of defense in the airways. Exposure to harmful substances and certain infections can lead to dysfunction or depletion of AMs. Importantly, these conditions have been associated with increased risk of sepsis and acute lung injury. *Staphylococcus aureus* enterotoxins are superantigens that induce oligoclonal activation of T cells and a robust cytokine release, leading to systemic inflammatory response and tissue injury. This study investigated the relationship between *S. aureus* enterotoxins and AMs. Following inhalation, *S. aureus* enterotoxin was preferentially bound to AMs and the binding was independent of MHC II. Furthermore, the enterotoxin was internalized and its presence in the cells decreased by 24 h after exposure. Ablation of AMs in CD169-DTR mice was associated with increased activation of enterotoxin-specific T cells and enhanced cytokine release into circulation. Thus, conditions causing depletion of AMs may increase the risk of *S. aureus* enterotoxin-induced diseases.

Introduction

Alveolar macrophages (AMs) are specialized tissue-resident cells that play a crucial role in lung development, homeostasis, and immune surveillance. Their unique position in the lung alveoli enables them to sample pathogens, inhaled particulates and other

environmental cues. Their reciprocal interactions with neighboring cells through various receptors and cytokine/chemokine axis can then alarm the immune system and orchestrate responses to remove potential threats and respond to tissue injury, making them the first line of pulmonary immune defense (226, 227). AMs have been shown to play a critical anti-inflammatory role in a number of disease animal models, including influenza, asthma, and acute lung injury (228-233) but they could be also pro-inflammatory (234, 235).

AMs are a relatively stable population of cells with very slow turnover rate; however, if the injury is severe enough, AMs may be depleted and later replenished from circulating monocytes or from *in situ* proliferation (226, 227). Exposure to various substances, pathogens and their products may lead to AM depletion or impaired function; these include influenza (236), bacterial pneumonia (237) cigarette smoke (238), anesthesia (239), diabetes (240), or alcohol consumption (241). Importantly, many of these conditions or exposures have been associated with increased risk of serious infections and development of systemic inflammatory response syndrome (SIRS)/sepsis and acute respiratory distress syndrome (ARDS). In particular, influenza can be complicated by a secondary bacterial pneumonia, which leads to higher rates of hospitalization and death (242). Increased alcohol consumption and cigarette smoke exposure have been associated with increased risk of SIRS/septic shock and ARDS, respectively (243-246). Finally, a number of chronic conditions, particularly diabetes mellitus, and immunosuppressive state are well-described comorbidities in sepsis patients (7, 72, 247). Altogether, these studies suggest that depletion or impaired function of AMs may be associated with increased risk of serious infection, sepsis and ARDS.

Staphylococcus aureus enterotoxins are a group of potent bacterial toxins that bypass the classical antigen processing and presentation, directly bind to MHC II on antigen-presenting cells and crosslink it with specific Vβ chains of T cell receptors. This unique feature of the so-called superantigens induces a massive inflammatory response marked by oligoclonal T cell activation and cytokine storm (10, 111). Superantigens have

been established as the mediators of toxic shock syndrome, a type of systemic inflammatory response, which can lead to tissue injury, shock and even death (9, 36). However, recent evidence suggest that they may be involved in a number of diseases, including pneumonia, endocarditis, and sepsis (9, 85, 96, 177). In fact, superantigens and superantigen-expressing *S. aureus* strains have been recovered from septic patients (79-81). *S. aureus* enterotoxins likely spread systemically from focal sites of infection rather than being directly produced in the bloodstream, as hemoglobin peptides were shown to inhibit superantigen production (9, 99, 100). The most common colonization site of *S. aureus* is the anterior nares (11); therefore, exposure to aerosolized or inhaled S. aureus enterotoxin may well mimic the route of dissemination. Accidental exposure to aerosolized *S. aureus* enterotoxin in humans was reported to cause systemic symptoms of fever, chills, headache, myalgia, cough, dyspnea, vomiting and diarrhea in humans (104). In non-human primates, aerosolized lethal doses of *S. aureus* enterotoxin caused severe pulmonary lesions and death in some subjects (98). Finally, *S. aureus* enterotoxin inhalation in mice was shown to cause systemic inflammatory response, involving rapid activation of T cells, cytokine release, recruitment of innate cells and subsequent lung injury (34, 39, 183).

The relationship between AMs and *S. aureus* enterotoxins has not been fully explored. *In vitro* stimulation of human AMs with *S. aureus* enterotoxin A (SEA) induced IL-8 production in a dose-dependent manner (248). In another *in vitro* study, addition of macrophages (AMs or peritoneal macrophages) reduced proliferation of SEA-activated T cells via nitric oxide production (249). Although there is only a limited direct link between AMs and *S. aureus* enterotoxins, indirect evidence exists that shows a relationship between superantigens and conditions that deplete AMs. In particular, several reports from the 1980s described development of toxic shock syndrome in patients with influenza and influenza-like illness (250, 251). Furthermore, a recent study showed that the combination of cigarette smoke exposure and *S. aureus* enterotoxin B (SEB) induced greater extent of pulmonary inflammation than cigarette smoke or SEB alone (252). Based on these findings, we

hypothesized that AMs play a critical role in the inflammatory responses triggered by *S. aureus* enterotoxin inhalation.

Here we show that SEA was taken up by AMs upon inhalation and the enterotoxin was found intracellularly and not on cell surface. Perhaps surprisingly, this binding was independent of MHC II expression as SEA was similarly taken up by AMs of WT and MHC $II^{-/-}$ mice. AMs in the murine lung express sialoadhesin, also known as CD169 on their surface (229, 253). Thus, to study the role of AMs, CD169-diphteria toxin receptor (DTR) mice were treated with diphtheria toxin (DT) and then exposed to SEA. The absence of AMs was associated with increased CD25 expression on SEA-specific T cells but this effect was only observed when lower concentrations of SEA were administered. Finally, SEA-exposed CD169-DTR mice also showed a significantly greater cytokine secretion to blood compared to WT mice. Thus, AMs may represent a defense mechanism against *S. aureus* enterotoxins as their depletion may increase the severity of toxic shock or other *S. aureus* enterotoxin-induced diseases.

Results

S. aureus enterotoxin preferentially binds to alveolar macrophages in MHC II-independent manner

One of the crucial properties of *S. aureus* enterotoxins is their ability to rapidly induce oligoclonal activation of T cells, which is accompanied by a massive inflammatory response and cytokine storm (10). However, how SEA and other enterotoxins spread systemically, especially from the airways as anterior nares are a common site of *S. aureus* colonies (11) is not fully understood. In our previous studies we uncovered that SEA permeates into blood immediately after inhalation and is found in the serum rather than bound to cells (183). The ability to access circulatory system from airway mucosa is likely an important feature that enables the toxin to spread systemically and activate T cells in lymphoid tissues within

minutes of inhalation (30, 183). Furthermore, using a titration curve, the concentration of SEA in serum after inhalation was estimated to be only a small fraction of the total amount inhaled by a mouse (~ less than 1/35; unpublished data shown in Fig. 3-2). Intriguingly, in another report using mass spectrometry, we showed that SEA could be recovered from BAL fluid at 16 h after inhalation and the toxin preserved its biological activity (254). These findings suggested that when SEA is inhaled, only a small portion enters the circulation while the remainder may be retained in the lung mucosa or perhaps neutralized by various defense mechanisms, such as defensins or phagocytosis.

Therefore, we sought to determine whether SEA binds to a certain cell population within the pulmonary tissue. Lung was obtained from mice 8 h after SEA or vehicle inhalation and examined by confocal microscopy for SEA using polyclonal anti-SEA antibody. Only mice exposed to SEA displayed cells that were SEA^+ (Fig. 5-1, A and B), confirming the specificity of the antibody. Surprisingly, it was found that SEA was preferentially bound to $CD11c^+CD169^+$ AMs (Fig. 5-1, A). In fact, a total of 87% of SEA^+ cells were also positive for CD11c and 64% were both $CD11c^+$ and $CD169^+$ (Fig. 5-1, C). To further define SEA binding to AMs, BAL fluid was obtained from mice 1, 4, or 24 h after SEA inhalation and BAL AMs defined as $CD45^+CD11c^+$SIGLEC F^+CD169^+ (Fig. 5-1, D) were stained for SEA. Importantly, no SEA was detected on the surface of AMs; however, there was a significant increase in SEA presence intracellularly peaking at 4 h (Fig. 5-1, E and F). Interestingly, there was no significant difference detected at 24 h after SEA (Fig. 5-1, F). Similar results were obtained when AMs from lung tissue were analyzed (Fig. 5-2, A). In contrast, lung dendritic cells showed increased SEA expression only at 24 h both on the surface and intracellularly (Fig. 5-2, B).

S. aureus enterotoxins are known for their ability to directly bind to MHC II molecules and crosslink them with specific Vβ chains of TCRs leading to a systemic inflammatory response (10). However, AMs were reported to only express low levels of MHC II under homeostatic conditions (226, 255) with MHC II expression increasing during an inflammatory

response, particularly in the presence of IFNγ (256). Furthermore, AMs tend to be poor antigen-presenters and may, in fact, inactivate T cells (257, 258). These findings suggested that SEA binding to AMs could be MHC II-independent. To assess whether SEA binds to AMs in MHC II-independent fashion, lung tissue was harvested from WT and MHC $II^{-/-}$ mice 8 h after SEA inhalation and analyzed by confocal microscopy. There was no difference in the number of SEA^+ cells between WT and MHC $II^{-/-}$ mice (Fig. 5-3, A and B). In addition, SEA^+ cells colocalized with CD11c marker with a similar frequency (Fig. 5-3, C). Finally, only a small fraction of SEA^+ cells colocalized with MHC II (Fig. 5-3, D) and in fact, we observed $CD11c^+$MHC II^+ dendritic cells with no significant SEA binding (Fig. 5-3, A, white arrows). Altogether, these results show for the first time that SEA binds to AMs in MHC II-independent manner.

Depletion of alveolar macrophages is associated with increased T cell activation and cytokine secretion

Next, we wanted to determine whether SEA binding to AMs impacts T cell activation and cytokine production. We hypothesized that AMs sequester a large portion of the inhaled toxin and neutralize it. Thus, AMs could play a protective role in SEA-induced inflammation. To investigate the role of AMs in SEA-induced inflammatory response, we used CD169-DTR mice to selectively deplete $CD169^+$ macrophages after DT administration. Because AMs express CD169 (Fig. 5-1), this technique can be used to study the role of AMs in pulmonary responses (229). Thus, CD169-DTR mice and WT control were treated with DT 2 days prior to SEA or vehicle inhalation. In order to avoid oversaturation of SEA dosage given to mice (which could lead to masking of differences between WT and CD69-DTR mice), the SEA dose was titrated (0.033, 0.1, 0.33, and 1 μg). Blood, lung and spleen were harvested 4 h after SEA or vehicle (0 μg) inhalation. Depletion of $CD169^+$ alveolar macrophages was confirmed in the lung by gating on $CD45^+CD11c^+$SIGLEC F^+CD169^+ cells (Fig. 5-4, A). The overall depletion of AMs was approximately 87% (Fig. 5-4, B). We first investigated the

effect of $CD169^+$ macrophage ablation on CD69 expression on SEA-specific $V\beta3^+$ T cells in the spleen. Interestingly, even with a low dose of SEA (0.033 µg), the percentage of $CD69^+$ $V\beta3^+$ T cells was 88.5% in WT mice and 89.8% in CD169-DTR mice, suggesting that a very small amount of SEA is sufficient to induce CD69 expression on T cells (Fig. 5-4, C and D). Thus, we concluded that CD69 expression might not be a sensitive marker to detect differences in T cell activation. In contrast, CD25 expression on $V\beta3^+$ T cells increased in a dose-dependent manner (Fig. 5-4, F). Importantly, CD169-DTR mice showed significantly greater percentage of $CD25^+$ $V\beta3^+$ T cells when 0.033 and 0.1 µg of SEA was administered (Fig. 5-4, E and F). There was no significant effect on CD25 expression with the higher doses of SEA (0.33 or 1 µg; Fig. 5-4, F). We also investigated the effect of AM ablation on the bystander $V\beta14^+$ T cells. There was no difference in the percentage of $CD69^+$ and $CD25^+$ of $V\beta14^+$ T cells with the exception of a significant increase in $CD25^+$ $V\beta14^+$ T cells in CD169-DTR mice after a dose of 0.033 µg SEA (Fig. 5-4, D and F, right panels).

A hallmark of toxic shock syndrome as well as sepsis is a robust release of cytokines into the bloodstream (36, 259). Therefore, we next investigated whether the depletion of $CD169^+$ macrophages affected cytokine secretion following SEA inhalation. Serum cytokine concentrations were measured by a multiplex assay in DT pre-treated WT and CD169-DTR mice 4 h after vehicle or SEA (0.033 or 0.1 µg) inhalation. There was no significant difference in the levels of serum cytokine when vehicle control was administered. However, following SEA inhalation, CD169-DTR mice had greater concentrations of serum G-CSF, IFNγ, TNF, IL-2, IL-6, and also IL-10 compared to WT mice (Fig. 5-5). These findings show that ablation of AMs is associated with increased expression of CD25 on SEA-specific $V\beta3^+$ T cells and also increased secretion of cytokines into the circulation.

Discussion

Superantigens such as *S. aureus* enterotoxins are potent bacterial toxins that can induce serious inflammatory responses and lethal shock (10). It has been estimated that

most strains of *S. aureus* are capable of producing superantigens (9, 260). However, *S. aureus* is also an extremely common commensal that permanently colonizes about 20% of all individuals (11). Thus, there is a disparity in understanding why *S. aureus* is so common in asymptomatic individuals and simultaneously, it can trigger a life-threatening inflammatory response. Although the mechanisms of how a commensal colonization can become pathogenic are not clear (260), it has been well established that patients who have colonization of anterior nares with *S. aureus* and particularly methicillin resistant *S. aureus* (MRSA) are more susceptible to hospital-acquired *S. aureus* infections (101-103). This suggests that various defense mechanisms must be in place to prevent the spread of the bacteria and limit the effects of the virulence factors; however, these mechanisms may be impaired in immunocompromised individuals in hospital settings.

Indeed, the immune system possesses several strategies to counteract the harmful effects of superantigens. First, It has been hypothesized that the production of antibodies against superantigens is protective and the lack of antibodies may a predisposing factor for the development of *S. aureus* infections and toxic shock syndrome (261-263). In particular, women with toxic shock syndrome had lower antibody titers to TSST-1 compared to healthy women with no prior history of toxic shock syndrome (262). Similarly, immunotherapy using antibodies specific to superantigens was found to be protective in animal models (264-266). In addition to antibodies, it has been shown that lactoferrin, an iron-binding glycoprotein located predominantly in mucosal secretions (267), can attenuate the inflammatory responses triggered by *S. aureus* enterotoxins (254, 268). Here we show that AMs may represent a key cellular defense mechanism that can reduce the effects of *S. aureus* enterotoxin-induced inflammation.

When staining for SEA in the lung tissue, we found that AMs preferentially bound SEA after inhalation and internalized it (Fig. 5-1). Interestingly, the intracellular presence of SEA in AMs increased in the first several hours but was not significantly different at 24 h (Fig. 5-1, F and 5-2, A). In addition, dendritic cells, which were hypothesized to bind a

significant amount of SEA due to their high MHC II expression, showed upregulation of SEA expression on surface and intracellularly only at 24 h after inhalation (Fig 5-2, B). Based on these findings, we postulate that the numerous and highly phagocytic AMs ingest SEA and thus reduce the ability of dendritic cells either in the lung mucosa or in other tissues to take up the antigen and present it. In fact, AMs have been shown to maintain the lung homeostasis by suppressing dendritic cell function (269, 270). The later presence of SEA on pulmonary dendritic cells could perhaps be due to antigen transfer from AMs to dendritic cells (271).

Superantigens, such as *S. aureus* enterotoxins, are known for their ability to bind to MHC II directly without antigen processing, which results in rapid oligoclonal activation of T cells and a cytokine storm (10). In addition, compared to SEB, SEA was found to have a greater affinity for MHC II due to its ability to not only bind the α chain but also the β chain of MHC II with a zinc-dependent binding site, which enabled SEA to stay on cell surface for at least 40 h (26). Interestingly, we found that the binding of SEA to AMs was independent of MHC II expression (Fig. 5-3). Binding of *S. aureus* enterotoxins to molecules other than MHC II have been previously reported. In particular, the costimulatory molecule CD28 and its ligand CD86 are crucial binding sites that enhance the severity of the inflammatory response triggered by *S. aureus* enterotoxin (27-29). Other binding sites for *S. aureus* enterotoxins have been reported, including MHC I (272), digalactosylceramide on kidney proximal tubular cells (273) and Gp130 receptor on adipocytes (274). These studies show that *S. aureus* enterotoxins may bind to several different molecules. Thus, it will be important to determine the identity of the binding site of SEA on AMs as well as the processing of the enterotoxin by these phagocytes.

Previous studies showed that following intranasal *S. aureus* enterotoxin exposure, mice experience a systemic oligoclonal T cell activation and cytokine release to blood (23, 34, 183, 275). To examine the role of AMs in the SEA-induced inflammatory response, WT and CD169-DTR mice were treated with DT and 2 days later, they were exposed to vehicle

or SEA. There was no difference in the expression of activation markers CD25 or CD69 on SEA-specific Vβ3$^+$ T cells as well as no significant change in serum cytokines when mice were administered vehicle control (Fig. 5-4 and 5-5). However, CD169-DTR exposed to SEA showed a significantly greater CD25 expression compared to WT mice (Fig. 5-4, F). This was only observed when lower amounts of SEA were given, suggesting that the higher doses of SEA saturate the level of T cell activation. Indeed, even 0.033 μg of SEA activated almost 90% of SEA-specific Vβ3$^+$ T cells in the spleen (Fig. 5-4, F). These findings emphasize the potency of SEA, which even in a small amount is sufficient to trigger a significant response. Furthermore, we examined the concentrations of serum cytokines commonly associated with toxic shock syndrome and sepsis, in particular, TNF, IFNγ, IL-2, and IL-6 (36, 75, 259). IL-10 and G-CSF were also analyzed. G-CSF, a growth factor that mobilizes neutrophils into circulation during acute inflammation (128), was previously found elevated in patients with bacterial infection (276, 277) while the anti-inflammatory cytokine IL-10 can be released in septic patients in attempt to counteract the hyper-inflammatory response (259). Importantly, SEA-exposed CD169-DTR mice had increased secretion of pro-inflammatory cytokines TNF, IFNγ, IL-2, IL-6 as well as G-CSF demonstrating that AM ablation is associated with enhanced inflammatory response following SEA inhalation (Fig. 5-5). Interestingly, the concentration of anti-inflammatory IL-10 was also elevated in CD169-DTR mice (Fig. 5-5). This is consistent with our previous study showing that SEA simultaneously induced the expression of both pro-inflammatory cytokines IL-2, TNF, and IFNγ and anti-inflammatory IL-10 in SEA-specific Vβ3$^+$ T cells (183). Thus, depletion of AMs was correlated with an overall enhancement of the SEA-induced immune response.

Finally, CD169 is expressed not only on AMs but also other macrophages, including marginal zone macrophages in the spleen and subcapsular sinus macrophages in the LNs (278, 279). Therefore, depletion of macrophage subsets other than AMs could also contribute to the enhanced inflammatory response observed in CD169-DTR mice. Similarly, it is also possible that DT injection and the subsequent cell apoptosis could play a role in the

increased inflammatory response in CD169-DTR mice. Therefore, further studies will be necessary to confirm the causal relationship between AMs and *S. aureus* enterotoxin-induced systemic inflammatory response.

In conclusion, here we show that AMs preferentially bind *S. aureus* enterotoxin in MHC II-independent manner and internalize it. Furthermore, AM ablation in CD169-DTR mice was associated with increased activation of SEA-specific $V\beta3^+$ T cells and enhanced secretion of cytokines into circulation. These findings could explain the development of toxic shock syndrome in patients with influenza infection (250, 251) as well as the increased risk of sepsis and ARDS in chronic alcohol users and smokers, respectively (243-246). Thus, dysfunction or depletion of AMs may be a critical risk factor for the development of *S. aureus* enterotoxin-induced inflammatory diseases.

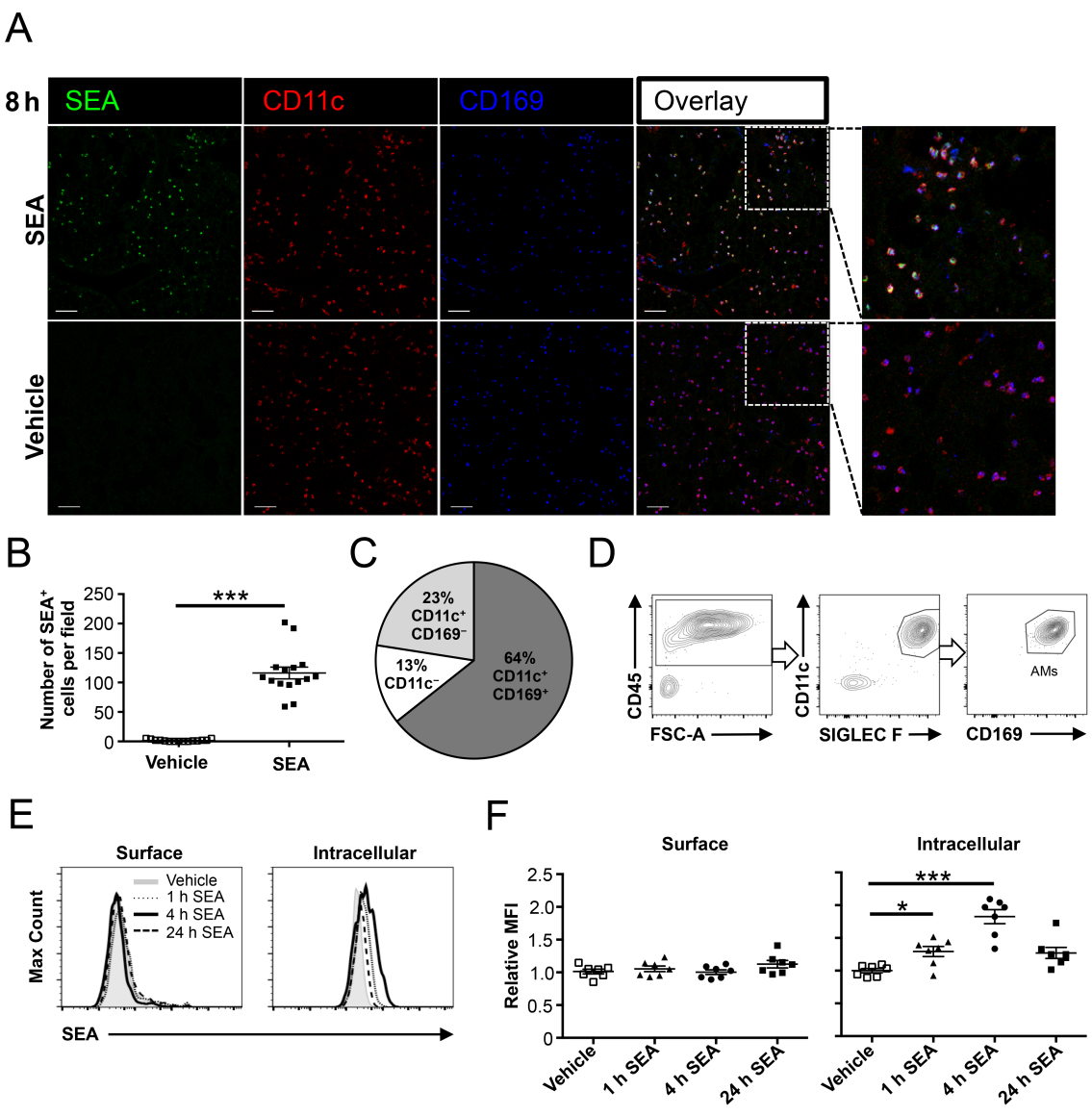

FIGURE 5-1: SEA preferentially binds to AMs upon inhalation. A) Representative confocal microscopy images of lung tissue 8 h after SEA or vehicle inhalation. Lung sections were stained with anti-SEA (green), anti-CD11c (red), and anti-CD169 (blue). Magnified images of the areas marked by white squares in the overlay panels are shown on the left. Size bar = 80 μm. 4 independent experiments with total n=5 per group. B) Number of SEA^+ cells per field. Three images from each mouse were quantified (4 independent experiments with n=5 per group) by Imaris (Bitplane). C) Percentage of $CD11c^+CD169^+$ and $CD11c^+CD169^-$ cells in all SEA^+ cells detected by confocal microscopy 8 h after SEA

inhalation. SEA^+ cells were colocalized with $CD11c^+$ cells and SEA^+CD11c^+ cells were further colocalized with CD169 by Imaris. The average percentage shown in the pie chart was calculated from 3 images per mouse (3 independent experiments with total n=4). D) Gating strategy to identify AMs in the BAL fluid by flow cytometry. BAL fluid was obtained 1, 4, or 24 h after SEA inhalation or from vehicle control (1 or 4 h) and AMs were identified as live $CD45^+CD11c^+$SIGLEC F^+CD169^+ cells. E) Representative histograms showing SEA expression on surface and intracellularly in BAL fluid AMs. F) Relative median fluorescent intensity (MFI) of SEA on surface and intracellularly in BAL fluid AMs 1, 4, or 24 h after SEA inhalation. MFI values are relative to the vehicle control (set as 1). Three independent experiments with total n=7 per group. Data are represented as mean ± SEM. Unpaired *t* test (B) or one-way ANOVA with Dunnett's test (F); **p*<0.05, ****p*<0.001.

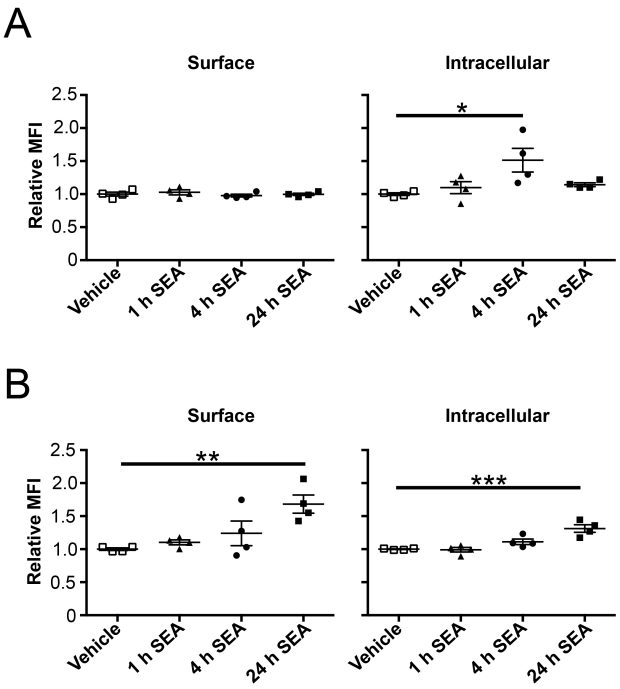

FIGURE 5-2: SEA presence in lung AMs and DCs. Lung tissue was harvested 1, 4, or 24 h after SEA inhalation or from vehicle control (1 or 4 h). AMs were identified as live $CD45^+CD11c^+$SIGLEC F^+CD169^+ cells and DCs as live $CD45^+CD11c^+$SIGLEC F^-MHC II^+. A) Relative median fluorescent intensity (MFI) of SEA on surface and intracellularly in lung

AMs 1, 4, or 24 h after SEA inhalation. B) Relative MFI of SEA on surface and intracellularly in lung DCs 1, 4, or 24 h after SEA inhalation. MFI values are relative to the vehicle control (set as 1). Two independent experiments with total n=4 per group. Data are represented as mean ± SEM. One-way ANOVA with Dunnett's test was used; *p<0.05, ** p<0.01, ***p<0.001.

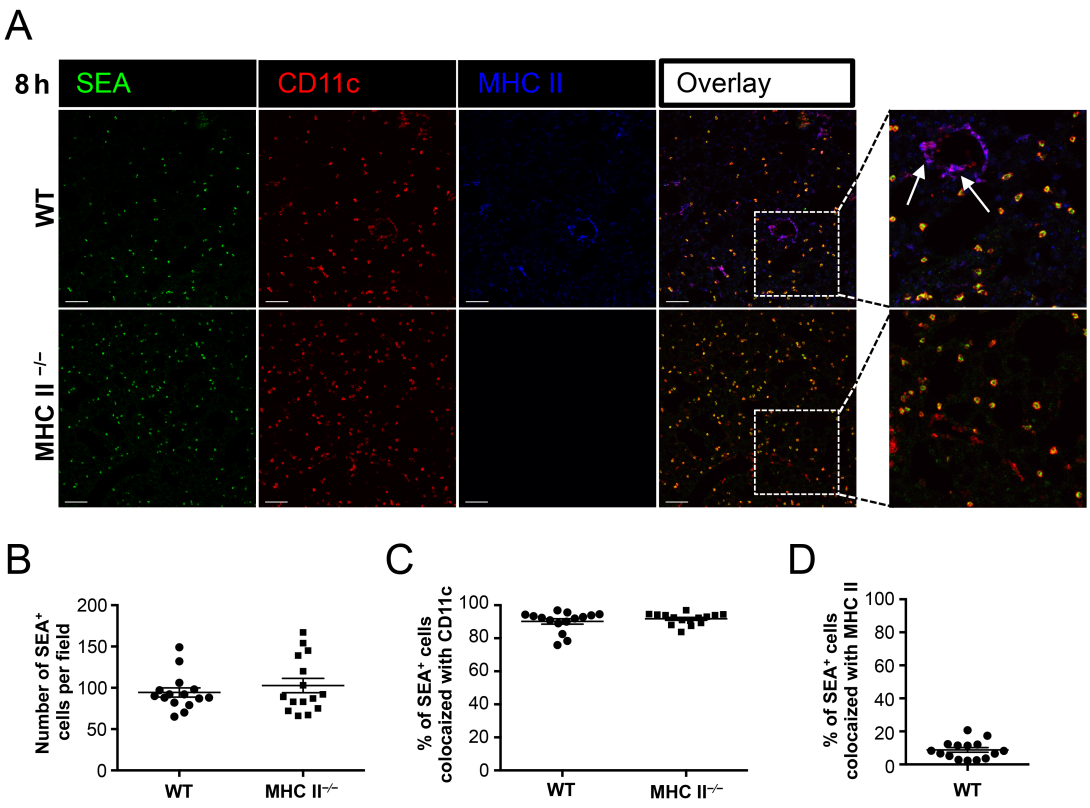

FIGURE 5-3: SEA binding to AMs is MHC II-independent. A) Representative confocal microscopy images comparing SEA binding in WT and MHC II$^{-/-}$ mice 8 h after SEA inhalation. Lung sections were stained with anti-SEA (green), anti-CD11c (red), and anti-MHC II (blue). Magnified images of the areas marked by white squares in the overlay panels are shown on the left. White arrows in the magnified panel (WT) point to dendritic cells (CD11c^{+}MHC II^{+}). Size bar = 80 µm. Three independent experiments with total n=5 per group. B) Number of SEA^{+} cells per field. Three images from each mouse were quantified (3 independent experiments with n=5 per group) by Imaris (Bitplane). C) Percentage of CD11c^{+}

cells in all SEA$^+$ cells detected by confocal microscopy 8 h after SEA inhalation. SEA$^+$ cells in WT and MHC II$^{-/-}$ mice were colocalized with CD11c$^+$ cells by Imaris (3 images per mouse; 3 independent experiments with n=5 per group). D) Percentage of MHC II$^+$ cells in all SEA$^+$ cells detected by confocal microscopy 8 h after SEA inhalation. SEA$^+$ cells in WT mice were colocalized with MHC II$^+$ cells by Imaris (3 images per mouse; 3 independent experiments with n=5 per group). Data are represented as mean ± SEM. Unpaired *t* test.

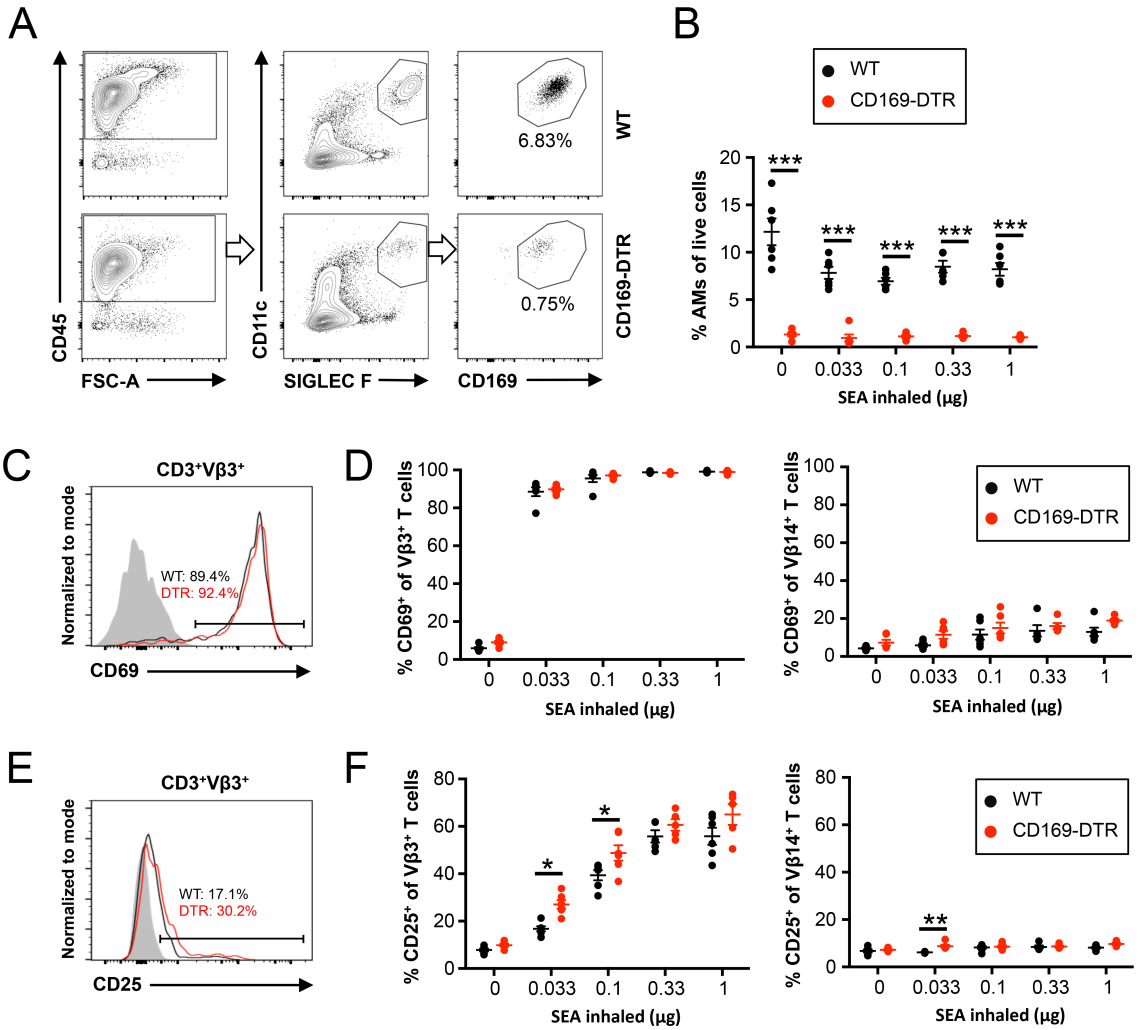

FIGURE 5-4: Depletion of CD169$^+$ cells leads to increased expression of CD25 on SEA-specific Vβ3$^+$ T cells. WT and CD169-DTR mice received DT 2 days prior to SEA or vehicle inhalation. Lung and spleen were removed 4 h after vehicle (0 µg) or SEA (0.033,

0.1, 0.33 or 1 µg) inhalation. A) and B) Representative flow cytometry plots (A) and scatter dot plot (B) showing depletion of AMs in lung (gated as live $CD45^+CD11c^+$SIGLEC F^+CD169^+ cells) in CD169-DTR mice compared to WT mice. The percentage of AMs is relative to all live cells. C) Representative histogram of CD69 expression in live $CD45^+CD3^+V\beta3^+$ cells in WT (black) and CD169-DTR (red) mice 4 h after 0.033 µg SEA inhalation. Gray = isotype control. D) Percentage of $CD69^+$ cells in $V\beta3^+$ (left) and $V\beta14^+$ (right) T cells 4 h after 0, 0.033, 0.1, 0.33 or 1 µg of SEA inhalation. E) Representative histogram of CD25 expression in live $CD45^+CD3^+V\beta3^+$ cells in WT (black) and CD169-DTR (red) mice 4 h after 0.033 µg SEA inhalation. Gray = isotype control. F) Percentage of $CD25^+$ cells in $V\beta3^+$ (left) and $V\beta14^+$ (right) T cells 4 h after 0, 0.033, 0.1, 0.33 or 1 µg of SEA inhalation. The data were compiled from 3 independent experiments with total n=5-6 per group. Two-way ANOVA with Sidak's test; *p<0.05, **p<0.01, ***p<0.001.

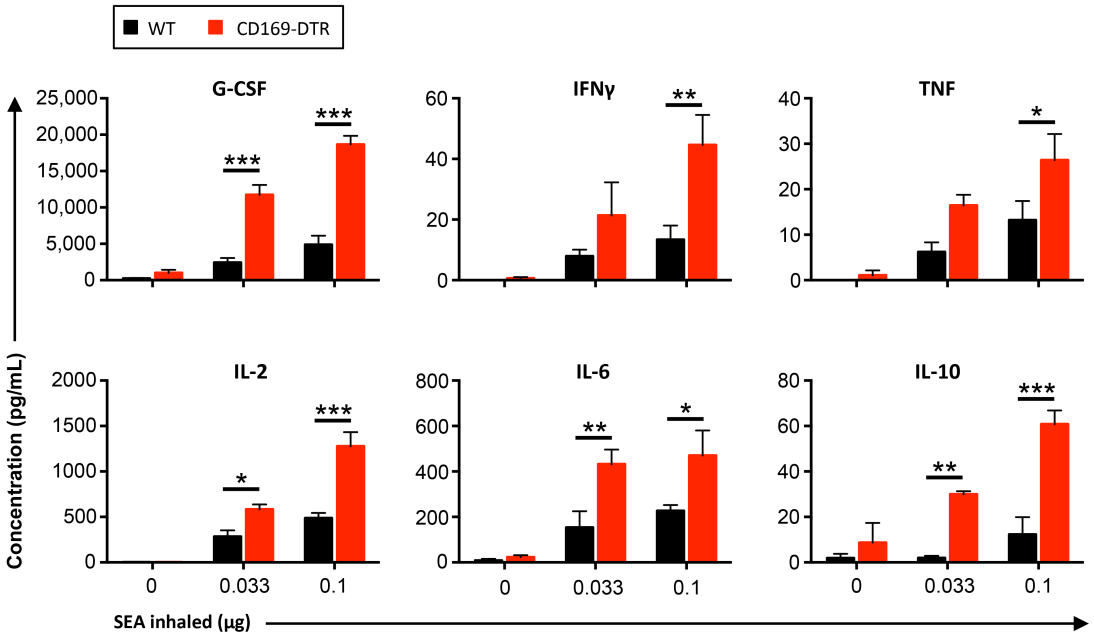

FIGURE 5-5: Depletion of $CD169^+$ cells increases the concentration of serum cytokines after SEA inhalation. Serum was obtained from tail blood 4 h after vehicle (0 µg)

or SEA (0.033 or 0.1 μg) inhalation. The concentrations of different cytokines were measured by a bead-based multiplex assay (EMD Millipore). The data were compiled from 3 independent experiments with total n=6 per group. Two-way ANOVA with Sidak's test; *p<0.05, **p<0.01, ***p<0.001.

Chapter 6: Conclusions and Future Directions

Together with previous reports (30, 34, 39, 106, 254), these studies demonstrated the intricate pathways employed in *S. aureus* enterotoxin-induced inflammation and the key findings are shown in Fig. 6.1 and Fig. 6.2. Fig. 6.1 depicts the early inflammatory responses following SEA inhalation; in particular, how SEA spreads systemically from the airways and how the activated adaptive immunity triggers the recruitment of innate immune cells to blood, LNs and lung. Fig. 6.2 shows the pulmonary responses leading to lung injury 2 days after SEA inhalation. Although these findings uncovered various mechanisms in *S. aureus* enterotoxin-induced inflammation and potentially also in SIRS/sepsis and ALI/ARDS, there are several remaining questions.

Firstly, it will be important to further investigate the role of innate immune cells, particularly neutrophils and monocytes, in *S. aureus* enterotoxin inflammatory response. Both chapter 3 and chapter 4 demonstrated that neutrophils and inflammatory monocytes are recruited to blood, lymphoid tissues and lung (183, 275). However, it is not currently clear whether the recruitment and activation of innate cells contributes to the severity of the response or actual tissue injury. Neutrophils and monocytes are considered the first line of immune defense in acute inflammatory response and their non-specific products, such as reactive oxygen species and proteolytic enzymes, are thought to be responsible for the host's tissue injury (2-4). Thus, it will be important to determine to what extent the innate immune cells affect *S. aureus* enterotoxin-induced inflammatory response (e.g. in the T cell zone of the LNs following their recruitment) and cell damage (e.g. in the lung 2 days after inhalation).

Secondly, the role of AMs in systemic inflammation following *S. aureus* enterotoxin exposure warrants further studies. The findings of chapter 5 unraveled an important relationship between AMs, SEA and the subsequent systemic inflammatory response. In particular, depletion of AMs was associated with increased inflammation following SEA

inhalation. However, it is not known which receptor SEA binds on AMs to and how the macrophages process the enterotoxin intracellularly. Furthermore, usage of alternative AM ablation models (e.g. intrathoracic administration of DT in CD169-DTR mice) will establish a more direct link between AMs and *S. aureus* enterotoxins. These future studies may help to determine at-risk patients who may be more susceptible to *S. aureus* enterotoxin exposure.

Thirdly, chapter 4 uncovered that CD54 is a critical player in SEA-evoked lung injury and blocking CD54 many hours after the exposure significantly reduced inflammation and tissue damage (275). Although it was shown that therapeutic CD54 blockade significantly reduces T cell recruitment to lung, it is also possible that the direct engagement of CD54 with its binding partners (e.g. CD11a) plays a vital role in triggering damage to endothelial cells (196, 280). Furthermore, it will be interesting to explore whether such pathways are dependent on the presence of an antigen (i.e. SEA) or whether they can occur independently of TCR binding.

Finally, it will be critical to further establish the causal relationship between superantigens and the pathogenesis of SIRS/sepsis and ALI/ARDS in humans. Prior studies have preferentially focused on studying Gram-negative bacteria and particularly the effects of LPS on eliciting immune response and cell injury. However, a recent study showed that 47% of patients in intensive care units with a serious infection were infected with Gram-positive bacteria and *S. aureus* was present in 20% of cases (87). Thus, superantigens may represent a crucial trigger of SIRS/sepsis and ALI/ARDS. There is currently no standard test used to detect superantigens in patients. Ideally, such test would detect superantigen proteins in anterior nares, blood or BAL fluid of patients who are at risk or presenting with symptoms of SIRS or ALI. Detection of superantigen proteins would be preferable to analyzing gene expression in *S. aureus* strains that were extracted from patients as superantigens are not necessarily transcribed and translated continuously (10). Alternatively, a functional immunoassay could be used that would detect clonal T cell activation or expansion or the downstream effects, such as IL-2 production in a co-culture

assay of naïve T cells with BAL fluid or serum obtained from patients (183, 254). This would also demonstrate that the immune system is responding as some individuals may have neutralizing antibodies to superantigens.

In conclusion, *S. aureus* enterotoxins and other superantigens are potent but currently underrated virulence factors. Unlike LPS and other pathogen associated molecular patterns (PAMPs), they trigger a robust immune response through oligoclonal activation of T cells rather than pattern recognition receptors (PRRs). T cells then orchestrate other arms of the immune system, which results in systemic inflammatory response and organ damage. Thus, *S. aureus* enterotoxins and other superantigens trigger unique pathways that merit further investigation, especially in the field of SIRS/sepsis and ALI/ARDS. Understanding these mechanisms will enhance our knowledge of these devastating diseases and may lead to discovery of novel therapeutic targets.

EARLY IMMUNE RESPONSE

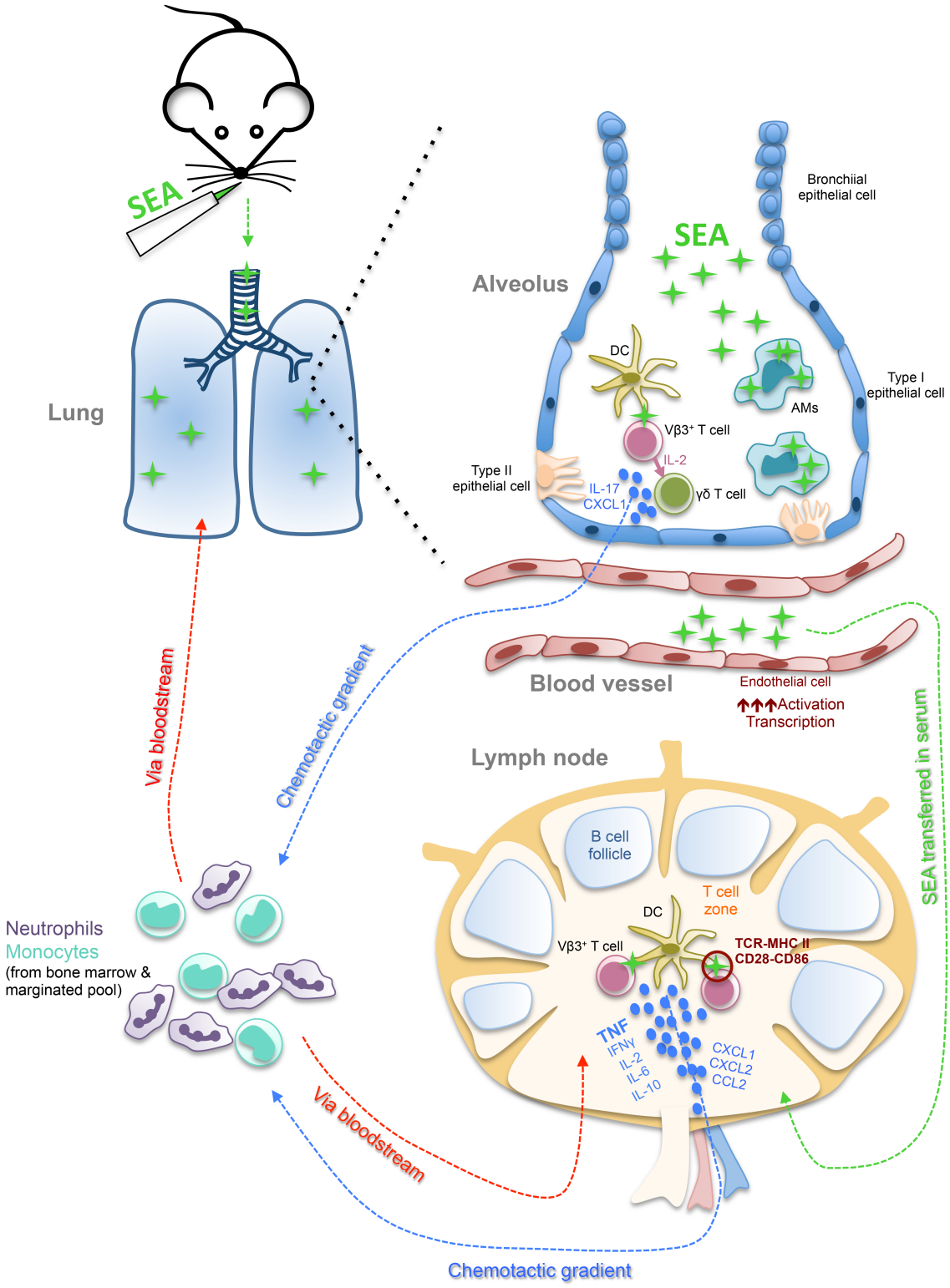

FIGURE 6.1: Summary of systemic inflammatory responses following SEA inhalation. SEA (marked as ✦) enters the airways through the nasal cavity and reaches the lung mucosa and individual alveoli. SEA gets trapped inside alveolar macrophages (AMs) which likely reduces the amount of the enterotoxin that gets into the circulation and the subsequent inflammatory response (Chapter 5; unpublished). SEA can be found in the blood within minutes of inhalation and it disseminates systemically. In LNs and spleen, SEA binds dendritic cells (DCs), particularly migratory DCs, and activates SEA-specific T cells (e.g. $V\beta3^+$) inducing a robust cytokine and chemokine release (marked as •). More specifically, TNF and CD28 signaling play unique but complementary roles in triggering systemic migration of the innate immune cells (neutrophils and inflammatory monocytes) from the bone marrow and likely also the marginated pool. The chemotactic gradient recruits the circulating neutrophils and monocytes into spleen and LNs, particularly the T cell zone (Chapter 3; (183)). Because SEA-specific T cells are also found in the lung under homeostatic conditions, they also become activated and secrete cytokines and chemokines, including CXCL1 and IL-12p40 (Chapter 4; (275)). Furthermore, the cytokine IL-2 plays a role in triggering IL-17 release from γδ T cells aiding the recruitment of neutrophils ((30); A. Ménoret, unpublished work). The pulmonary immune responses and/or the circulating cytokines induce activation of pulmonary endothelial cells, including pSTAT1 and MHC II upregulation and changes in gene transcription (Chapter 4; (275)).

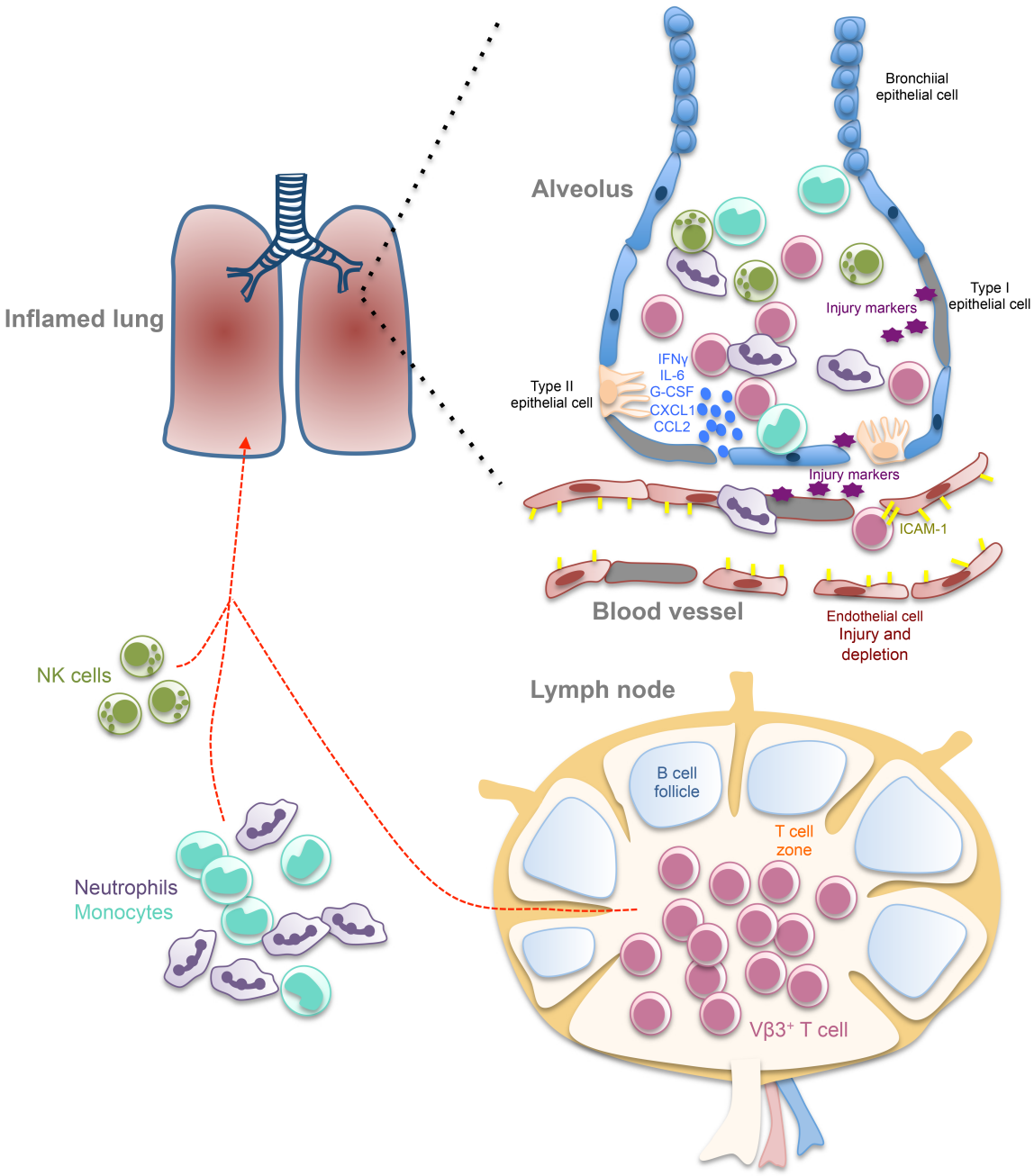

FIGURE 6.2: Summary of pulmonary inflammatory responses following SEA inhalation. Two days after SEA inhalation, the population of SEA-specific T cells (e.g. $V\beta3^+$) becomes significantly expanded within the lymphoid tissues. SEA-specific T cells and particularly $CD8^+$ T cells then accumulate in the lung (process dependent on $CD4^+$ T cell

help) and induce production of cytokines and chemokines, including IFNγ, IL-6, CXCL1 and CCL2 ((39) and also Chapter 4; (275)). These factors induce the recruitment of NK cells, neutrophils and monocytes to the lung ((30) and also Chapter 4; (275)). The population of pulmonary endothelial cells downregulates the expression of eNOS and upregulates Fas and CD54 (marked as). These cumulative inflammatory responses are largely dependent on CD54 expression and trigger injury to epithelial and endothelial cells (marked as grey cells with injury markers shown as) and increased lung permeability, further propagating the inflammation within the tissue (Chapter 4; (275)).

References

1. Ward, P. A., and A. B. Lentsch. 1999. The acute inflammatory response and its regulation. *Arch Surg* 134: 666-669.

2. Yang, J., L. Zhang, C. Yu, X. F. Yang, and H. Wang. 2014. Monocyte and macrophage differentiation: circulation inflammatory monocyte as biomarker for inflammatory diseases. *Biomark Res* 2: 1.

3. Kruger, P., M. Saffarzadeh, A. N. R. Weber, N. Rieber, M. Radsak, H. von Bernuth, C. Benarafa, D. Roos, J. Skokowa, and D. Hartl. 2015. Neutrophils: Between Host Defence, Immune Modulation, and Tissue Injury. *PLoS Pathog.* 11.

4. Mayadas, T. N., X. Cullere, and C. A. Lowell. 2014. The multifaceted functions of neutrophils. *Annu Rev Pathol* 9: 181-218.

5. Brown, K. A., and D. F. Treacher. 2006. Neutrophils as potential therapeutic targets in sepsis. *Discov Med* 6: 118-122.

6. Shen, X. F., K. Cao, J. P. Jiang, W. X. Guan, and J. F. Du. 2017. Neutrophil dysregulation during sepsis: an overview and update. *J Cell Mol Med*.

7. Iskander, K. N., M. F. Osuchowski, D. J. Stearns-Kurosawa, S. Kurosawa, D. Stepien, C. Valentine, and D. G. Remick. 2013. Sepsis: multiple abnormalities, heterogeneous responses, and evolving understanding. *Physiol. Rev.* 93: 1247-1288.

8. Bosma, K. J., R. Taneja, and J. F. Lewis. 2010. Pharmacotherapy for prevention and treatment of acute respiratory distress syndrome: current and experimental approaches. *Drugs* 70: 1255-1282.

9. Spaulding, A. R., W. Salgado-Pabón, P. L. Kohler, A. R. Horswill, D. Y. M. Leung, and P. M. Schlievert. 2013. Staphylococcal and Streptococcal Superantigen Exotoxins. *Clin Microbiol Rev* 26: 422-447.

10. Fraser, J. D., and T. Proft. 2008. The bacterial superantigen and superantigen-like proteins. *Immunol. Rev.* 225: 226-243.

11. Wertheim, H. F., D. C. Melles, M. C. Vos, W. van Leeuwen, A. van Belkum, H. A. Verbrugh, and J. L. Nouwen. 2005. The role of nasal carriage in Staphylococcus aureus infections. *Lancet Infect. Dis.* 5: 751-762.

12. Klevens, R. M., M. A. Morrison, J. Nadle, S. Petit, K. Gershman, S. Ray, L. H. Harrison, R. Lynfield, G. Dumyati, J. M. Townes, A. S. Craig, E. R. Zell, G. E. Fosheim, L. K. McDougal, R. B. Carey, and S. K. Fridkin. 2007. Invasive methicillin-resistant Staphylococcus aureus infections in the United States. *JAMA* 298: 1763-1771.

13. Naber, C. K. 2009. Staphylococcus aureus bacteremia: epidemiology, pathophysiology, and management strategies. *Clin. Infect. Dis.* 48 Suppl 4: S231-237.

14. Dantes, R., Y. Mu, R. Belflower, D. Aragon, G. Dumyati, L. H. Harrison, F. C. Lessa, R. Lynfield, J. Nadle, S. Petit, S. M. Ray, W. Schaffner, J. Townes, and S. Fridkin. 2013. National burden of invasive methicillin-resistant Staphylococcus aureus infections, United States, 2011. *JAMA Intern Med* 173: 1970-1978.

15. Foster, T. J. 2005. Immune evasion by staphylococci. *Nat Rev Microbiol* 3: 948-958.

16. Becker, K., A. W. Friedrich, G. Lubritz, M. Weilert, G. Peters, and C. Von Eiff. 2003. Prevalence of genes encoding pyrogenic toxin superantigens and exfoliative toxins among strains of Staphylococcus aureus isolated from blood and nasal specimens. *J Clin Microbiol* 41: 1434-1439.

17. Li, Y., R. Zhao, X. Zhang, Q. Han, X. Qian, G. Gu, J. Shi, and J. Xu. 2015. Prevalence of Enterotoxin Genes and spa Genotypes of Methicillin-resistant Staphylococcus aureus from a Tertiary Care Hospital in China. *J Clin Diagn Res* 9: Dc11-14.

18. Hu, D. L., K. Omoe, F. Inoue, T. Kasai, M. Yasujima, K. Shinagawa, and A. Nakane. 2008. Comparative prevalence of superantigenic toxin genes in meticillin-resistant and meticillin-susceptible Staphylococcus aureus isolates. *J Med Microbiol* 57: 1106-1112.

19. Czop, J. K., and M. S. Bergdoll. 1974. Staphylococcal enterotoxin synthesis during the exponential, transitional, and stationary growth phases. *Infect. Immun.* 9: 229-235.

20. Derzelle, S., F. Dilasser, M. Duquenne, and V. Deperrois. 2009. Differential temporal expression of the staphylococcal enterotoxins genes during cell growth. *Food Microbiol* 26: 896-904.

21. Yagi, J., J. Baron, S. Buxser, and C. A. Janeway, Jr. 1990. Bacterial proteins that mediate the association of a defined subset of T cell receptor:CD4 complexes with class II MHC. *J. Immunol.* 144: 892-901.

22. Herman, A., J. W. Kappler, P. Marrack, and A. M. Pullen. 1991. Superantigens: mechanism of T-cell stimulation and role in immune responses. *Annu. Rev. Immunol.* 9: 745-772.

23. Kumar, S., A. Menoret, S. M. Ngoi, and A. T. Vella. 2010. The systemic and pulmonary immune response to staphylococcal enterotoxins. *Toxins (Basel)* 2: 1898-1912.

24. Argudin, M. A., M. C. Mendoza, and M. R. Rodicio. 2010. Food poisoning and Staphylococcus aureus enterotoxins. *Toxins (Basel)* 2: 1751-1773.

25. Kozono, H., D. Parker, J. White, P. Marrack, and J. Kappler. 1995. Multiple binding sites for bacterial superantigens on soluble class II MHC molecules. *Immunity* 3: 187-196.

26. Pless, D. D., G. Ruthel, E. K. Reinke, R. G. Ulrich, and S. Bavari. 2005. Persistence of zinc-binding bacterial superantigens at the surface of antigen-presenting cells contributes to the extreme potency of these superantigens as T-cell activators. *Infect. Immun.* 73: 5358-5366.

27. Arad, G., R. Levy, I. Nasie, D. Hillman, Z. Rotfogel, U. Barash, E. Supper, T. Shpilka, A. Minis, and R. Kaempfer. 2011. Binding of Superantigen Toxins into the CD28 Homodimer Interface Is Essential for Induction of Cytokine Genes That Mediate Lethal Shock. *PLoS Biol* 9.

28. Levy, R., Z. Rotfogel, D. Hillman, A. Popugailo, G. Arad, E. Supper, F. Osman, and R. Kaempfer. 2016. Superantigens hyperinduce inflammatory cytokines by enhancing the B7-2/CD28 costimulatory receptor interaction. *Proc. Natl. Acad. Sci. USA* 113: E6437-e6446.

29. Kaempfer, R., G. Arad, R. Levy, D. Hillman, I. Nasie, and Z. Rotfogel. 2013. CD28: direct and critical receptor for superantigen toxins. *Toxins (Basel)* 5: 1531-1542.

30. Kumar, S., S. L. Colpitts, A. Menoret, A. L. Budelsky, L. Lefrancois, and A. T. Vella. 2013. Rapid alphabeta T-cell responses orchestrate innate immunity in response to Staphylococcal enterotoxin A. *Mucosal Immunol.* 6: 1006-1015.

31. Jupin, C., S. Anderson, C. Damais, J. E. Alouf, and M. Parant. 1988. Toxic shock syndrome toxin 1 as an inducer of human tumor necrosis factors and gamma interferon. *J. Exp. Med.* 167: 752-761.

32. Miethke, T., C. Wahl, K. Heeg, B. Echtenacher, P. H. Krammer, and H. Wagner. 1992. T cell-mediated lethal shock triggered in mice by the superantigen staphylococcal enterotoxin B: critical role of tumor necrosis factor. *J. Exp. Med.* 175: 91-98.

33. Bette, M., M. K. Schafer, N. van Rooijen, E. Weihe, and B. Fleischer. 1993. Distribution and kinetics of superantigen-induced cytokine gene expression in mouse spleen. *J. Exp. Med.* 178: 1531-1539.

34. Rajagopalan, G., M. M. Sen, M. Singh, N. S. Murali, K. A. Nath, K. Iijima, H. Kita, A. A. Leontovich, U. Gopinathan, R. Patel, and C. S. David. 2006. Intranasal exposure to staphylococcal enterotoxin B elicits an acute systemic inflammatory response. *Shock* 25: 647-656.

35. Rajagopalan, G., A. Y. Tilahun, Y. W. Asmann, and C. S. David. 2009. Early gene expression changes induced by the bacterial superantigen staphylococcal enterotoxin B and its modulation by a proteasome inhibitor. *Physiol Genomics* 37: 279-293.

36. Lappin, E., and A. J. Ferguson. 2009. Gram-positive toxic shock syndromes. *Lancet Infect. Dis.* 9: 281-290.

37. Peavy, D. L., W. H. Adler, and R. T. Smith. 1970. The mitogenic effects of endotoxin and staphylococcal enterotoxin B on mouse spleen cells and human peripheral lymphocytes. *J. Immunol.* 105: 1453-1458.

38. Smith, B. G., and H. M. Johnson. 1975. The effect of staphylococcal enterotoxins on the primary in vitro immune response. *J. Immunol.* 115: 575-578.

39. Muralimohan, G., R. J. Rossi, L. A. Guernsey, R. S. Thrall, and A. T. Vella. 2008. Inhalation of Staphylococcus aureus enterotoxin A induces IFN-gamma and CD8 T

cell-dependent airway and interstitial lung pathology in mice. *J. Immunol.* 181: 3698-3705.

40. Poindexter, N. J., and P. M. Schlievert. 1985. Toxic-shock-syndrome toxin 1-induced proliferation of lymphocytes: comparison of the mitogenic response of human, murine, and rabbit lymphocytes. *J. Infect. Dis.* 151: 65-72.

41. Li, Z. J., K. Omoe, K. Shinagawa, J. Yagi, and K. Imanishi. 2009. Interaction between superantigen and T-cell receptor Vbeta element determines levels of superantigen-dependent cell-mediated cytotoxicity of CD8(+) T cells in induction and effector phases. *Microbiol Immunol* 53: 451-459.

42. Takimoto, H., Y. Yoshikai, K. Kishihara, G. Matsuzaki, H. Kuga, T. Otani, and K. Nomoto. 1990. Stimulation of all T cells bearing V beta 1, V beta 3, V beta 11 and V beta 12 by staphylococcal enterotoxin A. *Eur. J. Immunol.* 20: 617-621.

43. Kawabe, Y., and A. Ochi. 1991. Programmed cell death and extrathymic reduction of Vbeta8+ CD4+ T cells in mice tolerant to Staphylococcus aureus enterotoxin B. *Nature* 349: 245-248.

44. McCormack, J. E., J. E. Callahan, J. Kappler, and P. C. Marrack. 1993. Profound deletion of mature T cells in vivo by chronic exposure to exogenous superantigen. *J. Immunol.* 150: 3785-3792.

45. White, J., A. Herman, A. M. Pullen, R. Kubo, J. W. Kappler, and P. Marrack. 1989. The V beta-specific superantigen staphylococcal enterotoxin B: stimulation of mature T cells and clonal deletion in neonatal mice. *Cell* 56: 27-35.

46. Renno, T., M. Hahne, and H. R. MacDonald. 1995. Proliferation is a prerequisite for bacterial superantigen-induced T cell apoptosis in vivo. *J. Exp. Med.* 181: 2283-2287.

47. Renno, T., M. Hahne, J. Tschopp, and H. R. MacDonald. 1996. Peripheral T cells undergoing superantigen-induced apoptosis in vivo express B220 and upregulate Fas and Fas ligand. *J. Exp. Med.* 183: 431-437.

48. Vella, A. T., J. E. McCormack, P. S. Linsley, J. W. Kappler, and P. Marrack. 1995. Lipopolysaccharide interferes with the induction of peripheral T cell death. *Immunity* 2: 261-270.

49. MacDonald, H. R., R. K. Lees, S. Baschieri, T. Herrmann, and A. R. Lussow. 1993. Peripheral T-cell reactivity to bacterial superantigens in vivo: the response/anergy paradox. *Immunol. Rev.* 133: 105-117.

50. Miethke, T., C. Wahl, K. Heeg, and H. Wagner. 1993. Acquired resistance to superantigen-induced T cell shock. V beta selective T cell unresponsiveness unfolds directly from a transient state of hyperreactivity. *J. Immunol.* 150: 3776-3784.

51. Lee, W. T., and E. S. Vitetta. 1992. Memory T cells are anergic to the superantigen staphylococcal enterotoxin B. *J. Exp. Med.* 176: 575-579.

52. Cauley, L. S., K. A. Cauley, F. Shub, G. Huston, and S. L. Swain. 1997. Transferable anergy: superantigen treatment induces CD4+ T cell tolerance that is reversible and requires CD4-CD8- cells and interferon gamma. *J. Exp. Med.* 186: 71-81.

53. Migita, K., K. Eguchi, Y. Kawabe, T. Tsukada, Y. Ichinose, S. Nagataki, and A. Ochi. 1995. Defective TCR-mediated signaling in anergic T cells. *J. Immunol.* 155: 5083-5087.

54. Sundstedt, A., and M. Dohlsten. 1998. In vivo anergized CD4+ T cells have defective expression and function of the activating protein-1 transcription factor. *J. Immunol.* 161: 5930-5936.

55. Attinger, A., H. Acha-Orbea, and H. R. MacDonald. 2000. Cutting edge: cell autonomous rather than environmental factors control bacterial superantigen-induced T cell anergy in vivo. *J. Immunol.* 165: 1171-1174.

56. Cauley, L. S., E. E. Miller, M. Yen, and S. L. Swain. 2000. Superantigen-induced CD4 T cell tolerance mediated by myeloid cells and IFN-gamma. *J. Immunol.* 165: 6056-6066.

57. Wang, Z. Q., T. Orlikowsky, A. Dudhane, V. Trejo, G. E. Dannecker, B. Pernis, and M. K. Hoffmann. 1998. Staphylococcal enterotoxin B-induced T-cell anergy is mediated by regulatory T cells. *Immunology* 94: 331-339.

58. Taylor, A. L., and M. J. Llewelyn. 2010. Superantigen-induced proliferation of human CD4+CD25- T cells is followed by a switch to a functional regulatory phenotype. *J. Immunol.* 185: 6591-6598.

59. Ivars, F. 2007. Superantigen-induced regulatory T cells in vivo. *Chem Immunol Allergy* 93: 137-160.

60. Grundstrom, S., L. Cederbom, A. Sundstedt, P. Scheipers, and F. Ivars. 2003. Superantigen-induced regulatory T cells display different suppressive functions in the presence or absence of natural CD4+CD25+ regulatory T cells in vivo. *J. Immunol.* 170: 5008-5017.

61. Sähr, A., S. Förmer, D. Hildebrand, and K. Heeg. 2015. T-cell activation or tolerization: the Yin and Yang of bacterial superantigens. *Frontiers in Microbiology* 6.

62. Salgado-Pabon, W., and P. M. Schlievert. 2014. Models matter: the search for an effective Staphylococcus aureus vaccine. *Nat Rev Microbiol* 12: 585-591.

63. Choi, Y. W., B. Kotzin, L. Herron, J. Callahan, P. Marrack, and J. Kappler. 1989. Interaction of Staphylococcus aureus toxin "superantigens" with human T cells. *Proc. Natl. Acad. Sci. USA* 86: 8941-8945.

64. O'Hehir, R. E., and J. R. Lamb. 1990. Induction of specific clonal anergy in human T lymphocytes by Staphylococcus aureus enterotoxins. *Proc. Natl. Acad. Sci. USA* 87: 8884-8888.

65. Todd, J., M. Fishaut, F. Kapral, and T. Welch. 1978. Toxic-shock syndrome associated with phage-group-I Staphylococci. *Lancet* 2: 1116-1118.

66. Shands, K. N., G. P. Schmid, B. B. Dan, D. Blum, R. J. Guidotti, N. T. Hargrett, R. L. Anderson, D. L. Hill, C. V. Broome, J. D. Band, and D. W. Fraser. 1980. Toxic-shock syndrome in menstruating women: association with tampon use and Staphylococcus aureus and clinical features in 52 cases. *N. Engl. J. Med.* 303: 1436-1442.

67. Davis, J. P., P. J. Chesney, P. J. Wand, and M. LaVenture. 1980. Toxic-shock syndrome: epidemiologic features, recurrence, risk factors, and prevention. *N. Engl. J. Med.* 303: 1429-1435.

68. Schlievert, P. M., K. N. Shands, B. B. Dan, G. P. Schmid, and R. D. Nishimura. 1981. Identification and characterization of an exotoxin from Staphylococcus aureus associated with toxic-shock syndrome. *J. Infect. Dis.* 143: 509-516.

69. DeVries, A. S., L. Lesher, P. M. Schlievert, T. Rogers, L. G. Villaume, R. Danila, and R. Lynfield. 2011. Staphylococcal toxic shock syndrome 2000-2006: epidemiology, clinical features, and molecular characteristics. *PLoS One* 6: e22997.

70. Descloux, E., T. Perpoint, T. Ferry, G. Lina, M. Bes, F. Vandenesch, I. Mohammedi, and J. Etienne. 2008. One in five mortality in non-menstrual toxic shock syndrome versus no mortality in menstrual cases in a balanced French series of 55 cases. *Eur J Clin Microbiol Infect Dis* 27: 37-43.

71. Horeczko, T., J. P. Green, and E. A. Panacek. 2014. Epidemiology of the Systemic Inflammatory Response Syndrome (SIRS) in the Emergency Department. *West J Emerg Med* 15: 329-336.

72. Angus, D. C., and T. van der Poll. 2013. Severe sepsis and septic shock. *N. Engl. J. Med.* 369: 840-851.

73. Martin, G. S. 2012. Sepsis, severe sepsis and septic shock: changes in incidence, pathogens and outcomes. *Expert Rev Anti Infect Ther* 10: 701-706.

74. Rittirsch, D., M. A. Flierl, and P. A. Ward. 2008. Harmful molecular mechanisms in sepsis. *Nat. Rev. Immunol.* 8: 776-787.

75. Aziz, M., A. Jacob, W. L. Yang, A. Matsuda, and P. Wang. 2013. Current trends in inflammatory and immunomodulatory mediators in sepsis. *J Leukoc Biol* 93: 329-342.

76. Martin, G. S., D. M. Mannino, S. Eaton, and M. Moss. 2003. The epidemiology of sepsis in the United States from 1979 through 2000. *N. Engl. J. Med.* 348: 1546-1554.

77. Vincent, J. L., J. Rello, J. Marshall, E. Silva, A. Anzueto, C. D. Martin, R. Moreno, J. Lipman, C. Gomersall, Y. Sakr, and K. Reinhart. 2009. International study of the prevalence and outcomes of infection in intensive care units. *JAMA* 302: 2323-2329.

78. Cohen, J. 2002. The immunopathogenesis of sepsis. *Nature* 420: 885-891.

79. Azuma, K., K. Koike, T. Kobayashi, T. Mochizuki, K. Mashiko, and Y. Yamamoto. 2004. Detection of circulating superantigens in an intensive care unit population. *Int. J. Infect. Dis.* 8: 292-298.

80. Ferry, T., D. Thomas, A. L. Genestier, M. Bes, G. Lina, F. Vandenesch, and J. Etienne. 2005. Comparative prevalence of superantigen genes in Staphylococcus aureus isolates causing sepsis with and without septic shock. *Clin. Infect. Dis.* 41: 771-777.

81. Humphreys, H., C. T. Keane, R. Hone, H. Pomeroy, R. J. Russell, J. P. Arbuthnott, and D. C. Coleman. 1989. Enterotoxin production by Staphylococcus aureus isolates from cases of septicaemia and from healthy carriers. *J Med Microbiol* 28: 163-172.

82. Prindeze, N. J., B. M. Amundsen, A. R. Pavlovich, D. W. Paul, B. C. Carney, L. T. Moffatt, and J. W. Shupp. 2014. Staphylococcal superantigens and toxins are detectable in the serum of adult burn patients. *Diagn Microbiol Infect Dis* 79: 303-307.

83. Aguilar, J. L., A. K. Varshney, X. Pechuan, K. Dutta, J. D. Nosanchuk, and B. C. Fries. 2016. Monoclonal antibodies protect from Staphylococcal Enterotoxin K (SEK) induced toxic shock and sepsis by USA300 Staphylococcus aureus. *Virulence*: 1-10.

84. Varshney, A. K., X. Wang, M. D. Scharff, J. MacIntyre, R. S. Zollner, O. V. Kovalenko, L. R. Martinez, F. R. Byrne, and B. C. Fries. 2013. Staphylococcal Enterotoxin B-specific monoclonal antibody 20B1 successfully treats diverse Staphylococcus aureus infections. *J. Infect. Dis.* 208: 2058-2066.

85. Salgado-Pabon, W., L. Breshears, A. R. Spaulding, J. A. Merriman, C. S. Stach, A. R. Horswill, M. L. Peterson, and P. M. Schlievert. 2013. Superantigens are critical for Staphylococcus aureus Infective endocarditis, sepsis, and acute kidney injury. *MBio* 4: e00494-00413.

86. Albertine, K. H., M. F. Soulier, Z. Wang, A. Ishizaka, S. Hashimoto, G. A. Zimmerman, M. A. Matthay, and L. B. Ware. 2002. Fas and fas ligand are up-regulated in pulmonary edema fluid and lung tissue of patients with acute lung injury and the acute respiratory distress syndrome. *Am. J. Pathol.* 161: 1783-1796.

87. Bellani, G., J. G. Laffey, T. Pham, E. Fan, L. Brochard, A. Esteban, L. Gattinoni, F. van Haren, A. Larsson, D. F. McAuley, M. Ranieri, G. Rubenfeld, B. T. Thompson, H. Wrigge, A. S. Slutsky, and A. Pesenti. 2016. Epidemiology, Patterns of Care, and Mortality for Patients With Acute Respiratory Distress Syndrome in Intensive Care Units in 50 Countries. *JAMA* 315: 788-800.

88. Matthay, M. A., and R. L. Zemans. 2011. The acute respiratory distress syndrome: pathogenesis and treatment. *Annu Rev Pathol* 6: 147-163.

89. Bhatia, M., and S. Moochhala. 2004. Role of inflammatory mediators in the pathophysiology of acute respiratory distress syndrome. *J. Pathol.* 202: 145-156.

90. Perl, M., J. Lomas-Neira, F. Venet, C. S. Chung, and A. Ayala. 2011. Pathogenesis of indirect (secondary) acute lung injury. *Expert Rev Respir Med* 5: 115-126.

91. Yu, Z. X., M. S. Ji, J. Yan, Y. Cai, J. Liu, H. F. Yang, Y. Li, Z. C. Jin, and J. X. Zheng. 2015. The ratio of Th17/Treg cells as a risk indicator in early acute respiratory distress syndrome. *Crit. Care* 19: 82.

92. Li, J. T., A. C. Melton, G. Su, D. E. Hamm, M. LaFemina, J. Howard, X. Fang, S. Bhat, K. M. Huynh, C. M. O'Kane, R. J. Ingram, R. R. Muir, D. F. McAuley, M. A. Matthay, and D. Sheppard. 2015. Unexpected Role for Adaptive alphabetaTh17 Cells in Acute Respiratory Distress Syndrome. *J. Immunol.* 195: 87-95.

93. Lesur, O., A. Kokis, C. Hermans, T. Fulop, A. Bernard, and D. Lane. 2000. Interleukin-2 involvement in early acute respiratory distress syndrome: relationship with polymorphonuclear neutrophil apoptosis and patient survival. *Crit. Care Med.* 28: 3814-3822.

94. Terpstra, M. L., J. Aman, G. P. van Nieuw Amerongen, and A. B. Groeneveld. 2014. Plasma biomarkers for acute respiratory distress syndrome: a systematic review and meta-analysis*. *Crit. Care Med.* 42: 691-700.

95. Huvenne, W., P. W. Hellings, and C. Bachert. 2013. Role of staphylococcal superantigens in airway disease. *Int. Arch. Allergy Immunol.* 161: 304-314.

96. Strandberg, K. L., J. H. Rotschafer, S. M. Vetter, R. A. Buonpane, D. M. Kranz, and P. M. Schlievert. 2010. Staphylococcal superantigens cause lethal pulmonary disease in rabbits. *J. Infect. Dis.* 202: 1690-1697.

97. Spaulding, A. R., Y. C. Lin, J. A. Merriman, A. J. Brosnahan, M. L. Peterson, and P. M. Schlievert. 2012. Immunity to Staphylococcus aureus secreted proteins protects rabbits from serious illnesses. *Vaccine* 30: 5099-5109.

98. Mattix, M. E., R. E. Hunt, C. L. Wilhelmsen, A. J. Johnson, and W. B. Baze. 1995. Aerosolized staphylococcal enterotoxin B-induced pulmonary lesions in rhesus monkeys (Macaca mulatta). *Toxicol Pathol* 23: 262-268.

99. Schlievert, P. M., L. C. Case, K. A. Nemeth, C. C. Davis, Y. Sun, W. Qin, F. Wang, A. J. Brosnahan, J. A. Mleziva, M. L. Peterson, and B. E. Jones. 2007. Alpha and beta chains of hemoglobin inhibit production of Staphylococcus aureus exotoxins. *Biochemistry* 46: 14349-14358.

100. Merriman, J. A., K. A. Nemeth, and P. M. Schlievert. 2014. Novel antimicrobial peptides that inhibit gram positive bacterial exotoxin synthesis. *PLoS One* 9: e95661.

101. Honda, H., M. J. Krauss, C. M. Coopersmith, M. H. Kollef, A. M. Richmond, V. J. Fraser, and D. K. Warren. 2010. Staphylococcus aureus Nasal Colonization and Subsequent Infection in Intensive Care Unit Patients: Does Methicillin Resistance Matter? *Infect Control Hosp Epidemiol* 31: 584-591.

102. Davis, K. A., J. J. Stewart, H. K. Crouch, C. E. Florez, and D. R. Hospenthal. 2004. Methicillin-resistant Staphylococcus aureus (MRSA) nares colonization at hospital admission and its effect on subsequent MRSA infection. *Clin. Infect. Dis.* 39: 776-782.

103. Safdar, N., and E. A. Bradley. 2008. The risk of infection after nasal colonization with Staphylococcus aureus. *Am J Med* 121: 310-315.

104. Rusnak, J. M., M. Kortepeter, R. Ulrich, M. Poli, and E. Boudreau. 2004. Laboratory Exposures to Staphylococcal Enterotoxin B. *Emerg Infect Dis* 10: 1544-1549.

105. Saeed, A. I., S. A. Rieder, R. L. Price, J. Barker, P. Nagarkatti, and M. Nagarkatti. 2012. Acute lung injury induced by Staphylococcal enterotoxin B: disruption of terminal vessels as a mechanism of induction of vascular leak. *Microsc Microanal* 18: 445-452.

106. Menoret, A., S. Kumar, and A. T. Vella. 2012. Cytochrome b5 and cytokeratin 17 are biomarkers in bronchoalveolar fluid signifying onset of acute lung injury. *PLoS One* 7: e40184.

107. Chen, H., S. Wu, R. Lu, Y. G. Zhang, Y. Zheng, and J. Sun. 2014. Pulmonary permeability assessed by fluorescent-labeled dextran instilled intranasally into mice with LPS-induced acute lung injury. *PLoS One* 9: e101925.

108. Grommes, J., S. Vijayan, M. Drechsler, H. Hartwig, M. Morgelin, R. Dembinski, M. Jacobs, T. A. Koeppel, M. Binnebosel, C. Weber, and O. Soehnlein. 2012. Simvastatin reduces endotoxin-induced acute lung injury by decreasing neutrophil recruitment and radical formation. *PLoS One* 7: e38917.

109. Murphy, S. L., K. D. Kochanek, J. Xu, and M. Heron. 2015. Deaths: Final Data for 2012. In *National Vital Statistics Reports*. National Center for Health Statistics, Hyattsville, MD.

110. Fields, B. A., E. L. Malchiodi, H. Li, X. Ysern, C. V. Stauffacher, P. M. Schlievert, K. Karjalainen, and R. A. Mariuzza. 1996. Crystal structure of a T-cell receptor beta-chain complexed with a superantigen. *Nature* 384: 188-192.

111. Li, H., A. Llera, E. L. Malchiodi, and R. A. Mariuzza. 1999. The structural basis of T cell activation by superantigens. *Annu. Rev. Immunol.* 17: 435-466.

112. Arad, G., R. Levy, D. Hillman, and R. Kaempfer. 2000. Superantigen antagonist protects against lethal shock and defines a new domain for T-cell activation. *Nat. Med.* 6: 414-421.

113. Schlievert, P. M. 1993. Role of superantigens in human disease. *J. Infect. Dis.* 167: 997-1002.

114. Kotzin, B. L., D. Y. Leung, J. Kappler, and P. Marrack. 1993. Superantigens and their potential role in human disease. *Adv. Immunol.* 54: 99-166.

115. Blank, C., A. Luz, S. Bendigs, A. Erdmann, H. Wagner, and K. Heeg. 1997. Superantigen and endotoxin synergize in the induction of lethal shock. *Eur. J. Immunol.* 27: 825-833.

116. Kearney, D. E., W. Wang, H. P. Redmond, and J. H. Wang. 2011. Bacterial superantigens enhance the in vitro proinflammatory response and in vivo lethality of the TLR2 agonist bacterial lipoprotein. *J. Immunol.* 187: 5363-5369.

117. Desachy, A., G. Lina, P. Vignon, A. Hashemzadeh, F. Denis, J. Etienne, B. Francois, and M. C. Ploy. 2007. Role of superantigenic strains in the prognosis of community-acquired methicillin-susceptible Staphylococcus aureus bacteraemia. *Clin. Microbiol. Infect.* 13: 1131-1133.

118. Kawabe, Y., and A. Ochi. 1990. Selective anergy of V beta 8+,CD4+ T cells in Staphylococcus enterotoxin B-primed mice. *J. Exp. Med.* 172: 1065-1070.

119. Rellahan, B. L., L. A. Jones, A. M. Kruisbeek, A. M. Fry, and L. A. Matis. 1990. In vivo induction of anergy in peripheral V beta 8+ T cells by staphylococcal enterotoxin B. *J. Exp. Med.* 172: 1091-1100.

120. Ward, N. S., B. Casserly, and A. Ayala. 2008. The compensatory anti-inflammatory response syndrome (CARS) in critically ill patients. *Clin. Chest Med.* 29: 617-625, viii.

121. Chtanova, T., M. Schaeffer, S. J. Han, G. G. van Dooren, M. Nollmann, P. Herzmark, S. W. Chan, H. Satija, K. Camfield, H. Aaron, B. Striepen, and E. A. Robey. 2008. Dynamics of neutrophil migration in lymph nodes during infection. *Immunity* 29: 487-496.

122. Abadie, V., E. Badell, P. Douillard, D. Ensergueix, P. J. Leenen, M. Tanguy, L. Fiette, S. Saeland, B. Gicquel, and N. Winter. 2005. Neutrophils rapidly migrate via lymphatics after Mycobacterium bovis BCG intradermal vaccination and shuttle live bacilli to the draining lymph nodes. *Blood* 106: 1843-1850.

123. Gorlino, C. V., R. P. Ranocchia, M. F. Harman, I. A. Garcia, M. I. Crespo, G. Moron, B. A. Maletto, and M. C. Pistoresi-Palencia. 2014. Neutrophils exhibit differential requirements for homing molecules in their lymphatic and blood trafficking into draining lymph nodes. *J. Immunol.* 193: 1966-1974.

124. Yang, C. W., B. S. Strong, M. J. Miller, and E. R. Unanue. 2010. Neutrophils influence the level of antigen presentation during the immune response to protein antigens in adjuvants. *J. Immunol.* 185: 2927-2934.

125. Brackett, C. M., J. B. Muhitch, S. S. Evans, and S. O. Gollnick. 2013. IL-17 promotes neutrophil entry into tumor-draining lymph nodes following induction of sterile inflammation. *J. Immunol.* 191: 4348-4357.

126. Nakano, H., K. L. Lin, M. Yanagita, C. Charbonneau, D. N. Cook, T. Kakiuchi, and M. D. Gunn. 2009. Blood-derived inflammatory dendritic cells in lymph nodes stimulate acute T helper type 1 immune responses. *Nat. Immunol.* 10: 394-402.

127. Cheong, C., I. Matos, J. H. Choi, D. B. Dandamudi, E. Shrestha, M. P. Longhi, K. L. Jeffrey, R. M. Anthony, C. Kluger, G. Nchinda, H. Koh, A. Rodriguez, J. Idoyaga, M. Pack, K. Velinzon, C. G. Park, and R. M. Steinman. 2010. Microbial stimulation fully differentiates monocytes to DC-SIGN/CD209(+) dendritic cells for immune T cell areas. *Cell* 143: 416-429.

128. Sadik, C. D., N. D. Kim, and A. D. Luster. 2011. Neutrophils cascading their way to inflammation. *Trends Immunol.* 32: 452-460.

129. Williams, A. E., and R. C. Chambers. 2014. The mercurial nature of neutrophils: still an enigma in ARDS? *Am. J. Physiol. Lung Cell. Mol. Physiol.* 306: L217-230.

130. Shi, C., and E. G. Pamer. 2011. Monocyte recruitment during infection and inflammation. *Nat. Rev. Immunol.* 11: 762-774.

131. Anandasabapathy, N., R. Feder, S. Mollah, S. W. Tse, M. P. Longhi, S. Mehandru, I. Matos, C. Cheong, D. Ruane, L. Brane, A. Teixeira, J. Dobrin, O. Mizenina, C. G. Park, M. Meredith, B. E. Clausen, M. C. Nussenzweig, and R. M. Steinman. 2014. Classical Flt3L-dependent dendritic cells control immunity to protein vaccine. *J. Exp. Med.* 211: 1875-1891.

132. Cerny, D., M. Haniffa, A. Shin, P. Bigliardi, B. K. Tan, B. Lee, M. Poidinger, E. Y. Tan, F. Ginhoux, and K. Fink. 2014. Selective susceptibility of human skin antigen presenting cells to productive dengue virus infection. *PLoS Pathog.* 10: e1004548.

133. Lee, S. C., S. A. Ju, B. H. Sung, S. K. Heo, H. R. Cho, E. A. Lee, J. D. Kim, I. H. Lee, S. M. Park, Q. T. Nguyen, J. H. Suh, and B. S. Kim. 2009. Stimulation of the molecule 4-1BB enhances host defense against Listeria monocytogenes infection in mice by inducing rapid infiltration and activation of neutrophils and monocytes. *Infect. Immun.* 77: 2168-2176.

134. Li, G., J. M. Sanders, M. H. Bevard, Z. Sun, J. W. Chumley, E. V. Galkina, K. Ley, and I. J. Sarembock. 2008. CD40 ligand promotes Mac-1 expression, leukocyte recruitment, and neointima formation after vascular injury. *Am. J. Pathol.* 172: 1141-1152.

135. Powell, J. D., J. A. Ragheb, S. Kitagawa-Sakakida, and R. H. Schwartz. 1998. Molecular regulation of interleukin-2 expression by CD28 co-stimulation and anergy. *Immunol. Rev.* 165: 287-300.

136. Coyle, A. J., and J. C. Gutierrez-Ramos. 2001. The expanding B7 superfamily: increasing complexity in costimulatory signals regulating T cell function. *Nat. Immunol.* 2: 203-209.

137. Vella, A. T., T. Mitchell, B. Groth, P. S. Linsley, J. M. Green, C. B. Thompson, J. W. Kappler, and P. Marrack. 1997. CD28 engagement and proinflammatory cytokines contribute to T cell expansion and long-term survival in vivo. *J. Immunol.* 158: 4714-4720.

138. Riley, J. L., M. Mao, S. Kobayashi, M. Biery, J. Burchard, G. Cavet, B. P. Gregson, C. H. June, and P. S. Linsley. 2002. Modulation of TCR-induced transcriptional profiles by ligation of CD28, ICOS, and CTLA-4 receptors. *Proc. Natl. Acad. Sci. USA* 99: 11790-11795.

139. Diehn, M., A. A. Alizadeh, O. J. Rando, C. L. Liu, K. Stankunas, D. Botstein, G. R. Crabtree, and P. O. Brown. 2002. Genomic expression programs and the integration of the CD28 costimulatory signal in T cell activation. *Proc. Natl. Acad. Sci. USA* 99: 11796-11801.

140. Acuto, O., and F. Michel. 2003. CD28-mediated co-stimulation: a quantitative support for TCR signalling. *Nat. Rev. Immunol.* 3: 939-951.

141. Kappler, J. W., A. Herman, J. Clements, and P. Marrack. 1992. Mutations defining functional regions of the superantigen staphylococcal enterotoxin B. *J. Exp. Med.* 175: 387-396.

142. Remick, D. G., G. R. Bolgos, J. Siddiqui, J. Shin, and J. A. Nemzek. 2002. Six at six: interleukin-6 measured 6 h after the initiation of sepsis predicts mortality over 3 days. *Shock* 17: 463-467.

143. Remick, D. G., G. Bolgos, S. Copeland, and J. Siddiqui. 2005. Role of interleukin-6 in mortality from and physiologic response to sepsis. *Infect. Immun.* 73: 2751-2757.

144. Damas, P., D. Ledoux, M. Nys, Y. Vrindts, D. De Groote, P. Franchimont, and M. Lamy. 1992. Cytokine serum level during severe sepsis in human IL-6 as a marker of severity. *Ann. Surg.* 215: 356-362.

145. Naffaa, M., B. F. Makhoul, A. Tobia, M. Kaplan, D. Aronson, W. Saliba, and Z. S. Azzam. 2013. Interleukin-6 at discharge predicts all-cause mortality in patients with sepsis. *Am. J. Emerg. Med.* 31: 1361-1364.

146. Torres, B. A., S. Kominsky, G. Q. Perrin, A. C. Hobeika, and H. M. Johnson. 2001. Superantigens: the good, the bad, and the ugly. *Exp. Biol. Med. (Maywood)* 226: 164-176.

147. Wikstrom, M. E., and P. A. Stumbles. 2007. Mouse respiratory tract dendritic cell subsets and the immunological fate of inhaled antigens. *Immunol. Cell Biol.* 85: 182-188.

148. Whitsett, J. A. 2002. Intrinsic and innate defenses in the lung: intersection of pathways regulating lung morphogenesis, host defense, and repair. *J. Clin. Invest.* 109: 565-569.

149. Vermaelen, K. Y., I. Carro-Muino, B. N. Lambrecht, and R. A. Pauwels. 2001. Specific migratory dendritic cells rapidly transport antigen from the airways to the thoracic lymph nodes. *J. Exp. Med.* 193: 51-60.

150. Kaukonen, K. M., M. Bailey, D. Pilcher, D. J. Cooper, and R. Bellomo. 2015. Systemic inflammatory response syndrome criteria in defining severe sepsis. *N. Engl. J. Med.* 372: 1629-1638.

151. Devi, S., Y. Wang, W. K. Chew, R. Lima, A. G. N, C. N. Mattar, S. Z. Chong, A. Schlitzer, N. Bakocevic, S. Chew, J. L. Keeble, C. C. Goh, J. L. Li, M. Evrard, B. Malleret, A. Larbi, L. Renia, M. Haniffa, S. M. Tan, J. K. Chan, K. Balabanian, T. Nagasawa, F. Bachelerie, A. Hidalgo, F. Ginhoux, P. Kubes, and L. G. Ng. 2013. Neutrophil mobilization via plerixafor-mediated CXCR4 inhibition arises from lung demargination and blockade of neutrophil homing to the bone marrow. *J. Exp. Med.* 210: 2321-2336.

152. Mourad, W., K. Mehindate, T. J. Schall, and S. R. McColl. 1992. Engagement of major histocompatibility complex class II molecules by superantigen induces inflammatory cytokine gene expression in human rheumatoid fibroblast-like synoviocytes. *J. Exp. Med.* 175: 613-616.

153. Diener, K., P. Tessier, J. Fraser, F. Kontgen, and S. R. McColl. 1998. Induction of acute inflammation in vivo by staphylococcal superantigens I: Leukocyte recruitment occurs independently of T lymphocytes and major histocompatibility complex Class II molecules. *Lab. Invest.* 78: 647-656.

154. Hampton, H. R., J. Bailey, M. Tomura, R. Brink, and T. Chtanova. 2015. Microbe-dependent lymphatic migration of neutrophils modulates lymphocyte proliferation in lymph nodes. *Nat. Commun.* 6: 7139.

155. Bradley, J. R. 2008. TNF-mediated inflammatory disease. *J. Pathol.* 214: 149-160.

156. Galea-Lauri, J., D. Darling, S. U. Gan, L. Krivochtchapov, M. Kuiper, J. Gaken, B. Souberbielle, and F. Farzaneh. 1999. Expression of a variant of CD28 on a subpopulation of human NK cells: implications for B7-mediated stimulation of NK cells. *J. Immunol.* 163: 62-70.

157. Venuprasad, K., P. P. Banerjee, S. Chattopadhyay, S. Sharma, S. Pal, P. B. Parab, D. Mitra, and B. Saha. 2002. Human neutrophil-expressed CD28 interacts with macrophage B7 to induce phosphatidylinositol 3-kinase-dependent IFN-gamma secretion and restriction of Leishmania growth. *J. Immunol.* 169: 920-928.

158. Pennington, J. E. 1993. Therapy with antibody to tumor necrosis factor in sepsis. *Clin. Infect. Dis.* 17 Suppl 2: S515-519.

159. Cohen, J., and J. Carlet. 1996. INTERSEPT: an international, multicenter, placebo-controlled trial of monoclonal antibody to human tumor necrosis factor-alpha in patients with sepsis. International Sepsis Trial Study Group. *Crit. Care Med.* 24: 1431-1440.

160. Abraham, E., R. Wunderink, H. Silverman, T. M. Perl, S. Nasraway, H. Levy, R. Bone, R. P. Wenzel, R. Balk, R. Allred, and et al. 1995. Efficacy and safety of monoclonal antibody to human tumor necrosis factor alpha in patients with sepsis syndrome. A randomized, controlled, double-blind, multicenter clinical trial. TNF-alpha MAb Sepsis Study Group. *JAMA* 273: 934-941.

161. Fisher, C. J., Jr., J. M. Agosti, S. M. Opal, S. F. Lowry, R. A. Balk, J. C. Sadoff, E. Abraham, R. M. Schein, and E. Benjamin. 1996. Treatment of septic shock with the tumor necrosis factor receptor:Fc fusion protein. The Soluble TNF Receptor Sepsis Study Group. *N. Engl. J. Med.* 334: 1697-1702.

162. Bongartz, T., A. J. Sutton, M. J. Sweeting, I. Buchan, E. L. Matteson, and V. Montori. 2006. Anti-TNF antibody therapy in rheumatoid arthritis and the risk of serious infections and malignancies: systematic review and meta-analysis of rare harmful effects in randomized controlled trials. *JAMA* 295: 2275-2285.

163. von Kockritz-Blickwede, M., M. Rohde, S. Oehmcke, L. S. Miller, A. L. Cheung, H. Herwald, S. Foster, and E. Medina. 2008. Immunological mechanisms underlying the genetic predisposition to severe Staphylococcus aureus infection in the mouse model. *Am. J. Pathol.* 173: 1657-1668.

164. Bermejo-Martin, J. F., E. Tamayo, G. Ruiz, D. Andaluz-Ojeda, R. Herran-Monge, A. Muriel-Bombin, M. Fe Munoz, M. Heredia-Rodriguez, R. Citores, J. Gomez-Herreras, and J. Blanco. 2014. Circulating neutrophil counts and mortality in septic shock. *Crit. Care* 18: 407.

165. Suntharalingam, G., M. R. Perry, S. Ward, S. J. Brett, A. Castello-Cortes, M. D. Brunner, and N. Panoskaltsis. 2006. Cytokine storm in a phase 1 trial of the anti-CD28 monoclonal antibody TGN1412. *N. Engl. J. Med.* 355: 1018-1028.

166. Saha, B., D. M. Harlan, K. P. Lee, C. H. June, and R. Abe. 1996. Protection against lethal toxic shock by targeted disruption of the CD28 gene. *J. Exp. Med.* 183: 2675-2680.

167. Saha, B., B. Jaklic, D. M. Harlan, G. S. Gray, C. H. June, and R. Abe. 1996. Toxic shock syndrome toxin-1-induced death is prevented by CTLA4Ig. *J. Immunol.* 157: 3869-3875.

168. Bone, R. C. 1996. Sir Isaac Newton, sepsis, SIRS, and CARS. *Crit. Care Med.* 24: 1125-1128.

169. Tamayo, E., A. Fernandez, R. Almansa, E. Carrasco, M. Heredia, C. Lajo, L. Goncalves, J. I. Gomez-Herreras, R. O. de Lejarazu, and J. F. Bermejo-Martin. 2011. Pro- and anti-inflammatory responses are regulated simultaneously from the first moments of septic shock. *Eur. Cytokine Netw.* 22: 82-87.

170. Novotny, A. R., D. Reim, V. Assfalg, F. Altmayr, H. M. Friess, K. Emmanuel, and B. Holzmann. 2012. Mixed antagonist response and sepsis severity-dependent dysbalance of pro- and anti-inflammatory responses at the onset of postoperative sepsis. *Immunobiology* 217: 616-621.

171. Matthay, M. A., L. B. Ware, and G. A. Zimmerman. 2012. The acute respiratory distress syndrome. *J. Clin. Invest.* 122: 2731-2740.

172. Seidenfeld, J. J., D. F. Pohl, R. C. Bell, G. D. Harris, and W. G. Johanson, Jr. 1986. Incidence, site, and outcome of infections in patients with the adult respiratory distress syndrome. *Am Rev Respir Dis* 134: 12-16.

173. Bauer, T. T., M. Valencia, J. R. Badia, S. Ewig, J. Gonzalez, M. Ferrer, and A. Torres. 2005. Respiratory microbiology patterns within the first 24 h of ARDS diagnosis: influence on outcome. *Chest* 128: 273-279.

174. Matute-Bello, G., C. W. Frevert, and T. R. Martin. 2008. Animal models of acute lung injury. *Am. J. Physiol. Lung Cell. Mol. Physiol.* 295: L379-L399.

175. Kollef, M. H., A. Shorr, Y. P. Tabak, V. Gupta, L. Z. Liu, and R. S. Johannes. 2005. Epidemiology and outcomes of health-care-associated pneumonia: results from a large US database of culture-positive pneumonia. *Chest* 128: 3854-3862.

176. Powers, M. E., and J. Bubeck Wardenburg. 2014. Igniting the fire: Staphylococcus aureus virulence factors in the pathogenesis of sepsis. *PLoS Pathog.* 10: e1003871.

177. Wilson, G. J., K. S. Seo, R. A. Cartwright, T. Connelley, O. N. Chuang-Smith, J. A. Merriman, C. M. Guinane, J. Y. Park, G. A. Bohach, P. M. Schlievert, W. I. Morrison, and J. R. Fitzgerald. 2011. A novel core genome-encoded superantigen contributes to lethality of community-associated MRSA necrotizing pneumonia. *PLoS Pathog.* 7: e1002271.

178. Parker, D., C. L. Ryan, F. Alonzo, 3rd, V. J. Torres, P. J. Planet, and A. S. Prince. 2015. CD4+ T cells promote the pathogenesis of Staphylococcus aureus pneumonia. *J. Infect. Dis.* 211: 835-845.

179. Desouza, I. A., C. F. Franco-Penteado, E. A. Camargo, C. S. Lima, S. A. Teixeira, M. N. Muscara, G. De Nucci, and E. Antunes. 2005. Inflammatory mechanisms underlying the rat pulmonary neutrophil influx induced by airway exposure to staphylococcal enterotoxin type A. *Br J Pharmacol* 146: 781-791.

180. Rajagopalan, G., K. Iijima, M. Singh, H. Kita, R. Patel, and C. S. David. 2006. Intranasal exposure to bacterial superantigens induces airway inflammation in HLA class II transgenic mice. *Infect. Immun.* 74: 1284-1296.

181. Peterson, B. T., E. J. Miller, and D. Morris. 1999. Neutrophil influx and migration in rabbit airways in response to staphylococcal enterotoxin-A. *Exp Lung Res* 25: 41-54.

182. Herz, U., R. Ruckert, K. Wollenhaupt, T. Tschernig, U. Neuhaus-Steinmetz, R. Pabst, and H. Renz. 1999. Airway exposure to bacterial superantigen (SEB) induces lymphocyte-dependent airway inflammation associated with increased airway responsiveness--a model for non-allergic asthma. *Eur. J. Immunol.* 29: 1021-1031.

183. Svedova, J., N. Tsurutani, W. Liu, K. M. Khanna, and A. T. Vella. 2016. TNF and CD28 Signaling Play Unique but Complementary Roles in the Systemic Recruitment of Innate Immune Cells after Staphylococcus aureus Enterotoxin A Inhalation. *J. Immunol.* 196: 4510-4521.

184. Takeshita, W. M., V. O. Gushiken, A. P. Ferreira-Duarte, A. S. Pinheiro-Torres, I. A. Roncalho-Buck, D. M. Squebola-Cola, G. C. Mello, G. F. Anhe, E. Antunes, and I. A. DeSouza. 2015. Staphylococcal enterotoxin A regulates bone marrow granulocyte trafficking during pulmonary inflammatory disease in mice. *Toxicol Appl Pharmacol* 287: 267-275.

185. Walter, J. M., J. Wilson, and L. B. Ware. 2014. Biomarkers in acute respiratory distress syndrome: from pathobiology to improving patient care. *Expert Rev Respir Med* 8: 573-586.

186. Ganter, M. T., M. J. Cohen, K. Brohi, B. B. Chesebro, K. L. Staudenmayer, P. Rahn, S. C. Christiaans, N. D. Bir, and J. F. Pittet. 2008. Angiopoietin-2, marker and mediator of endothelial activation with prognostic significance early after trauma? *Ann. Surg.* 247: 320-326.

187. Nicholson, D. W., A. Ali, N. A. Thornberry, J. P. Vaillancourt, C. K. Ding, M. Gallant, Y. Gareau, P. R. Griffin, M. Labelle, Y. A. Lazebnik, and et al. 1995. Identification and inhibition of the ICE/CED-3 protease necessary for mammalian apoptosis. *Nature* 376: 37-43.

188. Amir, E.-a. D., K. L. Davis, M. D. Tadmor, E. F. Simonds, J. H. Levine, S. C. Bendall, D. K. Shenfeld, S. Krishnaswamy, G. P. Nolan, and D. Pe'er. 2013. viSNE enables visualization of high dimensional single-cell data and reveals phenotypic heterogeneity of leukemia. *Nat Biotech* 31: 545-552.

189. Maxwell, J. R., R. J. Rossi, S. J. McSorley, and A. T. Vella. 2004. T cell clonal conditioning: a phase occurring early after antigen presentation but before clonal expansion is impacted by Toll-like receptor stimulation. *J. Immunol.* 172: 248-259.

190. Heiss, C., A. Rodriguez-Mateos, and M. Kelm. 2015. Central Role of eNOS in the Maintenance of Endothelial Homeostasis. *Antioxid Redox Signal* 22: 1230-1242.

191. Pober, J. S., and W. C. Sessa. 2007. Evolving functions of endothelial cells in inflammation. *Nat. Rev. Immunol.* 7: 803-815.

192. Hashimoto, S., A. Kobayashi, K. Kooguchi, Y. Kitamura, H. Onodera, and H. Nakajima. 2000. Upregulation of two death pathways of perforin/granzyme and FasL/Fas in septic acute respiratory distress syndrome. *Am J Respir Crit Care Med* 161: 237-243.

193. Li, J. H., M. S. Kluger, L. A. Madge, L. Zheng, A. L. Bothwell, and J. S. Pober. 2002. Interferon-gamma augments CD95(APO-1/Fas) and pro-caspase-8 expression and sensitizes human vascular endothelial cells to CD95-mediated apoptosis. *Am. J. Pathol.* 161: 1485-1495.

194. Urayama, S., A. Kawakami, N. Matsuoka, M. Tsuboi, T. Nakashima, Y. Kawabe, T. Koji, and K. Eguchi. 1997. Fas/Fas ligand interaction regulates cytotoxicity of CD4+ T cells against staphylococcal enterotoxin B-pulsed endothelial cells. *Biochem Biophys Res Commun* 239: 782-788.

195. Hamai, A., F. Meslin, H. Benlalam, A. Jalil, M. Mehrpour, F. Faure, Y. Lecluse, P. Vielh, M. F. Avril, C. Robert, and S. Chouaib. 2008. ICAM-1 has a critical role in the regulation of metastatic melanoma tumor susceptibility to CTL lysis by interfering with PI3K/AKT pathway. *Cancer Res* 68: 9854-9864.

196. Anikeeva, N., K. Somersalo, T. N. Sims, V. K. Thomas, M. L. Dustin, and Y. Sykulev. 2005. Distinct role of lymphocyte function-associated antigen-1 in mediating effective cytolytic activity by cytotoxic T lymphocytes. *Proc. Natl. Acad. Sci. USA* 102: 6437-6442.

197. Rahman, A., and F. Fazal. 2009. Hug tightly and say goodbye: role of endothelial ICAM-1 in leukocyte transmigration. *Antioxid Redox Signal* 11: 823-839.

198. Aggarwal, N. R., L. S. King, and F. R. D'Alessio. 2014. Diverse macrophage populations mediate acute lung inflammation and resolution. *Am. J. Physiol. Lung Cell. Mol. Physiol.* 306: L709-725.

199. Risso, K., G. Kumar, M. Ticchioni, C. Sanfiorenzo, J. Dellamonica, F. Guillouet-de Salvador, G. Bernardin, C. H. Marquette, and P. M. Roger. 2015. Early infectious acute respiratory distress syndrome is characterized by activation and proliferation of alveolar T-cells. *Eur J Clin Microbiol Infect Dis* 34: 1111-1118.

200. D'Alessio, F. R., K. Tsushima, N. R. Aggarwal, E. E. West, M. H. Willett, M. F. Britos, M. R. Pipeling, R. G. Brower, R. M. Tuder, J. F. McDyer, and L. S. King. 2009. CD4+CD25+Foxp3+ Tregs resolve experimental lung injury in mice and are present in humans with acute lung injury. *J. Clin. Invest.* 119: 2898-2913.

201. Aeffner, F., B. Bolon, and I. C. Davis. 2015. Mouse Models of Acute Respiratory Distress Syndrome: A Review of Analytical Approaches, Pathologic Features, and Common Measurements. *Toxicol Pathol* 43: 1074-1092.

202. Schlievert, P. M. 2009. Cytolysins, Superantigens, and Penumonia due to Community-Associated Methicillin-Resistant Staphylococcus aureus. *J. Infect. Dis.* 200: 676-678.

203. Delgoffe, G. M., and D. A. A. Vignali. 2013. STAT heterodimers in immunity: A mixed message or a unique signal? *Jakstat* 2.

204. Carman, C. V., and R. Martinelli. 2015. T Lymphocyte-Endothelial Interactions: Emerging Understanding of Trafficking and Antigen-Specific Immunity. *Front Immunol* 6: 603.

205. Muller, A. M., C. Cronen, K. M. Muller, and C. J. Kirkpatrick. 2002. Heterogeneous expression of cell adhesion molecules by endothelial cells in ARDS. *J. Pathol.* 198: 270-275.

206. Lang, J. D., and J. M. Hickman-Davis. 2005. One-hit, two-hit . . . is there really any benefit? *Clin Exp Immunol* 141: 211-214.

207. Rieder, S. A., P. Nagarkatti, and M. Nagarkatti. 2012. Multiple anti-inflammatory pathways triggered by resveratrol lead to amelioration of staphylococcal enterotoxin B-induced lung injury. *Br J Pharmacol* 167: 1244-1258.

208. Sun, J., G. P. Law, C. C. Bridges, and R. J. McKallip. 2012. CD44 as a novel target for treatment of staphylococcal enterotoxin B-induced acute inflammatory lung injury. *Clin Immunol* 144: 41-52.

209. Uchakina, O. N., C. M. Castillejo, C. C. Bridges, and R. J. McKallip. 2013. The role of hyaluronic acid in SEB-induced acute lung inflammation. *Clin Immunol* 146: 56-69.

210. Rao, R., P. S. Nagarkatti, and M. Nagarkatti. 2015. Δ(9) Tetrahydrocannabinol attenuates Staphylococcal enterotoxin B-induced inflammatory lung injury and prevents mortality in mice by modulation of miR-17-92 cluster and induction of T-regulatory cells. *Br J Pharmacol* 172: 1792-1806.

211. Matute-Bello, G., W. C. Liles, K. P. Steinberg, P. A. Kiener, S. Mongovin, E. Y. Chi, M. Jonas, and T. R. Martin. 1999. Soluble Fas ligand induces epithelial cell apoptosis in humans with acute lung injury (ARDS). *J. Immunol.* 163: 2217-2225.

212. Matute-Bello, G., R. K. Winn, M. Jonas, E. Y. Chi, T. R. Martin, and W. C. Liles. 2001. Fas (CD95) Induces Alveolar Epithelial Cell Apoptosis in Vivo : Implications for Acute Pulmonary Inflammation. *Am. J. Pathol.* 158: 153-161.

213. Xu, H., J. A. Gonzalo, Y. St Pierre, I. R. Williams, T. S. Kupper, R. S. Cotran, T. A. Springer, and J. C. Gutierrez-Ramos. 1994. Leukocytosis and resistance to septic shock in intercellular adhesion molecule 1-deficient mice. *J. Exp. Med.* 180: 95-109.

214. Damle, N. K., K. Klussman, G. Leytze, and P. S. Linsley. 1993. Proliferation of human T lymphocytes induced with superantigens is not dependent on costimulation by the CD28 counter-receptor B7. *J. Immunol.* 150: 726-735.

215. Krakauer, T. 1994. Costimulatory receptors for the superantigen staphylococcal enterotoxin B on human vascular endothelial cells and T cells. *J Leukoc Biol* 56: 458-463.

216. Labuda, T., J. Wendt, G. Hedlund, and M. Dohlsten. 1998. ICAM-1 costimulation induces IL-2 but inhibits IL-10 production in superantigen-activated human CD4+ T cells. *Immunology* 94: 496-502.

217. Boyd, A. W., S. O. Wawryk, G. F. Burns, and J. V. Fecondo. 1988. Intercellular adhesion molecule 1 (ICAM-1) has a central role in cell-cell contact-mediated immune mechanisms. *Proc. Natl. Acad. Sci. USA* 85: 3095-3099.

218. Riesbeck, K., A. Billstrom, J. Tordsson, T. Brodin, K. Kristensson, and M. Dohlsten. 1998. Endothelial cells expressing an inflammatory phenotype are lysed by superantigen-targeted cytotoxic T cells. *Clin Diagn Lab Immunol* 5: 675-682.

219. Woodfin, A., M. Beyrau, M. B. Voisin, B. Ma, J. R. Whiteford, P. L. Hordijk, N. Hogg, and S. Nourshargh. 2016. ICAM-1-expressing neutrophils exhibit enhanced effector functions in murine models of endotoxemia. *Blood* 127: 898-907.

220. Mulligan, M. S., G. O. Till, C. W. Smith, D. C. Anderson, M. Miyasaka, T. Tamatani, R. F. Todd, 3rd, T. B. Issekutz, and P. A. Ward. 1994. Role of leukocyte adhesion molecules in lung and dermal vascular injury after thermal trauma of skin. *Am. J. Pathol.* 144: 1008-1015.

221. Lundberg, A. H., K. Fukatsu, L. Gaber, S. Callicutt, M. Kotb, H. Wilcox, K. Kudsk, and A. O. Gaber. 2001. Blocking pulmonary ICAM-1 expression ameliorates lung injury in established diet-induced pancreatitis. *Ann. Surg.* 233: 213-220.

222. Mileski, W. J., D. Burkhart, J. L. Hunt, R. J. Kagan, J. R. Saffle, D. N. Herndon, D. M. Heimbach, A. Luterman, R. W. Yurt, C. W. Goodwin, and J. Hansborough. 2003. Clinical effects of inhibiting leukocyte adhesion with monoclonal antibody to intercellular adhesion molecule-1 (enlimomab) in the treatment of partial-thickness burn injury. *J Trauma* 54: 950-958.

223. Kavanaugh, A. F., L. S. Davis, L. A. Nichols, S. H. Norris, R. Rothlein, L. A. Scharschmidt, and P. E. Lipsky. 1994. Treatment of refractory rheumatoid arthritis with a monoclonal antibody to intercellular adhesion molecule 1. *Arthritis Rheum* 37: 992-999.

224. Salmela, K., L. Wramner, H. Ekberg, I. Hauser, O. Bentdal, L. E. Lins, H. Isoniemi, L. Backman, N. Persson, H. H. Neumayer, P. F. Jorgensen, C. Spieker, B. Hendry, A. Nicholls, G. Kirste, and G. Hasche. 1999. A randomized multicenter trial of the anti-ICAM-1 monoclonal antibody (enlimomab) for the prevention of acute rejection and delayed onset of graft function in cadaveric renal transplantation: a report of the European Anti-ICAM-1 Renal Transplant Study Group. *Transplantation* 67: 729-736.

225. Mannick, J. A., M. L. Rodrick, and J. A. Lederer. 2001. The immunologic response to injury. *J Am Coll Surg* 193: 237-244.

226. Hussell, T., and T. J. Bell. 2014. Alveolar macrophages: plasticity in a tissue-specific context. *Nat. Rev. Immunol.* 14: 81-93.

227. Morales-Nebreda, L., A. V. Misharin, H. Perlman, and G. R. Budinger. 2015. The heterogeneity of lung macrophages in the susceptibility to disease. *Eur Respir Rev* 24: 505-509.

228. Mathie, S. A., K. L. Dixon, S. A. Walker, V. Tyrrell, M. Mondhe, V. B. O'Donnell, L. G. Gregory, and C. M. Lloyd. 2015. Alveolar macrophages are sentinels of murine pulmonary homeostasis following inhaled antigen challenge. *Allergy* 70: 80-89.

229. Purnama, C., S. L. Ng, P. Tetlak, Y. A. Setiagani, M. Kandasamy, S. Baalasubramanian, K. Karjalainen, and C. Ruedl. 2014. Transient ablation of alveolar macrophages leads to massive pathology of influenza infection without affecting cellular adaptive immunity. *Eur. J. Immunol.* 44: 2003-2012.

230. Schneider, C., S. P. Nobs, A. K. Heer, M. Kurrer, G. Klinke, N. van Rooijen, J. Vogel, and M. Kopf. 2014. Alveolar macrophages are essential for protection from respiratory failure and associated morbidity following influenza virus infection. *PLoS Pathog.* 10: e1004053.

231. Bang, B. R., E. Chun, E. J. Shim, H. S. Lee, S. Y. Lee, S. H. Cho, K. U. Min, Y. Y. Kim, and H. W. Park. 2011. Alveolar macrophages modulate allergic inflammation in a murine model of asthma. *Exp Mol Med* 43: 275-280.

232. Beck-Schimmer, B., R. Schwendener, T. Pasch, L. Reyes, C. Booy, and R. C. Schimmer. 2005. Alveolar macrophages regulate neutrophil recruitment in endotoxin-induced lung injury. *Respir Res* 6: 61.

233. Traeger, T., W. Kessler, A. Hilpert, M. Mikulcak, M. Entleutner, P. Koerner, A. Westerholt, K. Cziupka, N. van Rooijen, C. D. Heidecke, and S. Maier. 2009. Selective depletion of alveolar macrophages in polymicrobial sepsis increases lung injury, bacterial load and mortality but does not affect cytokine release. *Respiration* 77: 203-213.

234. Prakash, A., K. R. Mesa, K. Wilhelmsen, F. Xu, J. M. Dodd-o, and J. Hellman. 2012. Alveolar Macrophages and Toll-like Receptor 4 Mediate Ventilated Lung Ischemia Reperfusion Injury in Mice. *Anesthesiology* 117: 822-835.

235. Hashimoto, S., J. F. Pittet, K. Hong, H. Folkesson, G. Bagby, L. Kobzik, C. Frevert, K. Watanabe, S. Tsurufuji, and J. Wiener-Kronish. 1996. Depletion of alveolar macrophages decreases neutrophil chemotaxis to Pseudomonas airspace infections. *Am J Physiol* 270: L819-828.

236. Ghoneim, H. E., P. G. Thomas, and J. A. McCullers. 2013. Depletion of alveolar macrophages during influenza infection facilitates bacterial superinfections. *J. Immunol.* 191: 1250-1259.

237. Gonzalez-Juarbe, N., R. P. Gilley, C. A. Hinojosa, K. M. Bradley, A. Kamei, G. Gao, P. H. Dube, M. A. Bergman, and C. J. Orihuela. 2015. Pore-Forming Toxins Induce Macrophage Necroptosis during Acute Bacterial Pneumonia. *PLoS Pathog.* 11: e1005337.

238. Aoshiba, K., J. Tamaoki, and A. Nagai. 2001. Acute cigarette smoke exposure induces apoptosis of alveolar macrophages. *Am. J. Physiol. Lung Cell. Mol. Physiol.* 281: L1392-1401.

239. Kotani, N., C. Y. Lin, J. S. Wang, J. M. Gurley, F. P. Tolin, F. Michelassi, H. S. Lin, W. S. Sandberg, and M. F. Roizen. 1995. Loss of alveolar macrophages during anesthesia and operation in humans. *Anesth Analg* 81: 1255-1262.

240. Ferracini, M., J. O. Martins, M. R. Campos, D. B. Anger, and S. Jancar. 2010. Impaired phagocytosis by alveolar macrophages from diabetic rats is related to the

deficient coupling of LTs to the Fc gamma R signaling cascade. *Mol Immunol* 47: 1974-1980.

241. Liang, Y., F. L. Harris, D. P. Jones, and L. A. Brown. 2013. Alcohol induces mitochondrial redox imbalance in alveolar macrophages. *Free Radic Biol Med* 65: 1427-1434.

242. van der Sluijs, K. F., T. van der Poll, R. Lutter, N. P. Juffermans, and M. J. Schultz. 2010. Bench-to-bedside review: Bacterial pneumonia with influenza - pathogenesis and clinical implications. *Crit. Care* 14: 219.

243. O'Brien, J. M., Jr., B. Lu, N. A. Ali, G. S. Martin, S. K. Aberegg, C. B. Marsh, S. Lemeshow, and I. S. Douglas. 2007. Alcohol dependence is independently associated with sepsis, septic shock, and hospital mortality among adult intensive care unit patients. *Crit. Care Med.* 35: 345-350.

244. Calfee, C. S., M. A. Matthay, K. N. Kangelaris, E. D. Siew, D. R. Janz, G. R. Bernard, A. K. May, P. Jacob, C. Havel, N. L. Benowitz, and L. B. Ware. 2015. Cigarette Smoke Exposure and the Acute Respiratory Distress Syndrome. *Crit. Care Med.* 43: 1790-1797.

245. Hsieh, S. J., H. Zhuo, N. L. Benowitz, B. T. Thompson, K. D. Liu, M. A. Matthay, and C. S. Calfee. 2014. Prevalence and impact of active and passive cigarette smoking in acute respiratory distress syndrome. *Crit. Care Med.* 42: 2058-2068.

246. Moazed, F., and C. S. Calfee. 2014. Environmental risk factors for acute respiratory distress syndrome. *Clin. Chest Med.* 35: 625-637.

247. Wang, H. E., N. I. Shapiro, R. Griffin, M. M. Safford, S. Judd, and G. Howard. 2012. Chronic medical conditions and risk of sepsis. *PLoS One* 7: e48307.

248. Miller, E. J., S. Nagao, F. K. Carr, J. M. Noble, and A. B. Cohen. 1996. Interleukin-8 (IL-8) is a major neutrophil chemotaxin from human alveolar macrophages stimulated with staphylococcal enterotoxin A (SEA). *Inflamm Res* 45: 386-392.

249. Isobe, K., and I. Nakashima. 1992. Feedback suppression of staphylococcal enterotoxin-stimulated T-lymphocyte proliferation by macrophages through inductive nitric oxide synthesis. *Infect. Immun.* 60: 4832-4837.

250. MacDonald, K. L., M. T. Osterholm, C. W. Hedberg, C. G. Schrock, G. F. Peterson, J. M. Jentzen, S. A. Leonard, and P. M. Schlievert. 1987. Toxic shock syndrome. A newly recognized complication of influenza and influenzalike illness. *JAMA* 257: 1053-1058.

251. Prechter, G. C., and A. K. Gerhard. 1989. Postinfluenza toxic shock syndrome. *Chest* 95: 1153-1154.

252. Huvenne, W., E. A. Lanckacker, O. Krysko, K. R. Bracke, T. Demoor, P. W. Hellings, G. G. Brusselle, G. F. Joos, C. Bachert, and T. Maes. 2011. Exacerbation of cigarette smoke-induced pulmonary inflammation by Staphylococcus aureus enterotoxin B in mice. *Respir Res* 12: 69.

253. Ducreux, J., P. R. Crocker, and R. Vanbever. 2009. Analysis of sialoadhesin expression on mouse alveolar macrophages. *Immunol Lett* 124: 77-80.

254. Ménoret, A., J. Svedova, B. Behl, and A. T. Vella. 2015. Trace Levels of Staphylococcal Enterotoxin Bioactivity Are Concealed in a Mucosal Niche during Pulmonary Inflammation. *PLoS One* 10.

255. Misharin, A. V., L. Morales-Nebreda, G. M. Mutlu, G. R. S. Budinger, and H. Perlman. 2013. Flow Cytometric Analysis of Macrophages and Dendritic Cell Subsets in the Mouse Lung. *Am J Respir Cell Mol Biol* 49: 503-510.

256. Fulton, S. A., S. M. Reba, R. K. Pai, M. Pennini, M. Torres, C. V. Harding, and W. H. Boom. 2004. Inhibition of Major Histocompatibility Complex II Expression and Antigen Processing in Murine Alveolar Macrophages by Mycobacterium bovis BCG and the 19-Kilodalton Mycobacterial Lipoprotein. *Infect. Immun.* 72: 2101-2110.

257. Chelen, C. J., Y. Fang, G. J. Freeman, H. Secrist, J. D. Marshall, P. T. Hwang, L. R. Frankel, R. H. DeKruyff, and D. T. Umetsu. 1995. Human alveolar macrophages present antigen ineffectively due to defective expression of B7 costimulatory cell surface molecules. *J. Clin. Invest.* 95: 1415-1421.

258. Blumenthal, R. L., D. E. Campbell, P. Hwang, R. H. DeKruyff, L. R. Frankel, and D. T. Umetsu. 2001. Human alveolar macrophages induce functional inactivation in antigen-specific CD4 T cells. *J Allergy Clin Immunol* 107: 258-264.

259. Schulte, W., J. Bernhagen, and R. Bucala. 2013. Cytokines in sepsis: potent immunoregulators and potential therapeutic targets--an updated view. *Mediators Inflamm* 2013: 165974.

260. Xu, S. X., and J. K. McCormick. 2012. Staphylococcal superantigens in colonization and disease. *Front Cell Infect Microbiol* 2: 52.

261. Verkaik, N. J., C. P. de Vogel, H. A. Boelens, D. Grumann, T. Hoogenboezem, C. Vink, H. Hooijkaas, T. J. Foster, H. A. Verbrugh, A. van Belkum, and W. J. van Wamel. 2009. Anti-staphylococcal humoral immune response in persistent nasal carriers and noncarriers of Staphylococcus aureus. *J. Infect. Dis.* 199: 625-632.

262. Bonventre, P. F., C. Linnemann, L. S. Weckbach, J. L. Staneck, C. R. Buncher, E. Vigdorth, H. Ritz, D. Archer, and B. Smith. 1984. Antibody responses to toxic-shock-syndrome (TSS) toxin by patients with TSS and by healthy staphylococcal carriers. *J. Infect. Dis.* 150: 662-666.

263. Holtfreter, S., K. Roschack, P. Eichler, K. Eske, B. Holtfreter, C. Kohler, S. Engelmann, M. Hecker, A. Greinacher, and B. M. Broker. 2006. Staphylococcus aureus carriers neutralize superantigens by antibodies specific for their colonizing strain: a potential explanation for their improved prognosis in severe sepsis. *J. Infect. Dis.* 193: 1275-1278.

264. Larkin, E. A., B. G. Stiles, and R. G. Ulrich. 2010. Inhibition of toxic shock by human monoclonal antibodies against staphylococcal enterotoxin B. *PLoS One* 5: e13253.

265. Nilsson, I. M., M. Verdrengh, R. G. Ulrich, S. Bavari, and A. Tarkowski. 1999. Protection against Staphylococcus aureus sepsis by vaccination with recombinant staphylococcal enterotoxin A devoid of superantigenicity. *J. Infect. Dis.* 180: 1370-1373.

266. Hu, D. L., K. Omoe, S. Sasaki, H. Sashinami, H. Sakuraba, Y. Yokomizo, K. Shinagawa, and A. Nakane. 2003. Vaccination with nontoxic mutant toxic shock syndrome toxin 1 protects against Staphylococcus aureus infection. *J. Infect. Dis.* 188: 743-752.

267. Actor, J. K., S. A. Hwang, and M. L. Kruzel. 2009. Lactoferrin as a Natural Immune Modulator. *Curr Pharm Des* 15: 1956-1973.

268. Hayworth, J. L., K. J. Kasper, M. Leon-Ponte, C. A. Herfst, D. Yue, W. C. Brintnell, D. M. Mazzuca, D. E. Heinrichs, E. Cairns, J. Madrenas, D. W. Hoskin, J. K. McCormick, and S. M. Haeryfar. 2009. Attenuation of massive cytokine response to the staphylococcal enterotoxin B superantigen by the innate immunomodulatory protein lactoferrin. *Clin Exp Immunol* 157: 60-70.

269. Condon, T. V., R. T. Sawyer, M. J. Fenton, and D. W. H. Riches. 2011. Lung dendritic cells at the innate-adaptive immune interface. *J Leukoc Biol* 90: 883-895.

270. Desch, A. N., P. M. Henson, and C. V. Jakubzick. 2013. Pulmonary dendritic cell development and antigen acquisition. *Immunol Res* 55: 178-186.

271. Girvan, A., F. E. Aldwell, G. S. Buchan, L. Faulkner, and M. A. Baird. 2003. Transfer of macrophage-derived mycobacterial antigens to dendritic cells can induce naive T-cell activation. *Scand J Immunol* 57: 107-114.

272. Häffner, A. C., K. Zepter, and C. A. Elmets. 1996. Major histocompatibility complex class I molecule serves as a ligand for presentation of the superantigen staphylococcal enterotoxin B to T cells. *Proc. Natl. Acad. Sci. USA* 93: 3037-3042.

273. Chatterjee, S., M. Khullar, and W. Y. Shi. 1995. Digalactosylceramide is the receptor for staphylococcal enterotoxin-B in human kidney proximal tubular cells. *Glycobiology* 5: 327-333.

274. Banke, E., K. Rodstrom, M. Ekelund, J. Dalla-Riva, J. O. Lagerstedt, S. Nilsson, E. Degerman, K. Lindkvist-Petersson, and B. Nilson. 2014. Superantigen activates the gp130 receptor on adipocytes resulting in altered adipocyte metabolism. *Metabolism* 63: 831-840.

275. Svedova, J., A. Ménoret, P. Mittal, J. M. Ryan, J. A. Buturla, and A. T. Vella. 2017. Therapeutic blockade of CD54 attenuates pulmonary barrier damage in T cell-induced acute lung injury. *American Journal of Physiology - Lung Cellular and Molecular Physiology*.

276. Pauksen, K., L. Elfman, A. K. Ulfgren, and P. Venge. 1994. Serum levels of granulocyte-colony stimulating factor (G-CSF) in bacterial and viral infections, and in atypical pneumonia. *Br J Haematol* 88: 256-260.

277. Kawakami, M., H. Tsutsumi, T. Kumakawa, H. Abe, M. Hirai, S. Kurosawa, M. Mori, and M. Fukushima. 1990. Levels of serum granulocyte colony-stimulating factor in patients with infections. *Blood* 76: 1962-1964.

278. Miyake, Y., K. Asano, H. Kaise, M. Uemura, M. Nakayama, and M. Tanaka. 2007. Critical role of macrophages in the marginal zone in the suppression of immune responses to apoptotic cell-associated antigens. *J. Clin. Invest.* 117: 2268-2278.

279. Junt, T., E. A. Moseman, M. Iannacone, S. Massberg, P. A. Lang, M. Boes, K. Fink, S. E. Henrickson, D. M. Shayakhmetov, N. C. Di Paolo, N. van Rooijen, T. R. Mempel, S. P. Whelan, and U. H. von Andrian. 2007. Subcapsular sinus macrophages in lymph nodes clear lymph-borne viruses and present them to antiviral B cells. *Nature* 450: 110-114.

280. Franciszkiewicz, K., A. Le Floc'h, M. Boutet, I. Vergnon, A. Schmitt, and F. Mami-Chouaib. 2013. CD103 or LFA-1 engagement at the immune synapse between cytotoxic T cells and tumor cells promotes maturation and regulates T-cell effector functions. *Cancer Res* 73: 617-628.